

การประยุกต์ของการควบคุมเชิงทำนายแบบจำลองกับระบบจราจรด้วยกรอบงานการ  
ควบคุมแบบกระจายตัวลำดับชั้น

นายจิรภัทร์ จิตต์เนื่อง

วิทยานิพนธ์นี้เป็นส่วนหนึ่งของการศึกษาตามหลักสูตรวิศวกรรมศาสตรมหาบัณฑิต

สาขาวิชาวิศวกรรมไฟฟ้า ภาควิชาวิศวกรรมไฟฟ้า

คณะวิศวกรรมศาสตร์ จุฬาลงกรณ์มหาวิทยาลัย

ปีการศึกษา 2561

ลิขสิทธิ์ของจุฬาลงกรณ์มหาวิทยาลัย

บทคัดย่อและแฟ้มข้อมูลฉบับเต็มของวิทยานิพนธ์ตั้งแต่ปีการศึกษา 2554 ที่ให้บริการในคลังปัญญาจุฬาฯ (CUIR)

เป็นแฟ้มข้อมูลของนิสิตเจ้าของวิทยานิพนธ์ที่ส่งผ่านทางบัณฑิตวิทยาลัย

The abstract and full text of theses from the academic year 2011 in Chulalongkorn University Intellectual Repository (CUIR) are the thesis authors' files submitted through the Graduate School.

APPLICATION OF MODEL PREDICTIVE CONTROL TO TRAFFIC SYSTEMS  
WITH HIERARCHICAL DISTRIBUTED CONTROL FRAMEWORK

Mr. Jeerapat Jitnaunt

A Thesis Submitted in Partial Fulfillment of the Requirements  
for the Degree of Master of Engineering Program in Electrical Engineering  
Department of Electrical Engineering  
Faculty of Engineering  
Chulalongkorn University  
Academic Year 2018  
Copyright of Chulalongkorn University

Thesis Title                    APPLICATION OF MODEL PREDICTIVE CONTROL TO TRAFFIC  
   WITH HIERARCHICAL DISTRIBUTED CONTROL FRAMEWORK

By                                    Mr. Jeerapat Jitnaunt

Field of Study                    Electrical Engineering

Thesis Advisor                    Professor David Banjerdpongchai, Ph.D.

---

Accepted by the Faculty of Engineering, Chulalongkorn University in Partial  
Fulfillment of the Requirements for the Master's Degree

..... Dean of the Faculty of Engineering  
(Professor Supot Teachavorasinskun, D.Eng.)

THESIS COMMITTEE

..... Chairman  
(Assistant Professor Manop Wongsaisuwas, D.Eng.)

..... Thesis Advisor  
(Professor David Banjerdpongchai, Ph.D.)

..... Examiner  
(Associate Professor Chaodit Aswakul, Ph.D.)

..... External Examiner  
(Associate Professor Waree Kongprawechnon, Ph.D.)

จิรภัทร์ จิตต์เนื่อง: การประยุกต์ของการควบคุมเชิงทำนายแบบจำลองกับระบบจราจร ด้วยกรอบงานการควบคุมแบบกระจายตัวลำดับชั้น. ( APPLICATION OF MODEL PREDICTIVE CONTROL TO TRAFFIC SYSTEMS WITH HIERARCHICAL DISTRIBUTED CONTROL FRAMEWORK ) อ.ที่ปรึกษาวิทยานิพนธ์  
หลัก : ศ. ดร. เดวิด บรรเจิดพงศ์ชัย, 89 หน้า.

การจราจรติดขัดภายในเมืองใหญ่เป็นปัญหาที่เรื้อรัง และส่งผลกระทบต่อ การพัฒนาอย่าง ยั่งยืนของการจราจรในเมือง โดยเฉพาะอย่างยิ่ง ระบบขนส่ง อีกทั้ง เป็นปัญหาส่งผลกระทบต่อคุณภาพชีวิตของประชาชนจำนวนมาก และเป็นตัวเร่งให้เกิดมลพิษทางอากาศเพิ่มมากขึ้น อีกด้วย หากโครงสร้างพื้นฐานสาธารณะ โลจิสติกส์ และระบบการขนส่งสาธารณะได้รับการปรับปรุง ให้มีประสิทธิภาพแล้ว จะสามารถบรรเทาการจราจรติดขัด วิทยานิพนธ์นี้มีวัตถุประสงค์เพื่อประยุกต์ การควบคุมเชิงทำนายแบบจำลองกับระบบจราจร ด้วยกรอบงานการควบคุมแบบกระจายตัวลำดับชั้น โครงสร้างของการควบคุมประกอบด้วยระดับชั้น 3 ระดับ ได้แก่ ระดับชั้นเครือข่าย, ระดับ ชั้นพื้นที่ และระดับชั้นทางแยก ตามลำดับ ในระดับชั้นเครือข่ายและ ระดับชั้นพื้นที่ การออกแบบ พิจารณาการหาอัตราการไหลของการจราจรแบบเหมาะสมที่สุดของเครือข่ายและของพื้นที่ตามลำดับ อัตราการไหลของการจราจรแบบเหมาะสมที่สุด ถูกส่งไปเป็นสัญญาณอ้างอิงสำหรับการควบคุมจราจร ในระดับชั้นทางแยก เพื่อคำนวณสัญญาณไฟจราจรแบบเหมาะสมที่สุดต่อไป สุดท้าย เราทดสอบ การควบคุมกับกรณีศึกษา โดยจำลองผลกับการจราจรในเขตสาทรที่มีแยกสัญญาณไฟ 10 แยก ดำรวจจราจรอาศัยข้อมูลปริมาณจราจรเพื่อควบคุมสัญญาณไฟจราจร เราเปรียบเทียบสมรรถนะ ของการควบคุมเชิงทำนายแบบจำลองกับของระบบควบคุมจราจรปัจจุบัน พบว่า การควบคุม เชิงทำนายแบบจำลองปรับปรุงการไหลรวมของจราจรทุกแยกมากขึ้นเกือบร้อยละ 2

ภาควิชา วิศวกรรมไฟฟ้า ..... ลายมือชื่อนิสิต .....  
สาขาวิชา วิศวกรรมไฟฟ้า ..... ลายมือชื่ออ.ที่ปรึกษาหลัก .....  
ปีการศึกษา 2561 .....

## 6070143221 : MAJOR ELECTRICAL ENGINEERING

KEYWORDS : TRAFFIC CONGESTION / TRAFFIC SIGNAL CONTROL / HIERARCHICAL DISTRIBUTED CONTROL FRAMEWORK / MODEL PREDICTIVE CONTROL

JEERAPAT JITNUANT : APPLICATION OF MODEL PREDICTIVE CONTROL TO TRAFFIC SYSTEMS WITH HIERARCHICAL DISTRIBUTED CONTROL FRAMEWORK.

ADVISOR : PROF. DAVID BANJERDPONGCHAI, Ph.D., 89 pp.

Traffic congestion is one of the chronic problems that degrades an urban traffic sustainable development especially the transport system. It seriously affects the quality of life of many people and becomes a catalyst of an increment of air pollution. If we can improve public infrastructure, logistics, and public transport system, they will reduce traffic congestion problem. This thesis aims to apply model predictive control (MPC) to traffic systems in a framework on hierarchical distributed control.

The control structure composes of three layers which are network layer, area layer, and intersection layer. On the network layer and area layer, the control design considers the optimal traffic flow of the network and area, respectively. The optimal traffic flow is distributed as the reference signal for each intersection to calculate the optimal traffic signal. Finally, we test the designed control on a case study by simulation of a Sathorn's traffic zone with ten intersections. Traffic polices rely on the traffic volume information to control the traffic lights. We compare the performance of MPC to that of existing traffic control system. The simulation result shows that MPC improves the the total traffic flow by almost 2%.

Department : ..... Electrical Engineering .....  
 Field of Study : ..... Electrical Engineering .....  
 Academic Year : ..... 2018 .....

Student's Signature .....  
 Advisor's Signature .....

## **Acknowledgments**

I would like to express my special appreciation and appreciates to my thesis supervisor, Professor David Banjerdpongchai for having given me continuous support, kind guidance and helpful advice since I was an undergraduate student.

I would like to thank Assistant Professor Manop Wongsaisuwan, Associate Professor Chaodit Aswakul, and Associate Professor Waree Kongprawechnon for kindly agreeing to be the committee members for my thesis examination.

I would also like to thank all students in Control Systems Research Laboratory for their great friendship and support. In particular, I would like to thank Associate Professor Chaodit Aswakul and his student for advice about traffic simulation.

Last but not least, I would like to thank my family for their understanding and supporting me throughout my life.

# Contents

|   | Page       |
|---|------------|
| <b>Abstract (Thai)</b> .....  | <b>iii</b> |
| <b>Abstract (English)</b> .....                                     | <b>v</b>   |
| <b>Acknowledgments</b> .....  | <b>vi</b>  |
| <b>Contents</b> .....   | <b>vii</b> |
| <b>List of Tables</b> .....   | <b>ix</b>  |
| <b>List of Figures</b> .....  | <b>x</b>   |
| <br>CHAPTER   |            |
| <b>I RESEARCH OVERVIEW</b> .....                                    | <b>1</b>   |
| 1.1 Introduction .....  | 1          |
| 1.2 Background .....  | 2          |
| 1.2.1 Traffic flow models .....                                     | 2          |
| 1.2.2 Traffic congestion indicators .....                           | 5          |
| 1.2.3 Traffic sensor .....  | 6          |
| 1.2.4 Optimization .....  | 7          |
| 1.2.5 Model predictive control .....                                | 8          |
| 1.2.6 Arrival and departure flow predictions .....                  | 9          |
| 1.3 Signalized intersection control techniques .....                | 9          |
| 1.4 Objective .....   | 14         |
| 1.5 Scope of work .....   | 14         |
| 1.6 Research methodology .....                                      | 14         |
| 1.7 Expected outcome .....  | 14         |
| <b>II HIERARCHICAL DISTRIBUTED CONTROL OF TRAFFIC NETWORK</b> ..... | <b>15</b>  |
| 2.1 Problem statement .....   | 15         |
| 2.2 Framework .....   | 15         |
| 2.3 Traffic models .....  | 16         |
| 2.3.1 Signalized intersection model .....                           | 16         |
| 2.3.2 Area model .....  | 24         |
| 2.3.3 Network model .....   | 26         |
| 2.4 Traffic data aggregation and distribution .....                 | 28         |

| CHAPTER   | Page      |
|---|-----------|
| 2.5 Control procedure for hierarchical distributed model predictive control . . . . . | 31        |
| <b>III PRELIMINARY RESULTS . . . . .</b>  | <b>35</b> |
| 3.1 Traffic scenario description . . . . .  | 35        |
| 3.2 Simulation results . . . . .  | 40        |
| 3.2.1 Fixed time control . . . . .  | 40        |
| 3.2.2 Hierarchical distributed control . . . . .                                      | 41        |
| 3.2.3 Comparison and summary . . . . .  | 43        |
| <b>IV APPLICATION TO SATHON MODEL . . . . .</b>                                       | <b>50</b> |
| 4.1 Traffic scenario description . . . . .  | 50        |
| 4.2 Experimental procedure . . . . .  | 62        |
| 4.3 Simulation results . . . . .  | 64        |
| 4.4 Summary . . . . .   | 81        |
| <b>V CONCLUSION . . . . .</b>   | <b>82</b> |
| <b>REFERENCES . . . . .</b>   | <b>83</b> |
| <b>APPENDIX . . . . .</b>   | <b>86</b> |
| <b>BIOGRAPHY . . . . .</b>  | <b>89</b> |

## List of Tables

| Table |   | Page |
|-------|---|------|
| 1.1   | Summary signalized intersection control approaches. . . . .               | 13   |
| 3.1   | Roadway information. . . . .  | 36   |
| 3.2   | Table of summary on traffic demand in boundary nodes. . . . .             | 36   |
| 3.3   | Table of summary on traffic volume in each road. . . . .                  | 37   |
| 3.4   | Summary of simulation results. . . . .                                    | 49   |
| 4.1   | Summary of traffic demand (veh/h) on the boundaries (outer area). . . . . | 51   |

## List of Figures

| Figure  | Page |
|---|------|
| 1.1 Fundamental diagrams of Speed-Flow-Density. . . . .                 | 3    |
| 1.2 Typical shock waves at a signalized intersection. . . . .           | 4    |
| 1.3 Vehicle queue model on a road. . . . .                              | 5    |
| 1.4 Inductive loop detector principle [21]. . . . .                     | 6    |
| 1.5 Example of loop detector installation on a road. . . . .            | 6    |
| 1.6 Illustration of gradient descent on a series of level sets. . . . . | 7    |
| 1.7 A discrete MPC scheme. . . . .                                      | 8    |
| 1.8 Traffic flow prediction model. . . . .                              | 9    |
| 1.9 Signalized intersection control techniques. . . . .                 | 10   |
| 1.10 Scheme of LQI control system. . . . .                              | 11   |
| 1.11 ANN flow chart. . . . .  | 12   |
| 1.12 Reinforcement learning flow chart. . . . .                         | 13   |
| 2.1 Hierarchical structure of traffic network. . . . .                  | 16   |
| 2.2 Example of a single road. . . . .                                   | 17   |
| 2.3 Example of flow pattern on an intersection. . . . .                 | 18   |
| 2.4 Example of signal pattern on an intersection. . . . .               | 19   |
| 2.5 Example of phase time diagram on traffic signal. . . . .            | 20   |
| 2.6 Example of traffic network schematic on 2nd area. . . . .           | 24   |
| 2.7 Example of a traffic schematic of network layer. . . . .            | 26   |
| 2.8 Example of time diagram on data aggregating. . . . .                | 28   |
| 2.9 Example of time diagram on data distributing. . . . .               | 29   |
| 2.10 Procedure diagram of network layer's controller. . . . .           | 32   |
| 2.11 Procedure diagram of area layer's controller. . . . .              | 33   |
| 2.12 Procedure diagram of intersection layer's controller. . . . .      | 34   |
| 3.1 An example scenario of a traffic network. . . . .                   | 35   |
| 3.2 Configure traffic lights on intersection $J_1$ . . . . .            | 37   |
| 3.3 Configure traffic lights on intersection $J_2$ . . . . .            | 39   |
| 3.4 Plot of states on fixed control. . . . .                            | 40   |
| 3.5 Plot of area $A_1$ on HDC with $\gamma = 20000$ . . . . .           | 41   |
| 3.6 Plot of area $A_2$ on HDC with $\gamma = 20000$ . . . . .           | 41   |
| 3.7 Plot of intersection $J_1$ on HDC with $\gamma = 20000$ . . . . .   | 42   |
| 3.8 Plot of intersection $J_2$ on HDC with $\gamma = 20000$ . . . . .   | 42   |
| 3.9 Plot of demand on area $A_1$ with varying $\gamma$ . . . . .        | 43   |

| Figure  | Page |
|---|------|
| 3.10 Plot of demand on area $A_2$ with varying $\gamma$ . . . . .                   | 43   |
| 3.11 Total mean vehicle queue-length comparison on the network. . . . .             | 44   |
| 3.12 Total traffic flow comparison on the network. . . . .                          | 44   |
| 3.13 Total delay comparison on the network. . . . .                                 | 45   |
| 3.14 Mean traffic flow rate on each road with varying $\gamma$ . . . . .            | 45   |
| 3.15 RMSE on flow tracking on each intersection. . . . .                            | 46   |
| 3.16 Mean vehicle-queue length on each intersection with varying $\gamma$ . . . . . | 46   |
| 3.17 Total mean traffic flow on the network. . . . .                                | 47   |
| 3.18 Mean traffic flow comparison on each road. . . . .                             | 47   |
| 3.19 Mean vehicle queue-length comparison on each road. . . . .                     | 48   |
| 3.20 Mean delay comparison on each road. . . . .                                    | 48   |
| 4.1 Traffic scenario of Sathorn's network zone. . . . .                             | 50   |
| 4.2 Area allocation on a scenario of Sathorn's network. . . . .                     | 51   |
| 4.3 The traffic light pattern of intersection $J_1$ . . . . .                       | 52   |
| 4.4 The traffic light pattern of intersection $J_2$ . . . . .                       | 53   |
| 4.5 The traffic light pattern of intersection $J_3$ . . . . .                       | 54   |
| 4.6 The traffic light pattern of intersection $J_4$ . . . . .                       | 55   |
| 4.7 The traffic light pattern of intersection $J_5$ . . . . .                       | 56   |
| 4.8 The traffic light pattern of intersection $J_6$ . . . . .                       | 57   |
| 4.9 The traffic light pattern of intersection $J_7$ . . . . .                       | 58   |
| 4.10 The traffic light pattern of intersection $J_8$ . . . . .                      | 59   |
| 4.11 The traffic light pattern of intersection $J_9$ . . . . .                      | 60   |
| 4.12 The traffic light pattern of intersection $J_{10}$ . . . . .                   | 61   |
| 4.13 The diagram of controllers, modules, and simulator. . . . .                    | 62   |
| 4.14 The diagram of experimental procedure. . . . .                                 | 63   |
| 4.15 Plot of control results of the network layer. . . . .                          | 64   |
| 4.16 Plot of control results of the 1st area. . . . .                               | 65   |
| 4.17 Plot of control results of the 2nd area. . . . .                               | 65   |
| 4.18 Plot of control results of the 3rd area. . . . .                               | 66   |
| 4.19 Plot of heat map on the network of Sathorn's network. . . . .                  | 66   |
| 4.20 Plot of control results of the 1st and 2nd intersection. . . . .               | 67   |
| 4.21 Plot of control results of the 3rd and 4th intersection. . . . .               | 67   |
| 4.22 Plot of control results of the 5th and 6th intersection. . . . .               | 68   |
| 4.23 Plot of control results of the 7th and 8th intersection. . . . .               | 68   |
| 4.24 Plot of control results of the 9th and 10th intersection. . . . .              | 69   |
| 4.25 Plot of control performance of network layer on 100% traffic. . . . .          | 69   |

| Figure   | Page |
|--|------|
| 4.26 Plot of control performance of 3 areas on 100% traffic. . . . .                     | 70   |
| 4.27 Plot of control performance of intersection $J_1 - J_5$ on 100% traffic. . . . .    | 71   |
| 4.28 Plot of control performance of intersection $J_6 - J_{10}$ on 100% traffic. . . . . | 72   |
| 4.29 Plot of control performance of network layer on 85% traffic. . . . .                | 73   |
| 4.30 Plot of control performance of 3 areas on 85% traffic. . . . .                      | 74   |
| 4.31 Plot of control performance of intersection $J_1 - J_5$ on 85% traffic. . . . .     | 75   |
| 4.32 Plot of control performance of intersection $J_6 - J_{10}$ on 85% traffic. . . . .  | 76   |
| 4.33 Plot of control performance of network layer on 75% traffic. . . . .                | 77   |
| 4.34 Plot of control performance of 3 areas on 75% traffic. . . . .                      | 78   |
| 4.35 Plot of control performance of intersection $J_1 - J_5$ on 75% traffic. . . . .     | 79   |
| 4.36 Plot of control performance of intersection $J_6 - J_{10}$ on 75% traffic. . . . .  | 80   |
| 4.37 Summary of the best control performances on three traffic conditions. . . . .       | 81   |

# CHAPTER I

## RESEARCH OVERVIEW

### 1.1 Introduction

Urban traffic congestion is a significant problem in city areas which difficulty to solve in a short time. The traffic problems can lead people to spend more time on the roadway, and it is the severe causes of pollution and energy efficiency problems. However, one possibility to solve traffic congestion without roadway reconstruction is the redesigning of the traffic signal control system.

Most traffic control methods were aimed at the same goal, which reduces the travel delay and traffic congestion on the intersections. Ioslovich et al. had used the feedback control to minimize the total delay on individual intersection based on continuous-time model [1]. Varga also considered on an individual intersection, and he proposed a controller that aims to minimize the vehicle queue length by using the Linear Quadratic Regulator (LQR) [2]. One strength of Varga's method is a time-varying model that adapts to the traffic flow measurement. Since the computation power of the modern computer has improved, the optimization technique has increasing popularity. The dynamic programming was used by [19], and it used to decide the next signal pattern by considering the linear cost function. Practically, traffic congestion does not depend on an intersection. It also implicated with adjacent intersections. Zaidi et al. had proposed the multiple-intersections traffic control, which is used the optimization technique over the various factors such that queue length and travel time [3]. This idea has also presented from other research [4, 5]. Model predictive control (MPC) is the most popular advanced control method based on iterative and finite-horizon optimization of a plant model. In the traffic control problems, MPC was used in literature [6] that minimizes the queue length and maximizes the traffic flow rate as every time horizon in the future to obtain the optimal traffic schedule for each intersection. Traffic problems were formed from the complex network that difficult to mitigate the traffic congestion on each road at the same time. A traffic network can separate the intersections into multiple areas. For one area, it can be assumed that it is a one control system that consists of many intersections. The setpoint of traffic flow on the area layer distribute into each intersection, and each intersection achieves by finding the optimal traffic signal. This idea can be called hierarchical control.

However, the traffic problems need to consider in the overview of traffic conditions on the network. Information on the traffic demand in the network is the parameter key to improve the traffic control that other literature has neglected. We can use the benefit of the traffic demand information to determine the traffic flow for each road. Furthermore, we also use the model predictive control to decide the optimal traffic solution by considering the predicted results on the time horizon. There-

fore, this work aims to establish a traffic control method by using the hierarchical distributed control framework (HDC). The traffic network has divided into three layers, which are network layer, area layer, and intersection layer. The role of each layer is described in Chapter 2. This work uses the model predictive control (MPC) to improve the performance of traffic flow in each intersection by using the predicted flow information from AI. We hypothesize that the changing of the cycle length of each intersection affects the control performance. The experiment is simulated with different cycle lengths to find a suitable weighting parameter that makes the best performance. Then, the results are compared to fixed control in terms of traffic flow (veh/h).

The methods and models used to designs the traffic control system in this work are described in Chapter 2. The simulation results in this work are summarized in Chapter 3. Finally, the conclusion is presented in Chapter 5.

## 1.2 Background

This section will describe the background of traffic models, which are the relationship of traffic flow, traffic density, and traffic speed. These models describe the basis of traffic dynamics and traffic conditions. Finally, the performance indices are calculated from equations in this section.

### 1.2.1 Traffic flow models

The basics of traffic variables which consist of the traffic flow, traffic speed, and traffic density, these variables must be presented the definition before the traffic analysis parts. Traffic flow describes the volume of the vehicles passed on a section per time, the relation of this value is described as

$$q = \frac{n}{\Delta t} \quad (1.1)$$

where  $q$  is the traffic flow in vehicles per unit time,  $n$  is the number of vehicles passed on some designated roadway point during time interval  $\Delta t$ , and  $\Delta t$  is the duration of time interval.

Traffic flow is usually used to specify the quantity of arrival flow rate and departure flow rate of vehicles on the road. When the arrival flow has high, it means that the traffic demand is high. However, if the departure flow rate has high, it means that the traffic condition is not congested.

The fundamental of traffic flow is described by Lighthill, Whitham and Richards (LWR) model [20,28], they had stated that the traffic flow is the multiplication of traffic density and mean speed in the road which given as

$$q = kv \quad (1.2)$$

where  $q$  is the flow rate (veh/time),  $k$  is the density (veh/space), and  $v$  is the mean speed (space/time).

While the traffic density has low, the traffic flow on the road will also be low. If the traffic condition is high density, the traffic flow on the road will also be high as well. However, while the

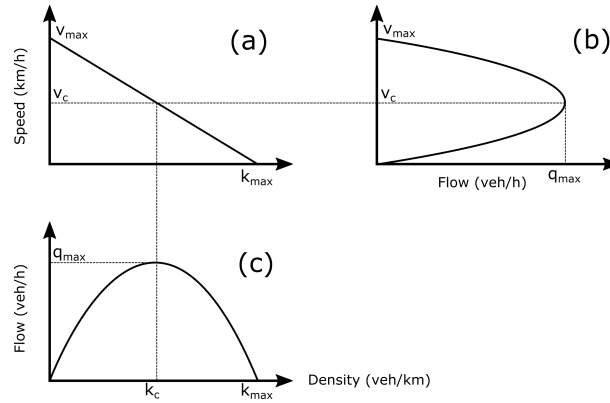


Figure 1.1: Fundamental diagrams of Speed-Flow-Density; (a) Speed-Density relationship, (b) Speed-Flow relationship, and (c) Flow-Density relationship.

traffic density has increased, the mean traffic speed will decrease in the opposite direction, which is illustrated in Figure 1.1 (a). Hence, the traffic flow relationship is the nonlinear function on the traffic density and traffic speed that will describe as follows.

### Speed-Density model

This part has described the relationships of traffic speed and traffic density when the maximum traffic speed and maximum traffic density on the road. Figure.1.1 (a). shown the negative linear relationship of traffic speed and traffic density. Mathematically, such a relationship can be expressed as

$$v = v_{\max} \left( 1 - \frac{k}{k_{\max}} \right) \quad (1.3)$$

where  $v$  is the vehicle-mean speed (km/h),  $v_{\max}$  is the free-flow speed (km/h),  $k$  is the traffic density (veh/km),  $k_{\max}$  is the maximum traffic density (veh/km).

### Flow-Density model

This part describes the relationship between traffic flow and traffic density by using knowledge from the Speed-Density model. A parabolic flow-density model can be described by using the assumption of a linear speed-density relationship (1.3), by substituting (1.3) into (1.1) we obtained

$$q = v_{\max} \left( k - \frac{k^2}{k_{\max}} \right) \quad (1.4)$$

This equation describes the relationship which shown in Figure 1.1 (c). When the traffic density is increased to the critical point  $k_c$ , the traffic flow will change in a downward direction. Due to the increase in traffic density, it affects the movement of vehicles to slow down as well.

The maximum flow rate  $q_{\max}$  as shown in Figure 1.1 (c) at the top of the curve, it can be evaluated by taking the derivative of equation (1.4) respect to density  $k$  and set it to zero. This gives

$$\frac{dq}{dk} = v_{\max} \left( 1 - \frac{2k}{k_{\max}} \right) = 0, \quad (1.5)$$

because of the free-flow speed  $v_{\max}$  is greater than zero, we obtained the critical density as

$$k_c = \frac{k_{\max}}{2}. \quad (1.6)$$

Then, we can calculate the critical velocity by substituting (1.6) into (1.3) gives

$$v_c = v_{\max} \left( 1 - \frac{k_{\max}}{2k_{\max}} \right) = \frac{v_{\max}}{2}. \quad (1.7)$$

Finally, we can calculate the maximum traffic flow by substituting (1.6) and (1.7) into (1.2) gives

$$q_{\max} = v_c k_c = \frac{v_{\max} k_{\max}}{4} \quad (1.8)$$

The maximum traffic flow is the variable that can be presented to the traffic capacity on the road.

### Shockwave theory

A limited of the fixed detector is an area covering, due to financial constraints for road authorities. An alternative approach to measuring the vehicle movement is to estimate the vehicle trajectory from information by using the kinematic wave theory (shock wave theory) [20] which has been commonly used to describe and analyze traffic flow dynamic.

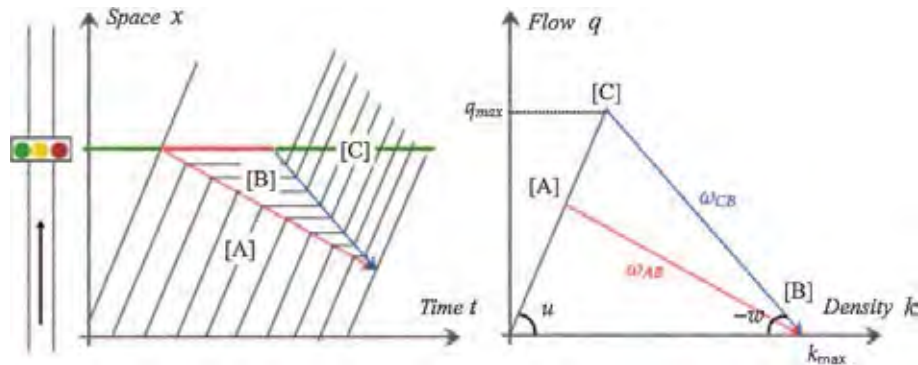


Figure 1.2: Typical shock waves at a signalized intersection; (a) time-space diagram, (b) triangular fundamental diagram ( $u$ : forward wave speed,  $w$ : backward wave speed), [29].

On the shock waves theory, the discharge rate  $q_{\text{out}}$  is equalled to  $q_{\max}$  which is obtained from (2.11). It is used to represent the dynamic of departure flow on the intersection.

### Store-and-forward traffic model

The basic traffic model for a single road which widely used in literatures [2, 7, 8] is represented by Figure 1.3, it based on the vehicle-conservation law. The number of vehicles in a road can be computed from the arrival rate and departure rate.

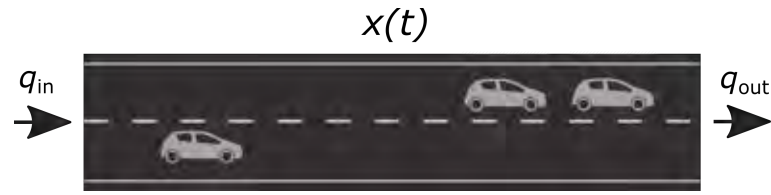


Figure 1.3: Vehicle queue model on a road.

The vehicle-conservation equation can be simplified in the discrete time model which given as

$$x(t + 1) = x(t) + (q_{in} - q_{out})\Delta t. \quad (1.9)$$

where  $x(t)$  is the number of vehicles in the road,  $q_{in}$  is the vehicles arrival rate,  $q_{out}$  is the vehicles departure rate,  $t$  is the time index, and  $\Delta t$  is the sampling period.

### 1.2.2 Traffic congestion indicators

#### Average Traffic Speed

A basic indicator to measures the traffic quality in a single road is the average traffic speed. The average speed in individual cars can evaluate directly, but in the macroscopic of traffic measurement cannot measure the vehicle speed in the road directly. Assuming a uniform speed, The average speed can be calculated using the linear relationship of traffic flow from equation (1.4) and can be rearranged by as:

$$\bar{v} = v_{max} \left( 1 - \frac{\frac{1}{T} \sum_{t=t_s}^T k(t)}{k_{max}} \right) \quad (1.10)$$

where  $t$  is the sample index,  $t_s$  is the start index of the sampling time,  $T$  is the sampling period and traffic density  $k(t)$  is obtained from measurement.

#### Traffic delay

The traffic performance on an intersection can be indicated by time delay. The traffic delay at a signalized intersection is caused by traffic signal control that is reduced the traffic flow volume and average traffic speed. The basic idea of this indicator is to measures the exceeding time when compared with uncongested traffic conditions while traveling through a road at a signalized intersection. Let assuming uniform speed, the travel time of each vehicle through a road of length  $\lambda$  at the free flow speed  $v_{max}$  is given as:

$$t_f = \frac{\lambda}{v_{max}} \quad (1.11)$$

With the congested traffic conditions, the travel time  $t_a$  of the vehicle with a uniform speed over the same road to reduced its speed  $v$  is given as:

$$t_a = \frac{\lambda}{v} \quad (1.12)$$

Because the traffic speed cannot be measured directly, we can simplify the above equation by substituting (1.10) into (1.12) gives

$$t_a = \frac{\lambda}{\bar{v}} \quad (1.13)$$

Then the delay for each vehicle to travelling through an signalized intersection can be calculated as:

$$d = t_a - t_f \quad (1.14)$$

However, the estimated travel time  $t_a$  is usually used to measure the traffic quality.

### 1.2.3 Traffic sensor

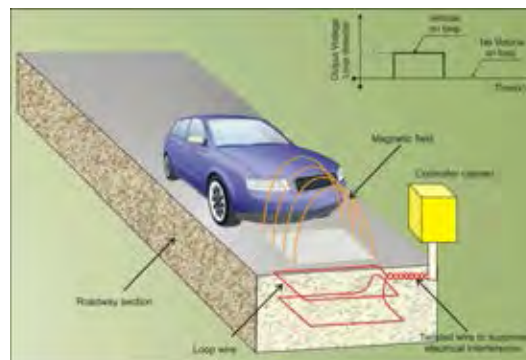


Figure 1.4: Inductive loop detector principle [21].

The inductive loop detector has shown in Figure 1.4 is used to detect vehicles passed at a designing point. When the vehicle drives over the detector wire loop, the detectors will be sensing the metal, and then the detector's state is activated. On the other hand, when the vehicle drives passed the detector wire loop, then the detector's state is deactivated.

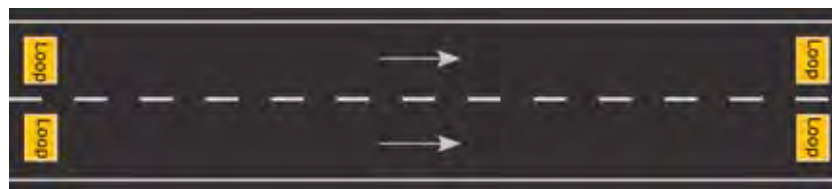


Figure 1.5: Example of loop detector installation on a road.

Traffic sensor that using in Bangkok's roadway is the loop detector which used to count the vehicles while passed the sensor. Figure 1.5 shows the example of a loop detector installation on Bangkok's roadway that each lane has the sensors at two points on the road, start and end of the road. Then, we can count the number of vehicles on the road by using conversation law.

### 1.2.4 Optimization

In the mathematical problem, an optimization method is a useful tool for finding the optimal solution which given the maximum reward or minimum penalty. In general, the reward and penalty are defined as the cost objective. The cost function of an optimization problem can be represented as follows:

- Given: a function  $f : \mathbb{R}^n \rightarrow \mathbb{R}$  from some set to the real numbers
- Sought: an element  $x^* \in \mathbb{R}^n$  such that  $f(x^*) \leq f(x)$  for all  $x \in \mathbb{R}^n$  ("minimization") or such that  $f(x^*) \geq f(x)$  for all  $x \in \mathbb{R}^n$  ("maximization")

A usual method used to find the maximum or minimum point in the cost objective function is the gradient descent method which is a first-order iterative optimization algorithm and also known as steepest descent that was invented by Cauchy in the 19th century [22].

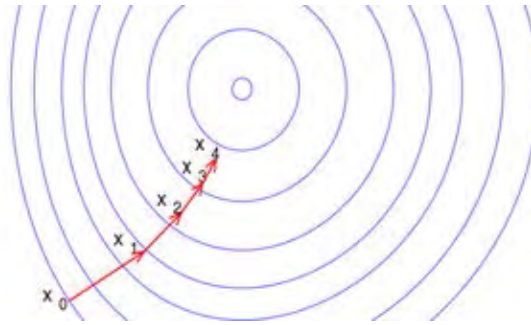


Figure 1.6: Illustration of gradient descent on a series of level sets.

Gradient descent is the method which finding the search direction for a multi-variable function  $f(x_k)$  and updating the parameter  $x_k$  for every iteration  $k$ . Figure 1.6. illustrates the searching of the solution  $x_k$ , the method will be stop when the solution meet the criteria such that  $\|x_k - x_{k-1}\|^2 \leq \varepsilon$ , where  $\varepsilon$  is a small constant value. To find the optimal solution, the search direction is determined from the derivative of function  $f(x_k)$ , and it called the gradient. The function  $f(x_k)$  is need to differentiable and the derivative  $\nabla f(x_k)$  is Lipschitz. Then, the update formula is described as follows:

$$x_{k+1} = x_k - \gamma_k \nabla f(x_k) \quad (1.15)$$

The step size  $\gamma_k$  is allowed to change at every iteration which satisfies the Wolfe conditions or the Barzilai-Borwein [23] method shown as following:

$$\gamma_k = \frac{(x_k - x_{k-1})^T [\nabla f(x_k) - \nabla f(x_{k-1})]}{\|\nabla f(x_k) - \nabla f(x_{k-1})\|^2} \quad (1.16)$$

However, this part is explained only a basic of unconstrained optimization using gradient descent method.

### 1.2.5 Model predictive control

Model predictive control (MPC) is the most popular control method that is based on iterative, finite-horizon optimization of a plant model while satisfying a set of constraints. It has been used in chemical plants, power system balancing models [25], and power electronics [26].

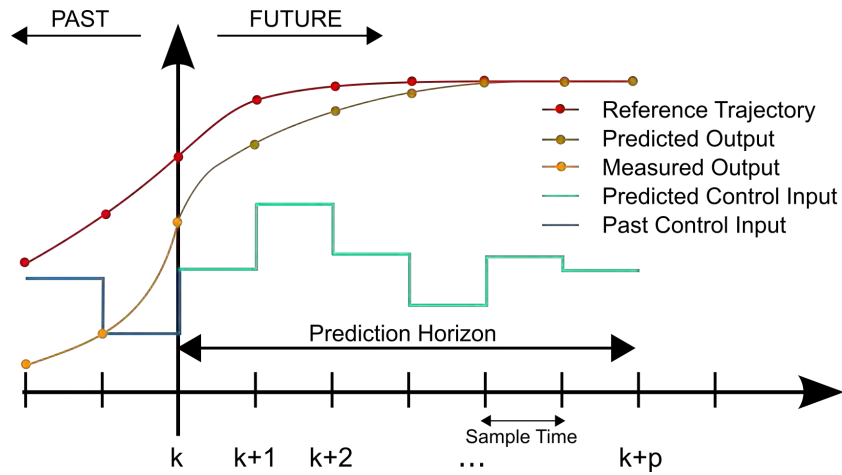


Figure 1.7: A discrete MPC scheme.

[source: [https://en.wikipedia.org/wiki/Model\\_predictive\\_control](https://en.wikipedia.org/wiki/Model_predictive_control)]

The key idea of MPC that illustrated in Figure 1.7 is the fact that it achieves the goal by finding the optimal control input and predicting the trajectory on finite time-horizon, only the first timeslot of control input is implemented. C.E. Garcia et al., [27] has stated that the idea of MPC can adapt to a non-particular system description. It can implement with state space, transfer matrix, and convolution type models. Model predictive control can be demonstrated by using a quadratic objective. This manipulated variables are selected to minimize the given objective function which can be written as follows:

$$\underset{\Delta u(k), \dots, \Delta u(k+m-1)}{\text{minimize}} \sum_{l=1}^p \|\hat{y}(k+l|k) - r(k+l)\|_{\Gamma_l}^2 + \|\Delta u(k+l-1)\|_{B_l}^2 \quad (1.17)$$

where

$\hat{y}(k+l|k)$  is the predicted value of  $y$  at time  $k+l$  based on information available at time  $k$ ,

$$\Delta u(k+l) = u(k+l) - u(k+l-1),$$

$p, m$  are the horizon length and the number of manipulated variable moves in the future, respectively,

$$\|x\|_Q^2 = x^T Q x,$$

$\Gamma_l, B_l$  are the weighting matrices.

The optimization is also available to add up the constraints to keep the process operating safely or shut the process down in a smooth manner. MPC is not limited to the kind of system, objective function, or optimization constraints depend on the application to select the proper technique.

### 1.2.6 Arrival and departure flow predictions

Traffic information is used to predict the traffic state in advance. Arrival rate and departure flow rate (veh/sec) are the information that shows the traffic quantity coming and traffic quantity departing. This paper uses machine learning to predict the traffic flow rate by using historical information.

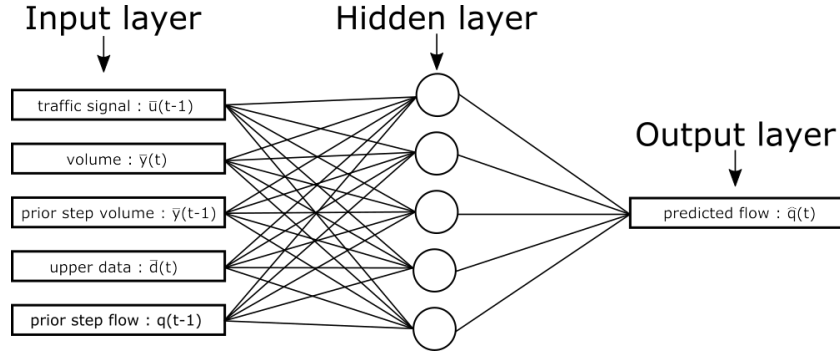


Figure 1.8: Traffic flow prediction model.

Figure 1.8 shown the prediction model using artificial neural network. The model structure is consists of 3 layers which are the input layer, hidden layer, and output layer. Normalized prior step traffic signal  $\bar{u}_{J_i}(t_{JC_i} - 1) = u_{J_i}(t_{JC_i})/\tau_i(t_{JC_i})$ , normalized volume  $\bar{y}_{J_i}(t_{JC_i}) = y_{J_i}(t_{JC_i})/\alpha$  and  $\bar{y}_{J_i}(t_{JC_i} - 1) = y_{J_i}(t_{JC_i} - 1)/\alpha$ , upper data from area layer  $\bar{d}(t_{JC_i}) = d_i(t_{JC_i})/\beta$ , and prior step flow rate  $q_i(t_{JC_i} - 1)$  are fed into the input layer, where  $\alpha$  and  $\beta$  is the constant value. The hidden layer is consists of multiple layers, each layer has connected with other layers by multiplying the weighting with input and taking the nonlinear function as the output. The output layer in this paper gives the prediction flow rate  $\hat{q}_i(t_{JC_i})$  which can be written as

$$\hat{q}_i(t_{JC_i}) = f(\bar{u}_{J_i}(t_{JC_i} - 1), \bar{y}_{J_i}(t_{JC_i}), \bar{y}_{J_i}(t_{JC_i} - 1), \bar{d}(t_{JC_i}), q_i(t_{JC_i} - 1)) \quad (1.18)$$

where  $f(\cdot)$  is represented the artificial neural network model.

### 1.3 Signalized intersection control techniques

The signalized intersection control method can be classified into four standard methods which are fixed time control, optimal control methods, optimization methods, and machine learning methods. The optimal control methods are the methods that used a control law for a given system such that a specific optimality criterion is achieved. Optimization methods are the methods that used the mathematics equations to explain the relation between cost or performance index and control input. Machine learning methods are methods that used historical data to find an unknown model. These signalized intersection control techniques categorized as shown in Figure 1.9 and the details of each method are described as follows.

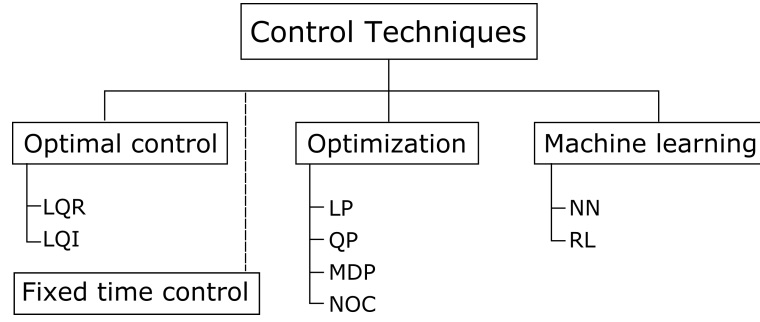


Figure 1.9: Signalized intersection control techniques.

### Fixed time control

The schedules of traffic signal in fixed time control will not change over time. The simplified way to determine the traffic signal for fixed time control is calculated from the proportional of traffic volume which is given by

$$u_{ij} = \begin{cases} \frac{V_{ij}}{\|V_i\|_1} \left( \tau_i^{(i)} - \tau_{\text{fix},ij} \cdot \dim(\rho_{\text{fix},i}^{(i)}) \right), & j \notin \rho_{\text{fix},i}^{(i)} \\ \tau_{\text{fix},ij}, & j \in \rho_{\text{fix},i}^{(i)} \end{cases} \quad (1.19)$$

where  $u_i = [u_{i1}, u_{i2}, \dots, u_{iN_{\rho^i}}]^T$  is the control signal vector which represent the duration time in seconds of each phase,  $\tau_{\text{fix},ij}$  is the duration of yellow time in seconds,  $\rho_{\text{fix},i}^{(i)}$  is the index set of yellow phase,  $i$  is the index of intersection,  $j$  is the index of phase, and  $V_{ij} \in [V_i]_{N_{\rho^i}} \{\mathbb{R}\}$  is the traffic volume (veh) corresponding to  $j$ th phase.

### Optimal control approaches

This approach is used the control law for a given system that explains the relations of traffic flow dynamics and traffic signals. The common approaches are Linear quadratic regulator control (LQR) and Linear quadratic integral control (LQI). These approaches are described as follows.

### Linear quadratic regulator control

Linear quadratic regulator control is used to find the optimal traffic control signal. This control technique is widely used in several control applications used state feedback control law. In the traffic signal control applications [2, 13] that deal with the discrete-time system, the control objective is used to minimize the vehicle queue-length on an intersection and finds the green periods of each phase. The general equation of control objective of LQR control is given as:

$$J(k) = \frac{1}{2} x^T(k) Q x(k) + \frac{1}{2} u^T(k) R u(k) \quad (1.20)$$

where  $x(k)$  is the state vector that represents the vehicle queue-length in each road at time index  $k$ ,  $u(k)$  is the control input that represents the green time periods of each phase at time index  $k$ ,  $Q$  is the weighting matrix of quadratic form on state vector, and  $R$  is the weighting matrix of quadratic form on control input vector.

### Linear quadratic integral control

Linear quadratic integral control is used to find the optimal traffic control signal which based on the predictive horizon. The predictive horizon is used to reduce the steady-state error for the desired reference by adding the integral of the error to state feedback control. The essential elements of the LQI control loop shown in Figure 1.10.

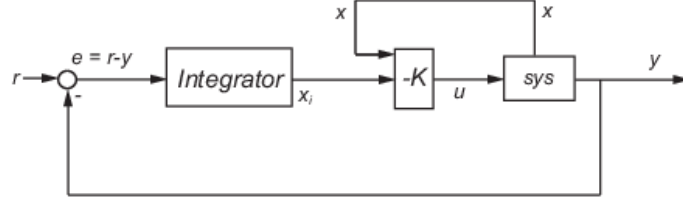


Figure 1.10: Scheme of LQI control system.

In the traffic signal control applications that proposed in [7], number of vehicles standing in a certain branch of the intersection is predicted on finite-horizon time, then the optimal control input such that green time periods of each phase are obtained in order to minimize the cost objective of LQI control that given as:

$$J(k) = \frac{1}{2} \sum_{i=1}^T \{x_i^T(k)Qx_i(k) + u_i^T(k)Ru_i(k)\} \quad (1.21)$$

where  $T$  is the length of the predictive horizon, and  $i$  is the time horizon index.

### Optimization approaches

This approach is used mathematics equations to explain the relation between traffic signal scheduling and cost such that vehicle queue-length, traffic density, and or traffic delay. The conventional approaches are Linear programming (LP), Quadratic programming (QP), Nonlinear optimal control (NOC), and Markov dynamic programming (MDP).

In several works of traffic signal control, the cost objective is usually used the linear form and quadratic form to minimize the total vehicle waiting at the intersections. Some works on signalized intersection control using linear programming are in [1, 6, 10, 11, 14]. Those works are dealing with a discrete-time system in which some works in [6, 10, 11, 14] are based on model predictive. However, some works in [3, 4, 9, 11] are using quadratic programming in the same goal to minimize the total vehicle queue-length. A work that was dealing with a nonlinear form of cost objective or using nonlinear optimal control is [11]. The difference from other works using LP and QP is more accurately on the traffic flow model that using the piecewise function to explain the dynamics. A work that was using Markov dynamic programming is [12]. Their work deals with a stochastic process and based on a discrete-time model. The goal of MDP is to choose a policy that will maximize some cumulative function of the random rewards or minimize some cumulative function of the random penalties infinite time horizon.

## Machine learning approaches

This approach uses historical data such that traffic flow and traffic queue-length to find an unknown model by using a training algorithm which given the optimal traffic signal scheduling. The conventional approaches are the Neural network (NN) and Reinforcement Learning (RL). These approaches are described as follows.

### Neural network

Artificial neural networks (ANN) are the simplest model of neural network (NN) that uses the historical data for learning the model by using an optimization algorithm to adjust the weights and biases of the model. ANN usually consists of an input layer, hidden layer, and output layer as illustrated in Figure 1.11. The input values from the input layer are fed into the hidden and output layer through the multiplication of weights and the addition of biases. The complexity of the model depends on the number of hidden layer and number of node in each layer, and the nonlinearity of the model depends on the type of activation function that selected in each layer.

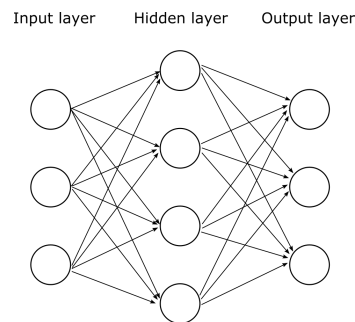


Figure 1.11: ANN flow chart.

A work on signalized intersection control using the Neural network is in [15]. They transformed the traffic measurements such that traffic flow rate and traffic density into the input vector of three traffic levels as high, medium, and low. Output vector that represents the optimal traffic signal plans which are obtained from the learning process through the back-propagation algorithm.

### Reinforcement learning

Reinforcement learning is an artificial intelligence approach to Machine learning. The critical idea of reinforcement learning is a machine learns to take actions in an environment to maximize cumulative reward or minimize the cumulative penalty. The basic flow chart of reinforcement learning is shown in Figure 1.12.

In the traffic signal control application, the elements in Figure 1.12 such that agent is defined as a traffic signal controller, where the environment is the traffic situation.

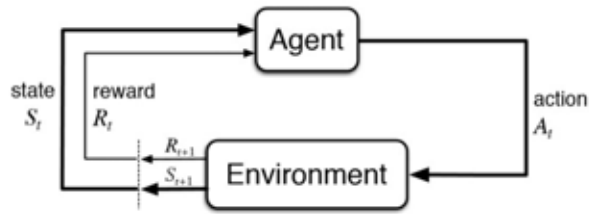


Figure 1.12: Reinforcement learning flow chart.

The action signals  $A_i$  that generated from the agent represents the traffic signal which is implemented to the real traffic systems, where the state  $S_i$  is the traffic measurements contained the vehicle queue lengths, and reward  $R_i$  that actually a penalty, in this case, is the traffic delay measurements received from taken an action such that signal plans, which is aimed to minimize. Some works on signalized intersection control using reinforcement learning are in [16–18].

Table 1.1: Summary signalized intersection control approaches.

| Reference | Tool/<br>Controller | Input parameters              | Objective                                 | MP  | MI  |
|-----------|---------------------|-------------------------------|---|-----|-----|
| [1]       | LP                  | I/O flow rates                | Minimize Queue lengths                    | No  | No  |
| [2]       | LQR                 | Queue lengths, I/O flow rates | Minimize Queue lengths                    | No  | No  |
| [3]       | QP                  | Queue lengths, I/O flow rates | Minimize Queue lengths                    | No  | Yes |
| [4]       | QP                  | I/O flow rates                | Minimize Queue lengths                    | Yes | Yes |
| [6]       | LP                  | Queue lengths, I/O flow rates | Minimize Queue lengths<br>& Maximize Flow | Yes | Yes |
| [7]       | LQI                 | Queue lengths, I/O flow rates | Minimize Queue lengths                    | Yes | No  |
| [9]       | QP                  | Queue lengths, I/O flow rates | Minimize Queue lengths                    | Yes | Yes |
| [10]      | LP                  | Queue lengths, I/O flow rates | Minimize travel time                      | Yes | Yes |
| [11]      | LP, QP,<br>NOC      | Queue lengths, I/O flow rates | Minimize Queue lengths                    | Yes | No  |
| [12]      | MDP                 | Queue lengths, I/O flow rates | Minimize Queue lengths                    | Yes | No  |
| [13]      | LQR                 | Queue lengths, I/O flow rates | Minimize Queue lengths                    | Yes | Yes |
| [14]      | LP                  | Queue lengths, I/O flow rates | Minimize waiting times                    | Yes | Yes |
| [15]      | NN                  | Queue lengths, I/O flow rates | Minimize delay                            | No  | Yes |
| [16]      | RL                  | Queue lengths, I/O flow rates | Minimize delay                            | No  | Yes |
| [17]      | RL                  | Queue lengths, I/O flow rates | Minimize delay                            | No  | Yes |
| [18]      | RL                  | Queue lengths, I/O flow rates | Minimize delay                            | No  | Yes |

MP - Model predictive, MI - Multiple intersections

The approaches for signalized intersection control are summarized in Table 3.1 which illustrated the control types, input parameters, control objective, based or non-based on model predictions (MP), and multiple or isolated intersection control.

#### **1.4 Objective**

1. To develop a traffic flow model with a linear time-invariant system.
2. To apply the hierarchical distributed structure and model predictive control to deal with traffic network.

#### **1.5 Scope of work**

1. This research considers the linear time-invariant system.
2. The application in this research is for traffic signal control.
3. The traffic demand and splitting flow rate in the model are assumed to be constant.
4. This research assumed the traffic network has no alleyway.
5. The numerical results are simulated by the SUMO traffic simulator.

#### **1.6 Research methodology**

1. Review the background of the traffic flow model and previous works of traffic signal control.
2. Design the HDMPC for traffic network layer, traffic area layer and signalized intersection layer.
3. Develop the computer program and analyze the numerical results.
4. Simulate and compare the results of HDMPC with fixed time control.
5. Write the thesis and conclude the simulation results.

#### **1.7 Expected outcome**

1. The hierarchical model and controller of a traffic network and signalized intersection for designing the traffic signal controller.
2. Computer codes of the traffic network controller.

# **CHAPTER II**

## **HIERARCHICAL DISTRIBUTED CONTROL OF TRAFFIC NETWORK**

This section describes the framework of this work, the characteristic of traffic network, and signalized intersection model. The hierarchical traffic model consists of three layers which are network layer, area layer, and intersection layer as shown in Figure 2.1. Furthermore, the detail of each model are described as follows.

### **2.1 Problem statement**

Two reasons caused the traffic congestion problem that occurred in Bangkok city. Firstly, the increased vehicles on the road network, which is a problem that cannot be solved in a control problem. Secondly, the reason is the improper traffic control system in Bangkok's traffic. The widely used traffic control systems in Bangkok city are the fixed time control and controller based on vehicle queue length measurement. Only vehicle queue length information in an individual intersection cannot treat the traffic congestion problem in the traffic network because of the traffic congestion was the problem on the overview of a network system. The limitation of the practice is the loop detector sensor. There is uncertainty in the measurement of vehicles counting on a road. However, the assumptions in these models are the vehicles in a road have no exit or enter the road between the loop detector sensor, and the traffic demand on the network is known.

### **2.2 Framework**

The goal of this work is to establish a traffic control method using the HDC framework. In this work, we consider the traffic problem by separating the model into three layers, namely, network layer, area layer, and intersection layer, as illustrated in Figure 2.1. The purpose of the network layer is used to estimate the traffic demand movement through the areas by grouping the intersections in the same area. Due to some intersection in the traffic network that is not controllable and not observable, it will be considered for writing in the graph on the network layer, and it will be eliminated into links. The purpose of the area layer is used to find the optimal traffic flow through the roads by using the information from the network layer. Moreover, the intersection layer is used to schedule the traffic signal plans by using the information from the area layer. We can assume that the network layer, area layer is the global layer, and the intersection layer is the local layer. The key idea of the global control is to improve the control performance of the local controller which associates exchanging information through the higher layer.

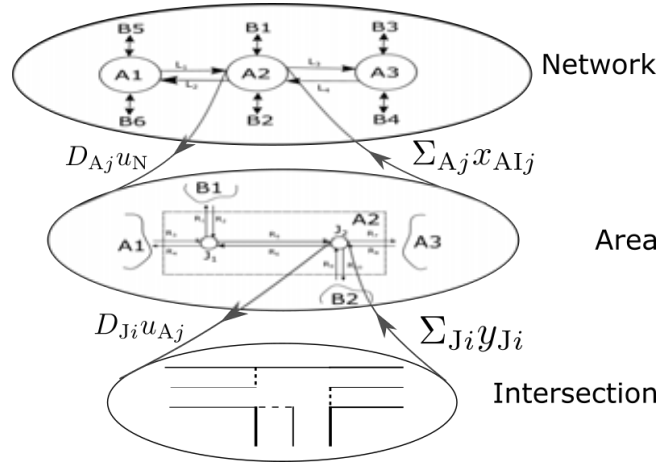


Figure 2.1: Hierarchical structure of traffic network.

where

- $x_{AI,j}$  is the traffic volume (veh) on each intersection in the  $j$ th area,
- $u_N$  is the optimal traffic flow (veh/h) between areas,
- $y_{Ji}$  is the traffic volume (veh) on each road in the  $i$ th intersection,
- $u_{Aj}$  is the optimal traffic flow (veh/h) for each road in  $j$ th area,
- $D_{Ji}$  and  $D_{Aj}$  are the distribution matrices of  $i$ th intersection and  $j$ th area respectively.
- $\Sigma_{Ji}$  and  $\Sigma_{Aj}$  are the aggregation matrices of  $i$ th intersection and  $j$ th area respectively.

Those three layers have different sampling periods in which the higher layer will be more extended sampling period than the lower layer because of traffic demand in the overview has slowly changed than the smaller layer. It can be explained as

$$T_s \leq T_A \leq T_N$$

where  $T_s$ ,  $T_A$ , and  $T_N$  are the sampling period in seconds of intersection, area, and network layer respectively. Mathematical techniques initialize the traffic models of each layer that will be illustrated as follows. However, it should be calibrated by using real measurement via the subspace identification technique [24].

## 2.3 Traffic models

### 2.3.1 Signalized intersection model

On the intersection layer, the used time indices in this layer had two kind,  $t_{JCi}$  is the time index for cycle time, and  $t_{JPi}$  is the time index for phase time. Those indices are illustrated with the example case in Figure 2.5. Furthermore, the macroscopic flow model of vehicles in a single road and a single signalized intersection are explained as follows.

### Single road

A single road model for explaining the traffic dynamic is described as follows. The  $r$ th road is comprised of  $N_{\text{dir},r}$  directions on an interconnection as shown in Figure 2.2. Thus, the state variable of  $r$ th road which represents the number of waiting vehicles in each direction is given as  $x_r(t_{\text{JC}i}) = [x_{r1}(t_{\text{JC}i}), x_{r2}(t_{\text{JC}i}), \dots, x_{rN_{\text{dir},r}}(t_{\text{JC}i})]^T$ .

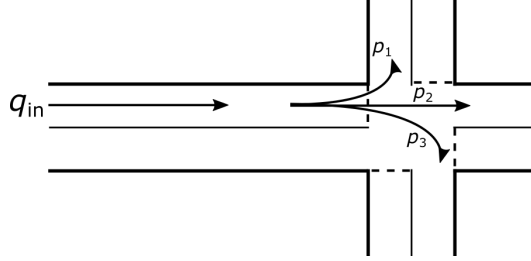


Figure 2.2: Example of a single road.

The dynamic of  $r$ th road can be expressed by using the discrete time-invariant state space models. This model describes the conservation of traffic flow, it can be written as follows:

$$x_r(t_{\text{JC}i} + 1) = x_r(t_{\text{JC}i}) + w_{\text{in},r}(t_{\text{JC}i}) - w_{\text{out},r}(t_{\text{JC}i}) \quad (2.1)$$

$$y_r(t_{\text{JC}i}) = C_r x_r(t_{\text{JC}i}) \quad (2.2)$$

where  $i$  is the index number of the intersection which  $r$ th road has been connected,  $y_r(t_{\text{JC}i}) \in \mathbb{R}^1$  is the output which represents the total of vehicle waiting in the  $r$ th road,  $\tau_i$  is the cycle length of traffic signal, and  $w_{\text{out},r}(t_{\text{JC}i}) \in \mathbb{R}^{N_{\text{dir},r}}$  is the number of departure vehicles which is estimated from (2.6).

Denote  $w_{\text{in},r}(t_{\text{JC}i}) \in \mathbb{R}^{N_{\text{dir},r}}$  the predicted of traffic input vector (veh) on each direction which is defined as

$$w_{\text{in},r}(t_{\text{JC}i}) = p_r q_{\text{in},r}(t_{\text{JC}i}) \tau_i. \quad (2.3)$$

The traffic input on the  $r$ th road which defined as  $q_{\text{in},r}(t_{\text{JC}i}) \in \mathbb{R}$ , it represents the arrival rate (veh/s). However, this work needs to estimate the number of vehicles waiting in each direction. It is estimated by multiplying with the splitting probability vector  $p_r \in \mathbb{R}^{N_{\text{dir},r}}$ , where  $p_r = [p_{r1}, p_{r2}, \dots, p_{rN_d}]^T$ . The output matrix  $C_r \in \mathbb{R}^{1 \times N_{\text{dir},r}}$  of the  $r$ th road is defined as

$$C_r = \mathbb{1}_{N_{\text{dir},r}}, \quad (2.4)$$

where  $\mathbb{1}_n$  is the either one row vector  $n$ -dimensional.

### Splitting flow estimator

The number of vehicles passed on each direction ( $w_{\text{out},r}$ ) in an intersection are challenging to determine when the information from the traffic sensor has low resolution. However, we can estimate the departed vehicles in each direction (veh) by using the total departed and arrived vehicle information in each road. The procedure to estimate is consists of one step which is the determining of

traffic movements in each direction at  $\rho$ th phase, where  $\rho = ph_i(t_{JP_i})$ , and  $ph_i(t_{JP_i})$  is a function for getting the phase index at time index  $t_{JP_i}$ .

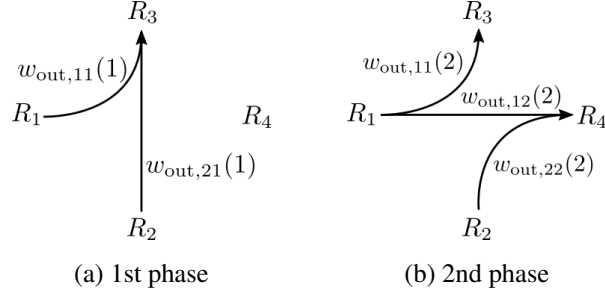


Figure 2.3: Example of flow pattern on an intersection.

Figure 2.3 illustrates the signal pattern on an intersection of an example case to demonstrate the estimating of splitting ratio and traffic movements of each direction at time  $t_{JP_i}$ . This example shows the incoming roads which are  $R_1$  and  $R_2$ , and outcome roads which are  $R_3$  and  $R_4$ . Incoming road  $r$  has total departed vehicles  $w_{out,r}(t_{JP_i})$  at time  $t_{JP_i}$ . Outcome road  $r$  has total arrived vehicles  $w_{in,r}(t_{JP_i})$  at time  $t_{JP_i}$ , the total arrived equal the total departed vehicles of other roads that associated on the same direction.

The example that showed in Figure 2.3 can be written in the linear relation which is given as follows:

$$\begin{bmatrix} w_{out,3}(1) \\ w_{out,4}(1) \end{bmatrix} = \begin{bmatrix} 1 & 0 & 1 & 0 \end{bmatrix} \begin{bmatrix} w_{in,11}(1) \\ w_{in,12}(1) \\ w_{in,21}(1) \\ w_{in,22}(1) \end{bmatrix} \quad \text{and} \quad \begin{bmatrix} w_{out,3}(2) \\ w_{out,4}(2) \end{bmatrix} = \begin{bmatrix} 1 & 0 & 0 & 0 \\ 0 & 1 & 0 & 1 \end{bmatrix} \begin{bmatrix} w_{in,11}(2) \\ w_{in,12}(2) \\ w_{in,21}(2) \\ w_{in,22}(2) \end{bmatrix}.$$

We can rewrite the above relations to

$$w_{in}(t_{JP_i}) = A_\rho w_{out}(t_{JP_i}) \quad \text{for } \rho = ph_i(t_{JP_i}). \quad (2.5)$$

Then, we define the constrained least squares problem to determine the number of departed vehicles in each direction  $w_{out}(t_{JP_i})$ , it given by

$$\underset{w_{out}(t_{JP_i})}{\text{minimize}} \|w_{in}(t_{JP_i}) - A_\rho w_{out}(t_{JP_i})\|^2 \quad (2.6)$$

subject to:

$$\sum_{j=1}^{N_{dir,r}} w_{out,rj}(t_{JP_i}) = \Sigma w_{in,r}(t_{JP_i}), \quad \text{for all } r, \quad (2.7)$$

where  $w_{out,r}(t_{JP_i}) = [w_{out,r1}(t_{JP_i}), w_{out,r2}(t_{JP_i}), \dots, w_{out,rN_{dir,r}}(t_{JP_i})]^T$  is the number of departed vehicles vector, and  $\Sigma w_{out,r}$  is the total of vehicles passed on  $r$ th road. Constraints (2.7) is used to balance the quality of arrived and departed vehicles on the  $r$ th road. So that, the splitting flow

probability can be estimated by counting the total departed vehicles on each direction and normalizing with  $\|\Sigma w_{\text{out},r}\|_1$ , where  $N$  is the horizon length. Then, the splitting flow probability  $p_r$  of  $r$ th road is given by

$$p_r = \frac{\Sigma w_{\text{out},r}}{\|\Sigma w_{\text{out},r}\|_1}. \quad (2.8)$$

We suggest to use the iterative optimization for determining the departed vehicles  $w_{\text{out}}(t_{\text{JP}i})$ .

### State estimator

Vehicles queue length in each direction that described on model (2.1) is non-measurable in practice. However, if we know the splitting flow probability, we can approximate the vehicles queue length in each direction by solving the optimization problem which is given as follows:

$$\underset{\hat{x}_r(t_{\text{JP}i})}{\text{minimize}} \|\hat{x}_r(t_{\text{JP}i}) - \hat{x}_r(t_{\text{JP}i} - 1) - w_{\text{in},r}(t_{\text{JP}i} - 1) + w_{\text{out},r}(t_{\text{JP}i} - 1)\|^2 \quad (2.9)$$

subject to:

$$\begin{aligned} \hat{x}_r(t_{\text{JP}i}) &\geq 0, \\ C_r \hat{x}_r(t_{\text{JP}i}) &= y_r(t_{\text{JP}i}), \end{aligned}$$

where  $y_r(t_{\text{JP}i})$  is the total number of vehicles in  $r$ th road which obtained from the measurement,  $\hat{x}_r(t_{\text{JP}i})$  represents the estimated vehicles queueing in each direction at time index  $t_{\text{JP}i}$ ,  $w_{\text{in},r}(t_{\text{JP}i})$  and  $w_{\text{out},r}(t_{\text{JP}i})$  are the total arrival and departed on  $r$ th road over time index  $[t_{\text{JP}i} - 1, t_{\text{JP}i}]$ .

### Signalized intersection model

The signalized intersection is illustrated the example signal pattern as Figure 2.4 and 2.5, the number of signal patterns (phases) is defined as  $N_{\rho i}$ .

The input signal  $u_{\text{J}i}(t_{\text{J}Ci}) = [u_{\text{J}i1}(t_{\text{J}Ci}), u_{\text{J}i2}(t_{\text{J}Ci}), \dots, u_{\text{J}iN_{\rho i}}(t_{\text{J}Ci})]^T$  is represented the traffic green time (sec) with time cycle is

$$\tau_i = \sum_{k=1}^{N_{\rho i}} u_{\text{J}ik}(t_{\text{J}Ci}), \quad \text{for } t_{\text{J}Ci} = 1, 2, \dots, T, \quad (2.10)$$

where  $T$  is the number of time control.

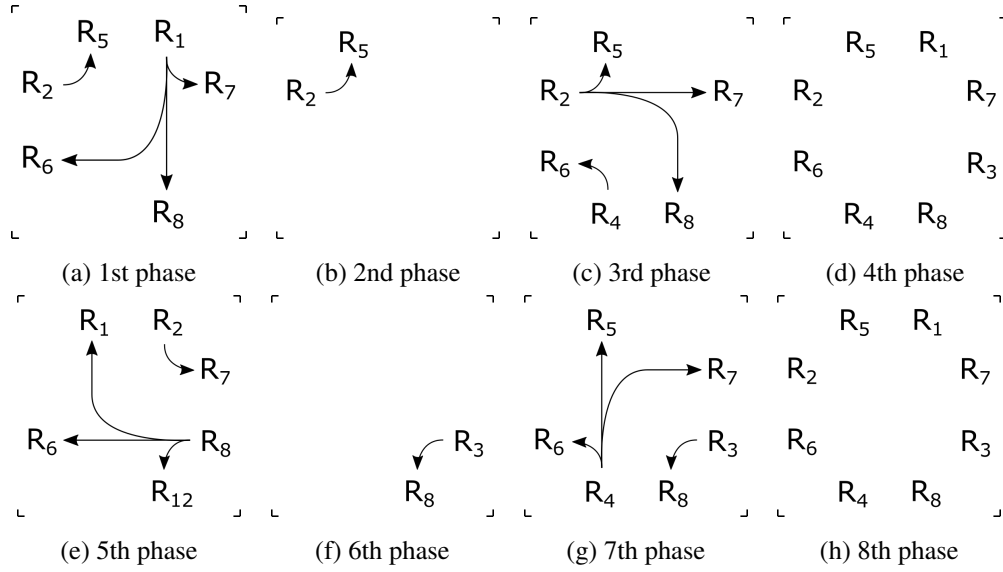


Figure 2.4: Example of signal pattern on an intersection.

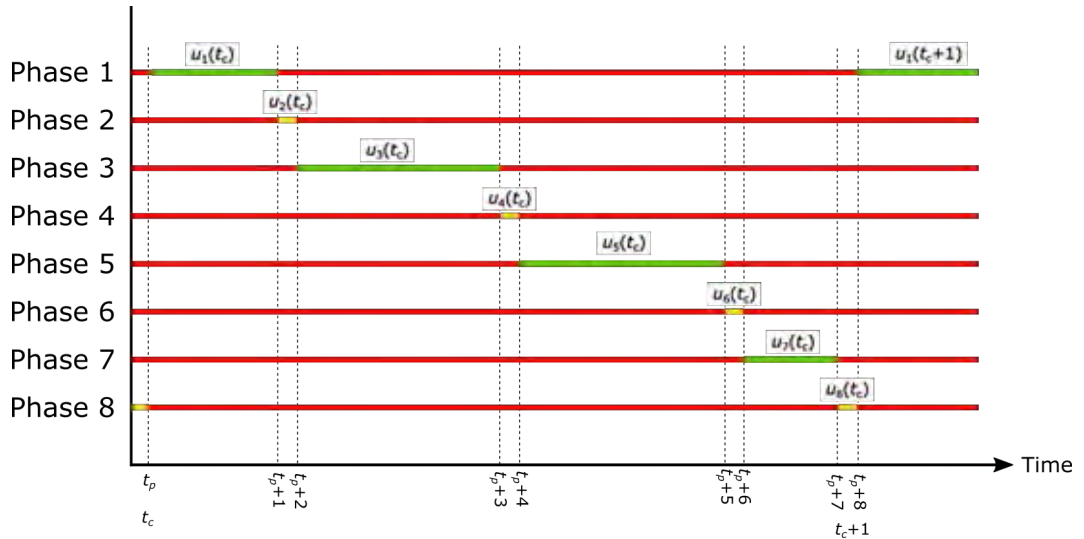


Figure 2.5: Example of phase time diagram on traffic signal.

The connected roads on the intersection are divided into incoming direction set  $R_{in}$  and outgoing direction set  $R_{out}$ . From the example intersection as Figure 2.4, we can define the incoming and outgoing direction set as follow:

$$R_{in} = \{R_1, R_2, R_3, R_4\},$$

$$R_{out} = \{R_5, R_6, R_7, R_8\}.$$

The traffic signal on an intersection is consists of  $N_{\rho_i}$  patterns. To examples, the intersection as Figure 2.4 is consist of 8 phases, then the available lanes set  $\mathcal{A}_k$  can be written as follows:

$$\mathcal{A}_1 = \{(R_1, 1), (R_1, 2), (R_1, 3), (R_2, 1)\} \quad \mathcal{A}_5 = \{(R_3, 1), (R_3, 2), (R_3, 3), (R_1, 1)\}$$

$$\mathcal{A}_2 = \{(R_2, 1)\}$$

$$\mathcal{A}_6 = \{(R_3, 1)\}$$

$$\begin{aligned}\mathcal{A}_3 &= \{(R_2, 1), (R_2, 2), (R_2, 3), (R_4, 1)\} & \mathcal{A}_7 &= \{(R_4, 1), (R_4, 2), (R_4, 3), (R_3, 1)\} \\ \mathcal{A}_4 &= \{\phi\} & \mathcal{A}_8 &= \{\phi\}\end{aligned}$$

where pair  $(R_i, j) \in \mathcal{A}_k$  is the set of road index  $R_i$  and direction index  $j$  of road  $R_i$ . The available source set  $\mathcal{S}_i$  of road  $R_i$  is represent the road and direction index of road that connected to road  $R_i$  through the traffic signals. The available source set  $\mathcal{S}_i$  of road  $R_i$  can be written from the example intersection as Figure 2.4 as

$$\begin{aligned}\mathcal{S}_1 &= \{\phi\} & \mathcal{S}_5 &= \{(R_2, 1), (R_3, 3), (R_4, 2)\} \\ \mathcal{S}_2 &= \{\phi\} & \mathcal{S}_6 &= \{(R_1, 1), (R_3, 2), (R_4, 1)\} \\ \mathcal{S}_3 &= \{\phi\} & \mathcal{S}_7 &= \{(R_1, 1), (R_2, 2), (R_4, 3)\} \\ \mathcal{S}_4 &= \{\phi\} & \mathcal{S}_8 &= \{(R_1, 2), (R_2, 3), (R_3, 1)\}\end{aligned}$$

where pair  $(R_j, k) \in \mathcal{S}_i$  is the set of road index  $R_j$  and direction index  $k$  of road  $R_j$ . According to the assumption that the saturation flow or out-flow rate is the maximum flow  $q_{\max}$ , we write the control matrix  $B_r$  for  $r$ th road as incoming direction ( $r \in R_{\text{in}}$ ), as follows:

$$w_{\text{out},r} \triangleq (B_r)_{(j,k)} = \begin{cases} -p_{rj}q_{\max}, & (R_i, j) \in \mathcal{A}_k \\ 0, & \text{Otherwise} \end{cases}$$

where  $B_r \in \mathbb{R}^{N_{\text{dir},r} \times N_{\rho i}}$ , and the control matrix for  $r$ th road as outgoing direction ( $r \in R_{\text{out}}$ ), as follows:

$$w_{\text{in},r} \triangleq (B_r)_{(k)} = \sum_{(R_s, j) \in (\mathcal{S}_r \cap \mathcal{A}_k)} p_{sj}q_{\max}.$$

where  $B_r \in \mathbb{R}^{1 \times N_{\rho i}}$ . The single road model can be extended to the intersection model by aggregating the vectors and matrices of each single road model, it can be written as follows:

$$\begin{aligned}x_{J_i}(t_{J_{C_i}} + 1) &= x_{J_i}(t_{J_{C_i}}) + B_{J_i}u_i(t_{J_{C_i}}) + w_{J_i}(t_{J_{C_i}}) \\ y_{J_i}(t_{J_{C_i}}) &= C_{J_i}x_{J_i}(t_{J_{C_i}})\end{aligned} \tag{2.11}$$

where

$$x_{J_i}(t_{J_{C_i}}) = \begin{bmatrix} x_1(t_{J_{C_i}}) \\ x_2(t_{J_{C_i}}) \\ \vdots \\ x_{N_{\text{rd}}}(t_{J_{C_i}}) \end{bmatrix}, w_{J_i}(t_{J_{C_i}}) = \begin{bmatrix} w_1(t_{J_{C_i}}) \\ w_2(t_{J_{C_i}}) \\ \vdots \\ w_{N_{\text{rd}}}(t_{J_{C_i}}) \end{bmatrix}, B_{J_i} = \begin{bmatrix} B_1 \\ B_2 \\ \vdots \\ B_{N_{\text{rd}}} \end{bmatrix}, C_{J_i} = \begin{bmatrix} C_1 & 0 & \cdots & 0 \\ 0 & C_2 & \cdots & 0 \\ \vdots & \vdots & \ddots & \vdots \\ 0 & 0 & \cdots & C_{N_{\text{rd}}} \end{bmatrix}.$$

The traffic input/output ( $w_r(t_{J_{C_i}})$ ) of  $r$ th road is defined depend on road direction. If  $r$ th road is incoming direction ( $r \in R_{\text{in}}$ ), then,  $w_r(t_{J_{C_i}}) = w_{\text{in},r}(t_{J_{C_i}})$ . If  $r$ th road is outgoing direction ( $r \in R_{\text{out}}$ ), then,  $w_r(t_{J_{C_i}}) = -w_{\text{out},r}(t_{J_{C_i}})$ .

**Hierarchical distributed model predictive control of intersections:** This part is presented the hierarchical distributed traffic control based model predictive control (HDMPC) which works on cycle-by-cycle control. The HDMPC model is given as follows:

$$X_{J,CL,i}(t_{JCi} + 1) = X_{J,CL,i}(t_{JCi}) + H_{J,CL,i}U_{J,CL,i}(t_{JCi}) + W_{J,CL,i}(t_{JCi}) \quad (2.12)$$

where

$$X_{J,CL,i}(t_{JCi}) = \left[ \bar{x}_{J_i}^T(t_{JCi}) \quad \bar{x}_{J_i}^T(t_{JCi} + 1|t_{JCi}) \quad \cdots \quad \bar{x}_{J_i}^T(t_{JCi} + N_p - 1|t_{JCi}) \right]^T,$$

$$U_{J,CL,i}(t_{JCi}) = \left[ u_{J_i}^T(t_{JCi}) \quad u_{J_i}^T(t_{JCi} + 1) \quad \cdots \quad u_{J_i}^T(t_{JCi} + N_p - 1) \right]^T,$$

$$W_{J,CL,i}(t_{JCi}) = \begin{bmatrix} w_{J_i}(t_{JCi}) \\ \vdots \\ w_{J_i}(t_{JCi}) \end{bmatrix}, \quad H_{J,CL,i} = \begin{bmatrix} B_{J_i} & \cdots & 0 \\ \vdots & \ddots & \vdots \\ B_{J_i} & \cdots & B_{J_i} \end{bmatrix}.$$

The average number of vehicles  $\bar{x}_{J_i}(t_{JCi})$  is collected from loop detector sensors with sampling period  $T_s$  second, the equation is given as:

$$\bar{x}_{J_i}(t_{JCi}) = \frac{1}{N_\rho} \sum_{k=0}^{N_\rho} \hat{x}_{J_i}(t_{JCi} - k) \quad (2.13)$$

where  $\hat{x}_{J_i}(k)$  is the estimated state obtained from (2.9).

This objective is used to minimize the vehicle queue length and maintain the optimal traffic flow at reference point  $q_{J_i}^*(t_{JCi})$  from the area layer (2.41). The optimal traffic signal of  $i$ th intersection is obtained by solving the minimization problem with prediction horizon  $N_p$ .

$$\underset{u_{J_i}(0), \dots, u_{J_i}(T)}{\text{minimize}} \sum_{t_{JCi}=0}^T \sum_{k=t_{JCi}}^{N_p} \{ \|\bar{x}_{J_i}(k+1|k)\|^2 + \gamma \|q_{J_i}^*(k) - \hat{q}_i(k)\|^2 \} \quad (2.14)$$

subject to following constraints for  $t_{JCi} = 0, \dots, T$ :

$$\tau_{\min,ij} \leq [u_{J_i}(t_{JCi})]_{(j)} \leq \tau_{\max,ij} \quad \text{for } \forall j \notin \rho_{\text{fix},i} \quad (2.15)$$

$$[u_{J_i}(t_{JCi})]_{(j)} = \tau_{\text{fix},ij} \quad \text{for } \forall j \in \rho_{\text{fix},i} \quad (2.16)$$

$$\|u_{J_i}(t_{JCi})\|_1 = \tau_i \quad (2.17)$$

$$|\tau_i^{-1} C_{J_i} B_{J_i} u_{J_i}(t_{JCi})| = \hat{q}_i(t_{JCi}) \quad (2.18)$$

where  $\tau_{\text{fix},ij}$ ,  $\tau_{\min,ij}$ , and  $\tau_{\max,ij}$  are the duration of fixed time, minimum, and maximum duration of green time of  $j$ th phase respectively,  $\gamma > 0$  is the weighting parameter, and  $\rho_{\text{fix},i}$  is the index set of fixed phase.

Constraint (2.15) is used to bound the green time at minimum duration  $\tau_{\min,ij}$  sec, (2.16) is used to fix duration at  $\tau_{\text{fix},ij}$  sec, and (2.17) is used to fix the summation of traffic signal to be a cycle length  $\tau_i$  sec. This problem can be simplified to

$$\underset{u_{J_i(0), \dots, u_{J_i}(T)}}{\text{minimize}} \sum_{t_{J_i}=0}^T \left\{ \|X_{J,CL,i}(t_{J_i} + 1)\|^2 + \gamma \|q_{J_i}^*(t_{J_i}) - \hat{q}_i(t_{J_i})\|^2 \right\} \quad (2.19)$$

where  $\hat{q}_i(t_{J_i}) = |(N_p \tau_i(t_{J_i}))^{-1} Q_i U_i(t_{J_i})|$  is the predicted flow, and  $Q_i = \begin{bmatrix} C_{J_i} B_{J_i} & \dots & C_{J_i} B_{J_i} \end{bmatrix}$  is the estimator matrix.

**Phase-to-phase intersection model:** This part, the cycle-to-cycle state space model from (2.11) can be expressed to phase-to-phase state space model using structure based model predictive control which is defined as follows:

$$\begin{aligned} x_{J_i}(t_{J_i} + 1) &= x_{J_i}(t_{J_i}) + \tilde{B}_{J_i}(t_{J_i}) u(t_{J_i}) + w(t_{J_i}) \\ y_{J_i}(t_{J_i}) &= C_{J_i} x_{J_i}(t_{J_i}) \end{aligned} \quad (2.20)$$

where  $\tilde{B}_{J_i}(t_{J_i})$  is the reduced time variant control matrix which depends on current phase index  $ph_i(t_{J_i})$ , the matrix is given as:

$$\tilde{B}_{J_i}(t_{J_i}) = B_{J_i, \rho} \quad \text{for } \rho = ph_i(t_{J_i}) \quad (2.21)$$

where  $B_{J_i, \rho}$  is the  $\rho$ th column vector in matrix  $B_{J_i}$ , where  $B_{J_i} = \begin{bmatrix} B_{J_i,1} & B_{J_i,2} & \dots & B_{J_i, N_{\rho i}} \end{bmatrix}$ . Then, we can define the model predictive of a signalized intersection which is given as:

$$Y_{J,PH,i}(t_{J_i}) = G_{J,PH,i} x_{J_i}(t_{J_i}) + H_{J,PH,i}(t_{J_i}) U_{J,PH,i}(t_{J_i}) \quad (2.22)$$

where

$$Y_{J,PH,i}(t_{J_i}) = \begin{bmatrix} y_{J_i}(t_{J_i} + 1) \\ y_{J_i}(t_{J_i} + 2) \\ \vdots \\ y_{J_i}(t_{J_i} + N_{\rho i}) \end{bmatrix}, U_{J,PH,i}(t_{J_i}) = \begin{bmatrix} u_{J_i}(t_{J_i}) \\ u_{J_i}(t_{J_i} + 1) \\ \vdots \\ u_{J_i}(t_{J_i} + N_{\rho i} - 1) \end{bmatrix},$$

$$G_{J,PH,i} = \begin{bmatrix} C_{J_i} \\ C_{J_i} \\ \vdots \\ C_{J_i} \end{bmatrix}, H_{J,PH,i}(t_{J_i}) = \begin{bmatrix} C_{J_i} \tilde{B}(t_{J_i}) & 0 & \dots & 0 \\ C_{J_i} \tilde{B}(t_{J_i}) & C_{J_i} \tilde{B}(t_{J_i} + 1) & \dots & 0 \\ \vdots & \vdots & \ddots & \vdots \\ C_{J_i} \tilde{B}(t_{J_i}) & C_{J_i} \tilde{B}(t_{J_i} + 1) & \dots & C_{J_i} \tilde{B}(t_{J_i} + N_{\rho i}) \end{bmatrix}.$$

The optimal traffic signal of  $i$ th intersection is obtained by solving the minimization problem for every step  $t_{J_i}$ .

$$\underset{u_{J_i(0), \dots, u_{J_i}(T)}}{\text{minimize}} \sum_{t_{J_i}=0}^T \sum_{k=t_{J_i}}^{N_{\rho i}} \left\{ \|\bar{x}_{J_i}(k+1|k)\|^2 + \gamma \|q_{J_i}^*(t_{J_i}) - \hat{q}_i(t_{J_i})\|_2^2 \right\} \quad (2.23)$$

subject to following constraints for  $t_{JPi} = 0, \dots, T$ :

$$u_j(t_{JPi}) \geq \tau_{\min,ij} \quad \text{for } \forall j \notin \rho_{\text{fix},i} \quad (2.24)$$

$$u_j(t_{JPi}) = \tau_{\text{fix},ij} \quad \text{for } \forall j \in \rho_{\text{fix},i} \quad (2.25)$$

$$\sum_{j=1}^{N_{\rho i}} u_{Ji}(t_{JPi} + j) = \tau_i \quad (2.26)$$

where  $\tau_{\text{fix},ij}$  and  $\tau_{\min,ij}$  are the duration of fixed time and minimum duration of green time respectively,  $\gamma > 0$  is the weighting parameter, and  $\rho_{\text{fix},i}$  is the index set of yellow phase. The estimation of traffic flow  $\hat{q}_i(t_{JPi})$  in second term of (2.23) can be written as:

$$\hat{q}_i(t_{JPi}) = |\tau_i^{-1} C_{Ji} B_{Ji} u_{Ji}(t_{JCi})| \quad (2.27)$$

The average number of vehicles  $\bar{x}_{Ji}(t_{JCi})$  is collected from loop detector sensors with sampling period  $T_s$  second, the equation is given as:

$$\bar{x}_{Ji}(t_{JCi}) = \frac{1}{n} \cdot P_{Ji} \sum_{k \in \varphi(t_{JCi})} y_{Ji}(k) \quad (2.28)$$

where  $P_{Ji} = \text{diag}(p_1, p_2, \dots, p_{N_{\text{rd}}})$ ,  $\varphi(t_{JCi}) = \{t_s | (t_{JCi} - 1)\tau_i \leq t_s T_s < t_{JCi}\tau_i\}$  is the set of time sample index  $t_s$  from time  $(t_{JCi} - 1)\tau_i$  to  $t_{JCi}\tau_i$  seconds, and the number  $n$  of sample index at time  $t_{JCi}$  is given by  $n = \dim(\varphi(t_{JCi}))$ .

### 2.3.2 Area model

Traffic area model is used to explain the traffic demand in an area and estimate the optimal traffic as it should be. This model explains the traffic remaining traffic volume on each node which composes of  $N_{\text{area},j}$  adjacent areas,  $N_{\text{bnd},j}$  boundaries (outer area),  $N_{\text{int},j}$  intersections, and the number of nodes in the  $j$ th area is defined as  $N_{\text{node},j} = 2N_{\text{bnd},j} + N_{\text{int},j}$ . Then, the model can be written as follows:

$$x_{Aj}(t_{Aj} + 1) = x_{Aj}(t_{Aj}) + B_{AFj} u_{Aj}(t_{Aj}) + B_{ABj} (T_A \dot{v}_{aj}(t_{Aj})) \quad (2.29)$$

where  $x_{Aj}(t_{Aj}) \in \mathbb{R}^{N_{\text{node},j}}$  is the state vector which represents demand in each node on  $j$ th area,  $u_{Aj}(t_{Aj}) \in \mathbb{R}^{N_{\text{rd},j}}$  is the traffic flow (veh/ $T_A$  sec) through the roads in the  $j$ th area,  $\dot{v}_{aj}(t_{Aj}) = [\dot{b}_1^T(t_{Aj}), \dot{b}_2^T(t_{Aj}), \dots, \dot{b}_{N_{\text{bnd},j}}^T(t_{Aj})]^T$  is the arrival and departure rate (veh/sec) of each boundary, where  $\dot{b}_k(t_{Aj}) = [\dot{b}_{\text{in},k}(t_{Aj}), \dot{b}_{\text{out},k}(t_{Aj})]^T$ ,  $\dot{b}_{\text{out},k}(t_{Aj})$  and  $\dot{b}_{\text{in},k}(t_{Aj})$  are the output traffic and input traffic demand rate (veh/sec) on  $k$ th boundary,  $B_{AFj} \in \mathbb{R}^{N_{\text{node},j} \times N_{\text{Ra}}}$  is the input matrix that represents the relation between nodes and roads inside  $j$ th area,  $B_{ABj} \in \mathbb{R}^{N_{\text{node},j} \times N_{\text{bnd},j}}$  is the input matrix that represents the relation between nodes and demand from outer area,  $N_{\text{rd},j}$  is the number of roads inside the  $j$ th area, and  $t_{Aj}$  is the time index of the  $j$ th area.

The area state vector composes of the boundary and intersection node which is defined as

$$x_{A,j}(t_{Aj}) \triangleq [x_{\text{AB},j}^T(t_{Aj}), x_{\text{AI},j}^T(t_{Aj})]^T,$$

where

- $x_{AB,j}(t_{A_j}) \triangleq [x_{AB,j}^{(1)T}(t_{A_j}), x_{AB,j}^{(2)T}(t_{A_j}), \dots, x_{AB,j}^{(N_{\text{bnd},j})T}(t_{A_j})]^T$  is the state vector has size  $2N_{\text{bnd},j} \times 1$  which represents the demand from boundaries where  $x_{AB,j}^i(t_{A_j}) \triangleq [x_{AB,j}^{(\text{in},i)}(t_{A_j}), x_{AB,j}^{(\text{out},i)}(t_{A_j})]^T$ ,
- $x_{AI,j}(t_{A_j}) \triangleq [x_{AI,j}^{(1)}(t_{A_j}), x_{AI,j}^{(2)}(t_{A_j}), \dots, x_{AI,j}^{(N_{\text{int},j})}(t_{A_j})]^T$  is the state vector has size  $N_{\text{int},j} \times 1$  which represents the demand from intersections inside the area.

We illustrate an example scenario to make the understanding to readers by giving the example area which showed in Figure 2.6 as follows.

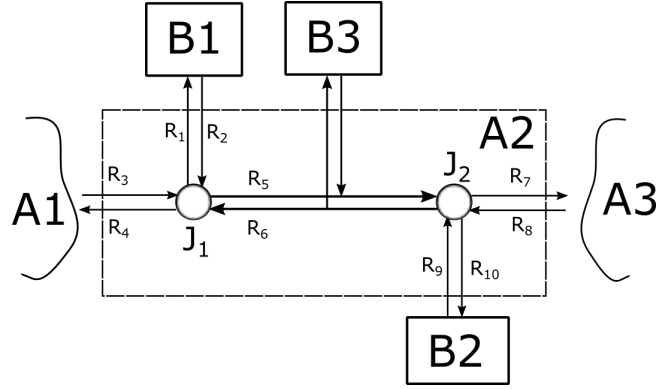


Figure 2.6: Example of traffic network schematic on 2nd area.

This area composes of two intersections, ten roads, and three boundaries. First, we define the state vector and input vector as

$$x_{A,j}(t_{A_j}) \triangleq [x_{AB,j}^{(1)T}(t_{A_j}), x_{AB,j}^{(2)T}(t_{A_j}), x_{AB,j}^{(3)T}(t_{A_j}), x_{AI,j}^{(1)}(t_{A_j}), x_{AI,j}^{(2)}(t_{A_j})]^T,$$

$$u_{A,j}(t_{A_j}) \triangleq [u_{A,j1}(t_{A_j}), u_{A,j2}(t_{A_j}), u_{A,j3}(t_{A_j}), u_{A,j4}(t_{A_j}), \dots, u_{A,j9}(t_{A_j}), u_{A,j10}(t_{A_j})]^T.$$

where  $x_{AB,j}^{(k)} \in x_{AB,j}$  and  $x_{AI,j}^{(k)} \in x_{AI,j}$  are the traffic demand on each node. Then, we can write the input matrix from nodes by referring to the position of states and input variables, it can be written as

$$B_{AF2} \triangleq \begin{bmatrix} \mu_{r1} & 0 & 0 & 0 & 0 & 0 & 0 & 0 & 0 & 0 \\ 0 & -1 & 0 & 0 & 0 & 0 & 0 & 0 & 0 & 0 \\ \hline 0 & 0 & 0 & 0 & 0 & 0 & 0 & 0 & 0 & \mu_{r10} \\ 0 & 0 & 0 & 0 & 0 & 0 & 0 & 0 & -1 & 0 \\ \hline 0 & 0 & 0 & 0 & 0 & \mu_{r6,b3} & 0 & 0 & 0 & 0 \\ 0 & 0 & 0 & 0 & -\mu_{b3,r5} & 0 & 0 & 0 & 0 & 0 \\ \hline -1 & \mu_{r2} & \mu_{r3} & -1 & -\mu_{j1,r5} & \mu_{r6,j1} & 0 & 0 & 0 & 0 \\ 0 & 0 & 0 & 0 & 1 & -1 & -1 & \mu_{r8} & \mu_{r9} & -1 \end{bmatrix}$$

This input matrix describes the relation of nodes and roads which are referred to as the direction of the road. The road which outcome direction on a node will be defined as -1, the  $k$ th road

which incoming direction will be defined as  $\mu_k$ , and others are defined as 0. The input matrix from boundaries is given as

$$B_{ABj} \triangleq \begin{bmatrix} I_{2N_{\text{bnd},j}} \\ 0_{N_{\text{int},j} \times 2N_{\text{bnd},j}} \end{bmatrix}.$$

### Hierarchical distributed control of area layer

The objective of the area layer is to find the optimal traffic flow of each road inside the area which mitigates the traffic congestion in the network. Then, we formulate the minimization problem to determine the feasible traffic flow inside the  $j$ th area for every step  $t_{Aj}$ .

$$\underset{u_{Aj}(0), \dots, u_{Ai}(T)}{\text{minimize}} \sum_{t_{Aj}=0}^T \|x_{Aj}(t_{Aj} + 1|t_{Aj})\|^2 \quad (2.30)$$

subject to the following constraints  $t_{Aj} = 0, 1, \dots, T$ :

$$0 \leq u_{Ajr}(t_{Aj}) \leq q_{\text{max},r}, \quad \text{for } \forall r, \quad (2.31)$$

$$\sum_{r \in R_{\text{in}}^i} \mu_r u_{Ajr}(t_{Aj}) \leq C_{\text{int},i} \times (T_A/3, 600), \quad \text{for } \forall i \in I_j, \quad (2.32)$$

$$|u_{Ajr_{\text{out}}}(t_{Aj}) - \sum_{(r_{\text{in}}, d) \in \mathcal{S}_{r_{\text{out}}}} \mu_{r_{\text{in}}} p_{r_{\text{in}}, d} u_{Ajr_{\text{in}}}(t_{Aj})| \leq \alpha, \quad \text{for } \forall r_{\text{out}} \in R_{\text{out}}^i \text{ and } \forall i \in I_j, \quad (2.33)$$

$$\sum_{r \in L_{Aj}^k} u_{Ajr}(t_{Aj}) = q_{Aj}^*(t_{Aj}), \quad \text{for } \forall k, \quad (2.34)$$

where  $R_{\text{in}}^i$  and  $R_{\text{out}}^i$  are the set of road's index corresponding to incoming and outcome direction of the  $i$ th intersection respectively,  $L_{Aj}^k$  is the set of road index on  $k$ th link in  $j$ th area,  $I_j$  is the set of intersection's index on  $j$ th area,  $C_{\text{int},i}$  is the capacity (veh/h) of  $i$ th intersection,  $q_{Aj}^*(t_{Aj})$  is the optimal traffic flow of  $k$ th link in  $j$ th area obtained from (2.40), and  $\alpha$  is the acceptable error of traffic flow.

The optimal solution  $u_{Aj}(t_{Aj})$  from (2.30) will be distributed to intersection layer, it represents the desired traffic flow (veh/ $T_A$  sec) on each road. Constraints (2.32) represents the maximum capacity ( $C_{\text{int},i}$ ) of  $i$ th intersection in vehicle per seconds, and the (2.33) represents the input flow of an outcome direction road is balanced with the ratio of output flow on incoming direction roads. However, the intersection capacity ( $C_{\text{int},i}$ ) is obtained from the assumption based on the measurement.

### 2.3.3 Network model

A traffic network model is used to explain the traffic demand in a network such that the traffic flow between areas. A traffic network is comprised of  $N_{\text{area}}$  areas and  $N_{\text{link}}$  links. Then, the model can be written as follows:

$$x_N(t_N + 1) = x_N(t_N) + B_{\text{NF}}u_N(t_N) + B_{\text{NB}}(v_N(t_N) + \dot{v}_N(t_N)T_N) + z_n(t_N)T_N \quad (2.35)$$

where  $x_N \in \mathbb{R}^{N_{\text{area}}}$  is the state vector of the network which represents the demand volume (veh) in each area,  $u_N \in \mathbb{R}^{N_{\text{link}}}$  is the input vector which represents the traffic flow (veh/ $T_N$  sec) on the links,  $B_{\text{NF}} \in \mathbb{R}^{N_{\text{area}} \times N_{\text{link}}}$  is the input matrix that represents the relation between areas,  $B_{\text{NB}} \in \mathbb{R}^{N_{\text{area}} \times 2N_{\text{bound}}}$  is the input matrix from boundaries to areas,  $z_n(t_N)$  is the demand in each area (veh/s),  $N_{\text{area}}$  is the number of areas,  $N_{\text{bound}}$  is the number of boundaries on network, and  $N_{\text{link}}$  is the number of links in network. The traffic demand from boundaries are defined on demand vector  $v_N(t_N) = [b_1^T(t_N), b_2^T(t_N), \dots, b_{N_{\text{bound}}}^T(t_N)]^T$ , where  $b_b(t_N) = [b_{\text{in},b}(t_N), b_{\text{out},b}(t_N)]^T$ ,  $b_{\text{out},b}(t_N)$  and  $b_{\text{in},b}(t_N)$  are the output traffic and input traffic demand (veh) on  $b$ th boundary, and  $\dot{v}_N(t_N) = [\dot{b}_1^T(t_N), \dot{b}_2^T(t_N), \dots, \dot{b}_{N_{\text{bound}}}^T(t_N)]^T$  is the arrival and departure rate (veh/sec) of each boundary, where  $\dot{b}_b(t_N) = [\dot{b}_{\text{in},b}(t_N), \dot{b}_{\text{out},b}(t_N)]^T$ ,  $\dot{b}_{\text{out},b}(t_N)$  and  $\dot{b}_{\text{in},b}(t_N)$  are the output traffic and input traffic demand rate (veh/sec) on  $b$ th boundary.

We illustrate an example scenario to make the understanding to the reader by giving the example area which showed in Figure 2.7 as follows.

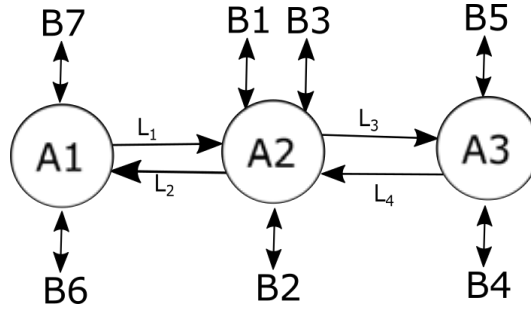


Figure 2.7: Example of a traffic schematic of network layer.

This network composes of three areas, four links, and six outer area. First, we define the state vector, input vector, and demand vector as

$$\begin{aligned} x_N(t_N) &\triangleq [x_{N1}^T(t_N), x_{N2}^T(t_N), x_{N3}^T(t_N)]^T, \\ u_N(t_N) &\triangleq [u_{N1}(t_N), u_{N2}(t_N), u_{N3}(t_N), u_{N4}(t_N)]^T, \\ v_N(t_N) &\triangleq [b_1^T(t_N), b_2^T(t_N), \dots, b_6^T(t_N)]^T. \end{aligned}$$

where  $a_j \in \mathbb{R}^2$  is the absolute demand (veh) on  $j$ th area and  $l_k \in \mathbb{R}^1$  is the traffic volume (veh) in  $k$ th link. Then, we can write the input matrix from area by referring to the position of states and input variables, there can be written as

$$B_{\text{NF}} \triangleq \begin{bmatrix} -1 & \mu_{12} & 0 & 0 \\ \mu_{11} & -1 & -1 & \mu_{14} \\ 0 & 0 & \mu_{13} & -1 \end{bmatrix}.$$

This input matrix describes the relation of areas and links which are referred to as the direction of a link. The link which outcome direction on an area will be defined as -1, the  $k$ th link which

incoming direction will be defined as  $\mu_{lk}$  and others are defined as 0. Note that a link can contain more roads, it depends on the area physical. The input matrix from boundaries is given as

$$B_{NB} \triangleq \left[ \begin{array}{cc|cc|cc|cc|cc|cc|cc} 0 & 0 & 0 & 0 & 0 & 0 & 0 & 0 & 0 & 0 & -1 & 1 & -1 & 1 \\ -1 & 1 & -1 & 1 & -1 & 1 & 0 & 0 & 0 & 0 & 0 & 0 & 0 & 0 \\ 0 & 0 & 0 & 0 & 0 & 0 & -1 & 1 & -1 & 1 & 0 & 0 & 0 & 0 \end{array} \right].$$

### Hierarchical distributed control of network layer

The goal of the network control aims to minimize the traffic demand between source and sink by finding the optimal traffic flow obtained from solving the optimization on time horizon  $T$ . We formulate the minimization problem to determine the optimal traffic flow on each link for every  $t_N$ .

$$\underset{u_N(0), \dots, u_N(T)}{\text{minimize}} \sum_{t_N=0}^T \|x_N(t_N + 1 | t_N)\|^2 \quad (2.36)$$

subject to the following constraints  $t_N = 0, 1, \dots, T$ :

$$q_{\min} \leq \mu_{lk} u_{Nk}(t_N) \leq C_{\text{link},k} \times (T_N/3, 600), \quad \text{for } \forall k, \quad (2.37)$$

where  $C_{\text{link},k}$  is the capacity (veh/h) of  $k$ th link,  $A_{bj}$  is the set of boundaries on  $j$ th area. The optimal solution  $u_N(t_N)$  of network layer from (2.36) will be used in the area layer. However, the traffic demand  $v_N(t_N)$  is necessary to forecast or use historical data.

## 2.4 Traffic data aggregation and distribution

### Traffic data aggregation

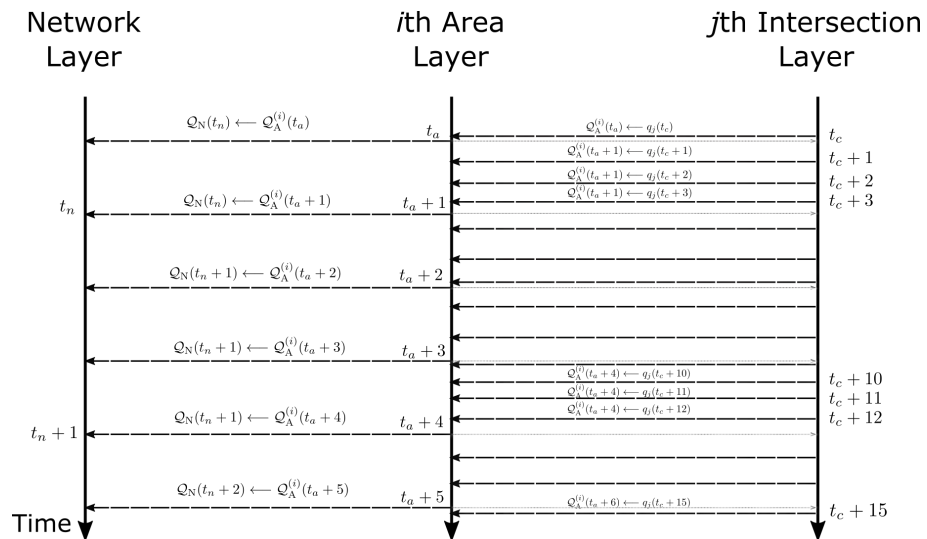


Figure 2.8: Example of time diagram on data aggregating.

The traffic measurement data from the intersection layer and area layer such that traffic flow and the number of the passing vehicles are aggregated onto the upper layer. Each layer had a different

sampling period to send the information up to the upper layer which is illustrated in Figure 2.8. However, the sampling period of each layer is appropriately defined by the user. The detail of data aggregation in the network layer and area layer are described as follows.

### Aggregation from intersection layer to area layer

On the intersection layer, the traffic output  $y_{ji}$  on  $i$ th intersection represents the number of vehicles (veh) on each road, it is aggregated to area layer via aggregation matrix  $\Sigma_{Ji}$ . The aggregation matrix will be aggregated the total vehicles of incoming direction roads on  $i$ th intersection, it can be described as

$$x_{AI,j}^{(i)}(t_{JCi}) \triangleq \Sigma_{Ji} y_{ji}(t_{JCi}) = \sum_{r \in R_{in}^i} y_{Jir}(t_{JCi}) \quad (2.38)$$

where  $R_{in}^i$  is the set of incoming direction roads on  $i$ th intersection. To illustrate the detail of the aggregation matrix on the example traffic area, the schematic from Figure 2.6 is used for example the aggregation matrix by assuming the number of roads on intersection  $J_1$  and  $J_2$  are 6 and 6 respectively. The state vector of intersection  $J_1$  and  $J_2$  are defined as  $y_{J1}^T(t_{JCi})$  and  $y_{J2}^T(t_{JCi})$ , where

$$y_{J1}(t_{JCi}) \triangleq [y_{J1,1}(t_{JCi}), y_{J1,2}(t_{JCi}), y_{J1,3}(t_{JCi}), y_{J1,4}(t_{JCi}), y_{J1,5}(t_{JCi}), y_{J1,6}(t_{JCi})]^T,$$

$$y_{J2}(t_{JCi}) \triangleq [y_{J2,5}(t_{JCi}), y_{J2,6}(t_{JCi}), y_{J2,7}(t_{JCi}), y_{J2,8}(t_{JCi}), y_{J2,9}(t_{JCi}), y_{J2,10}(t_{JCi})]^T.$$

Then, the matrices of intersection  $J_1$  and  $J_2$  are defined as

$$\Sigma_{J1} \triangleq \begin{bmatrix} 0 & 1 & 1 & 0 & 0 & 1 \end{bmatrix}, \quad \Sigma_{J2} \triangleq \begin{bmatrix} 1 & 0 & 0 & 1 & 1 & 0 \end{bmatrix}.$$

### Aggregation from area layer to network layer

On the area layer, the traffic state  $x_{AI,j}$  on  $j$ th area represents the total vehicles (veh) on each intersection, it is aggregated to the network layer via aggregation matrix  $\Sigma_{A_j}$ . The aggregation matrix will be aggregated the total vehicles of all intersections in  $j$ th area, it can be described as

$$x_{Nj}(t_{Aj}) \triangleq \Sigma_{A_j} x_{AI,j}(t_{Aj}) \quad (2.39)$$

where  $R_{in}^i$  is the set of incoming direction roads on  $i$ th intersection, and the aggregation matrix can be defined as  $\Sigma_{A_j} = \mathbb{1}^T$ .

### Traffic data distribution

The traffic information from the network layer and area layer such that traffic demand and optimal traffic flow had distributed into the lower layer. Each layer had a difference sampling period to send the traffic information into the lower layer which is illustrated in Figure 2.9. However, the sampling period of each layer must appropriately define by the user. The detail of the data distribution on the area layer and intersection layer are described as follows.

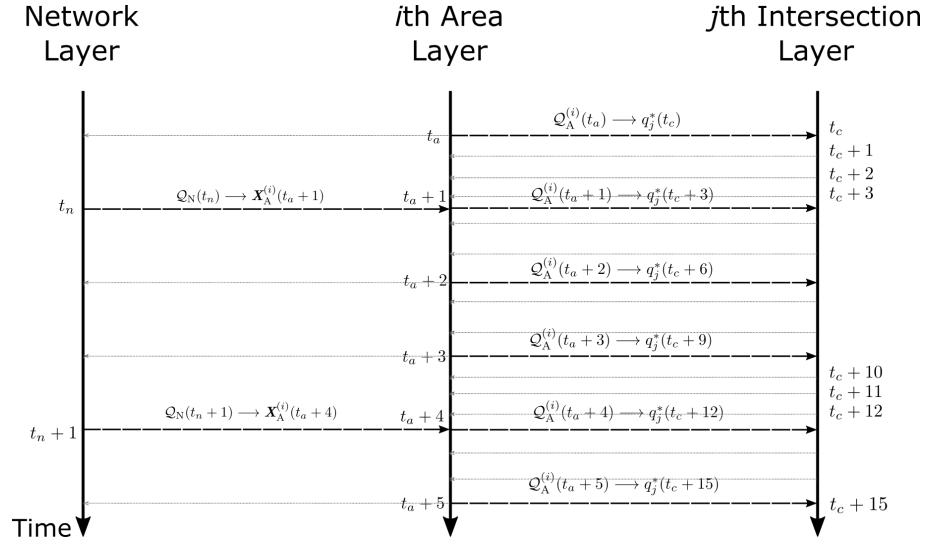


Figure 2.9: Example of time diagram on data distributing.

### Distribution data from network layer into area layer

Optimal traffic flow  $u_N$  from network layer is distributed into the  $j$ th area for keeping the traffic flow between area is optimal, it can be described by

$$q_{A_j}^*(t_{A_j}) = D_{A_j} u_N(t_{A_j}), \quad (2.40)$$

where  $q_{A_j}^*(t_{A_j})$  is the optimal signal from network layer which represents the traffic flow, and  $D_{A_j}$  is the distribution matrix which has dimension  $2N_{\text{area},j} \times N_{\text{link}}$ .

To illustrate the detail of the distribution matrix of example area  $A_1$  which the network schematic from Figure 2.7 and area  $A_1$  schematic from Figure 2.6 are used to example the distribution matrix as given by

$$D_{A_2} \triangleq \frac{T_A}{T_N} \cdot \begin{bmatrix} 1 & 0 & 0 & 0 \\ 0 & \mu_{12} & 0 & 0 \end{bmatrix}.$$

where the input vector of this intersection is defined as  $q_{A_j}^*(t_{A_j}) = [q_{A_{j1}}^*(t_{A_j}), q_{A_{j2}}^*(t_{A_j})]^T$  and upper signal is defined as  $u_N(t_{A_j}) = [u_{N1}(t_{A_j}), u_{N2}(t_{A_j}), u_{N3}(t_{A_j}), u_{N4}(t_{A_j})]^T$ .

### Distribution data from area layer into intersection layer

The desired traffic flow  $q_j^*(t_{JCi})$  is the optimal traffic flow which the network should be maintained to keep the total traffic flow of network at maximum.

$$q_j^*(t_{JCi}) = D_{J_i} u_{A_j}(t_{JCi}) \quad (2.41)$$

where  $u_{A_i}(t_{JCi})$  is the optimal signal from  $j$ th area, and  $D_{J_i}$  is the distribution matrix which has dimension  $N_{\text{rd}} \times N_{\text{Ra}}$ .

To illustrate the detail of this distribution matrix of intersection  $J_1$ , the schematic of area  $A_2$  from Figure 2.6 is used to example the distribution matrix as given by

$$D_{J1} \triangleq \frac{1}{T_A} \cdot \begin{bmatrix} 1 & 0 & 0 & 0 & 0 & 0 & 0 & 0 & 0 & 0 \\ 0 & \mu_2 & 0 & 0 & 0 & 0 & 0 & 0 & 0 & 0 \\ 0 & 0 & \mu_3 & 0 & 0 & 0 & 0 & 0 & 0 & 0 \\ 0 & 0 & 0 & 1 & 0 & 0 & 0 & 0 & 0 & 0 \\ 0 & 0 & 0 & 0 & 1 & 0 & 0 & 0 & 0 & 0 \\ 0 & 0 & 0 & 0 & 0 & \mu_6 & 0 & 0 & 0 & 0 \end{bmatrix}.$$

where the output vector of this intersection is defined as  $q_{Ji}^*(t_{JCi}) = [q_{Ji1}^*(t_{JCi}), q_{Ji2}^*(t_{JCi}), \dots, q_{Ji6}^*(t_{JCi})]^T$  and upper signal is defined as  $u_{Aj}(t_{JCi}) = [u_{Aj1}(t_{JCi}), u_{Aj2}(t_{JCi}), \dots, u_{Aj10}(t_{JCi})]^T$ .

## 2.5 Control procedure for hierarchical distributed model predictive control

This work has established the controller with three layers which are the network, area, and intersections. Those controllers are the asynchronous system, they have a communication socket to exchange the information with other controllers. Thus, the control procedure in this work is consists of three major steps which are described as follows:

**1. Configuring:** The first step to start the traffic control system, we define the roads, intersections, areas, and network. Next step, we define the pattern and sequence of traffic light  $(\mathcal{A}, \mathcal{S})$  for all intersections. Then, we run the first simulation with fixed control to obtain traffic datasets with real traffic conditions.

**2. Initializing:** In this step, the traffic dataset was obtained from real traffic conditions is the traffic volume (veh) passed on a section will be used to the following steps.

1. First, use the obtained dataset to determine the area demand  $z_n$ .
2. Second, use the obtained dataset to determine the boundary demand  $x_{AB,j}^i(0)$  for all  $j$ th area and  $i$ th boundary.
3. Lastly, use the obtained dataset to determine the splitting flow probability  $p_i$  for all  $i$ th intersection from (2.8).

**3. Controlling:** After we initialized the controllers, we will start up each controller to obtain the optimal traffic signal for each intersection. Due to controllers are the synchronous system, we will describe the procedure of each controller by dividing into three procedures as follows:

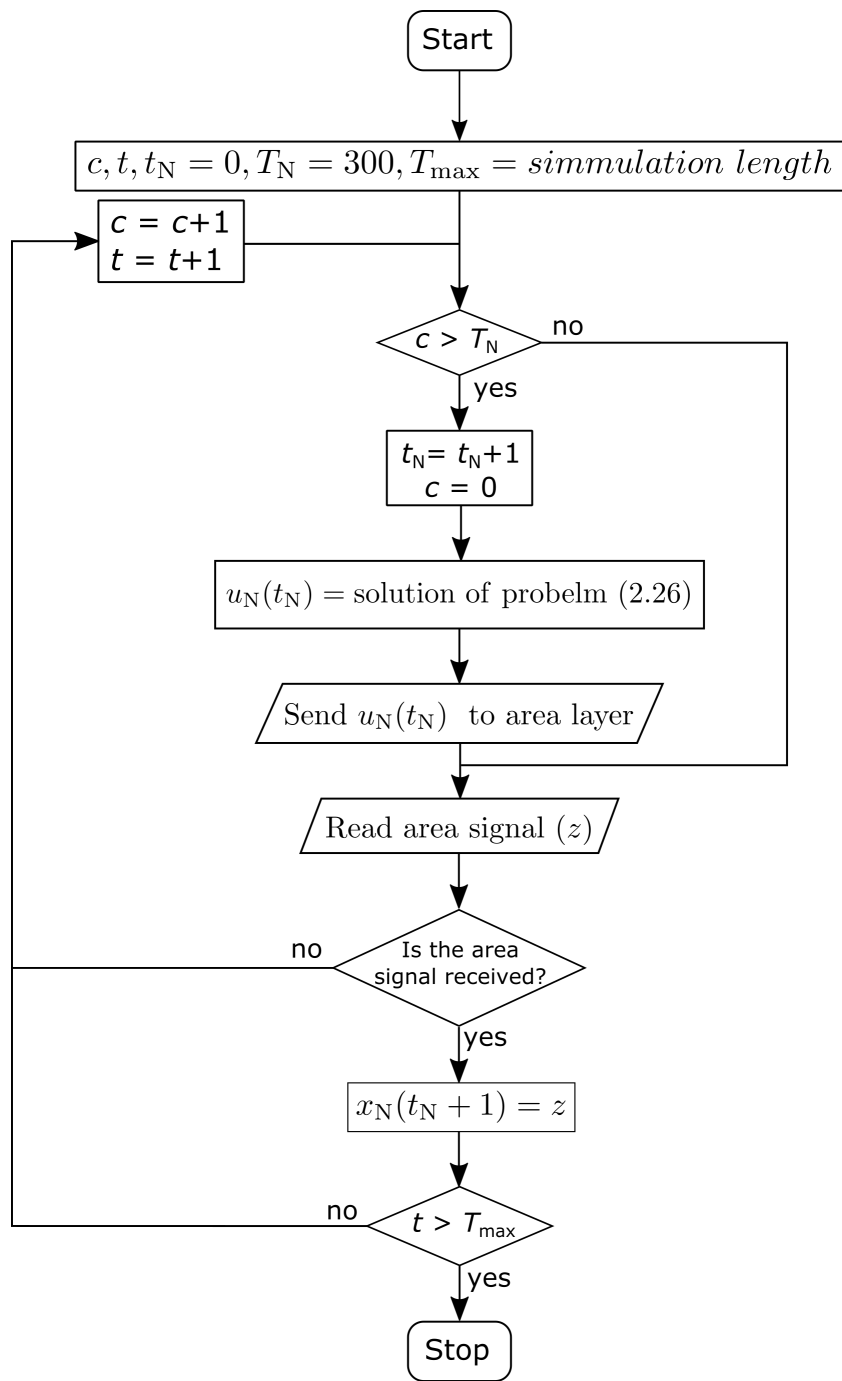


Figure 2.10: Procedure diagram of network layer's controller.

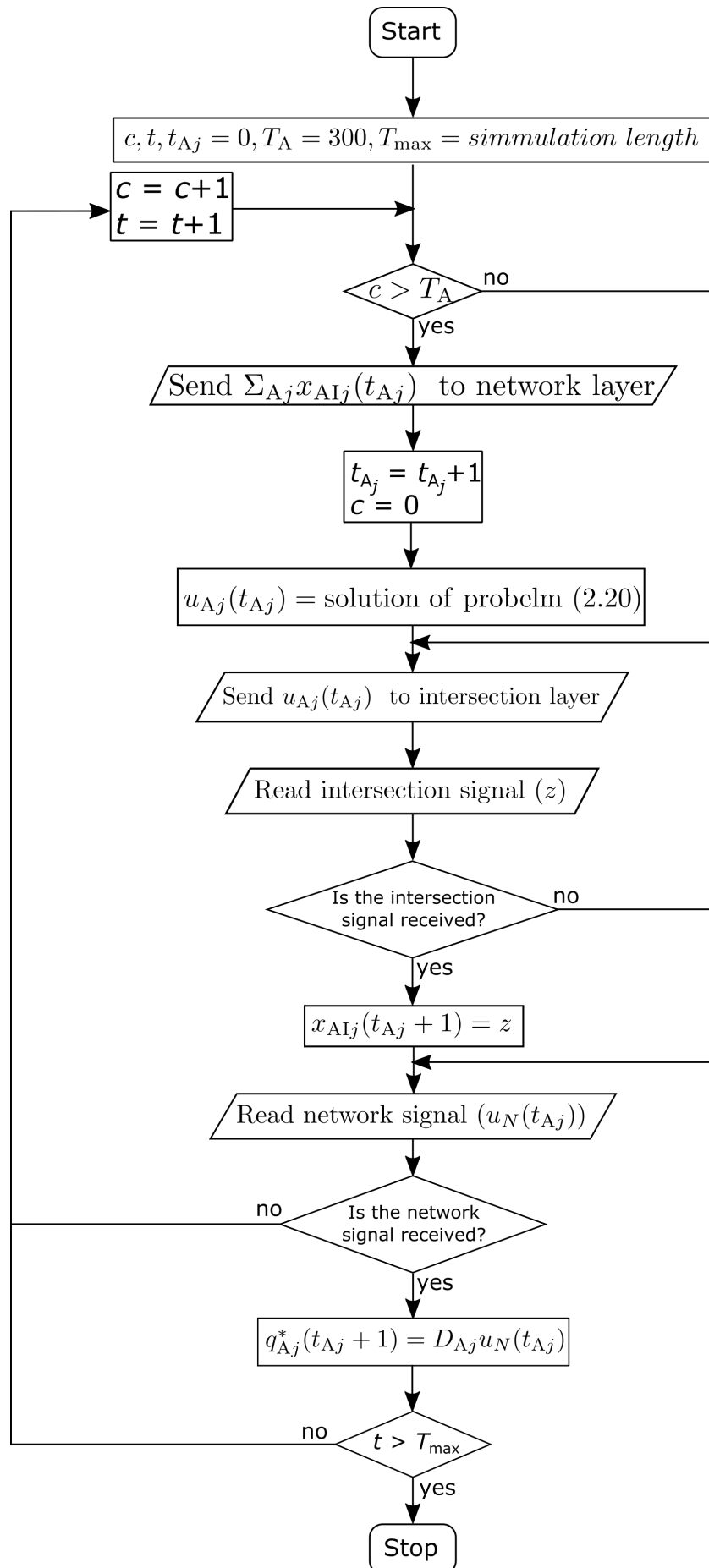


Figure 2.11: Procedure diagram of area layer's controller.

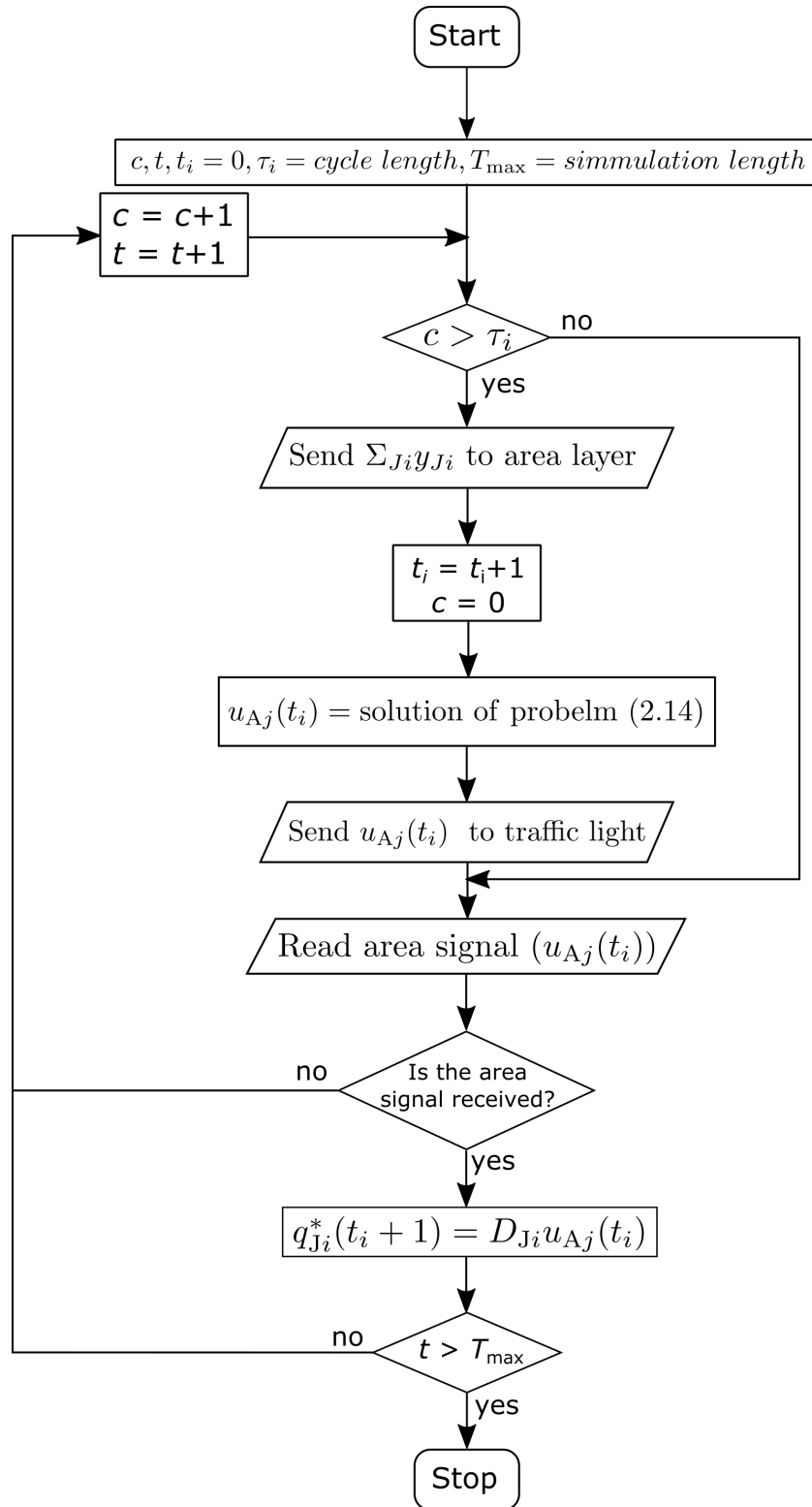


Figure 2.12: Procedure diagram of intersection layer's controller.

## CHAPTER III

### PRELIMINARY RESULTS

#### 3.1 Traffic scenario description

This section describes the scenario that has been simulated in this work are described. The scenario is set up in two areas which shows in Figures 3.1 with one intersection per area and consist of 14 roads. Their 14 road's characteristics are showed as Table 3.1. The simulation software in this work is used the SUMO traffic simulator. It's using the microscopic traffic model to simulate the results in real-time. We need to write the Python code to observe the traffic sensors and control the traffic lights via Traffic Control Interface (TraCI).

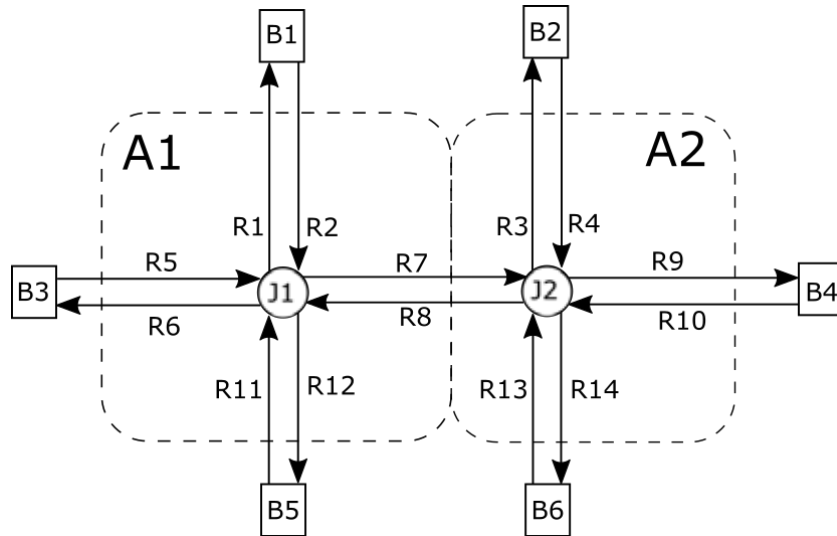


Figure 3.1: An example scenario of a traffic network.

Figure 3.1 shows the traffic network with two intersections connected to adjacent zones defined as the boundary B1, B2,..., and B6. We configure the traffic demand that traffic flow from the area A1 to A2 (11,000 veh) is more than from the area A2 to A1 (2,200 veh) which calculated from routing configuration in Table 3.3.

Table 3.1: Roadway information.

| <b>Road</b> | <b>Length (m)</b> | <b>Lane</b> | <b>From</b> | <b>To</b> | <b>Maximum speed (km/h)</b> |
|-------------|-------------------|-------------|-------------|-----------|-----------------------------|
| R1          | 183.10            | 3           | J1          | B1        | 50                          |
| R2          | 183.10            | 3           | B1          | J1        | 50                          |
| R3          | 183.10            | 3           | J2          | B2        | 50                          |
| R4          | 183.10            | 3           | B2          | J2        | 50                          |
| R5          | 183.15            | 3           | B3          | J1        | 50                          |
| R6          | 183.15            | 3           | J1          | B3        | 50                          |
| R7          | 169.50            | 3           | J1          | J2        | 50                          |
| R8          | 169.50            | 3           | J2          | J3        | 50                          |
| R9          | 186.40            | 3           | J2          | B4        | 50                          |
| R10         | 186.40            | 3           | B4          | J2        | 50                          |
| R11         | 186.25            | 3           | B5          | J1        | 50                          |
| R12         | 186.25            | 3           | J1          | B5        | 50                          |
| R13         | 186.25            | 3           | B6          | J2        | 50                          |
| R14         | 186.25            | 3           | J2          | B6        | 50                          |

In the SUMO simulator, we need to draw the road network by following the designed scenario as Figure 3.1. The illustrated information on Table 3.1 is used to draw the scenario and consists of road index, length of road in meter, number of the lane, available maximum vehicle speed, origin node, and destination node.

Table 3.2: Table of summary on traffic demand in boundary nodes.

| <b>Boundary</b> | <b>Source (veh)</b> | <b>Sink (veh)</b> |
|-----------------|---------------------|-------------------|
| B1              | 6,000               | 700               |
| B2              | 500                 | 500               |
| B3              | 4,000               | 500               |
| B4              | 400                 | 10,000            |
| B5              | 2,000               | 1,000             |
| B6              | 300                 | 500               |

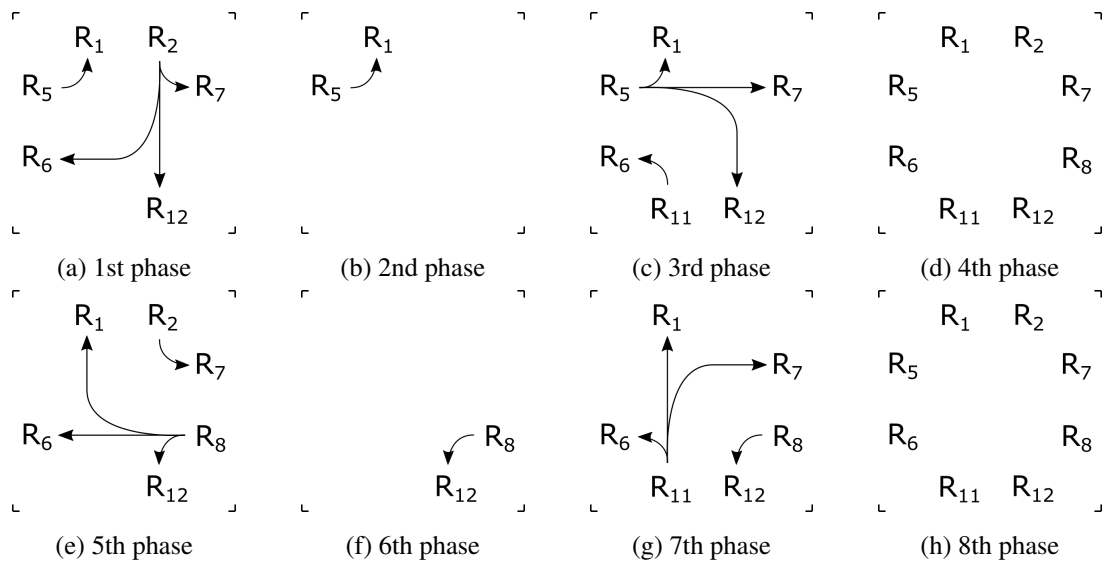
Table 3.3: Table of summary on traffic volume in each road.

| Road | Volume | Flow (veh/h) | Road | Volume | Flow (veh/h) |
|------|--------|--------------|------|--------|--------------|
| R1   | 700    | 2160         | R8   | 800    | 2160         |
| R2   | 6000   | 2880         | R9   | 10000  | 2520         |
| R3   | 500    | 2520         | R10  | 400    | 1080         |
| R4   | 500    | 1080         | R11  | 2000   | 2880         |
| R5   | 4000   | 3240         | R12  | 1000   | 1260         |
| R6   | 500    | 1620         | R13  | 300    | 1080         |
| R7   | 10600  | 5400         | R14  | 500    | 2160         |

The routing configuration from the simulator has been summarized into Table 3.2 that shows the traffic demand on each boundary node. Table 3.3 shows the summary of traffic volume on each road. This information is useful to calculate the cycle time and green time on a fixed time control case.

### Configuration of intersection $J_1$

The traffic light signal of intersection  $J_1$  is configured of 8 phases which showed on Figure 3.2. Phase index 2,4,6 and 7 are defined as the yellow phase which the time duration are fixed at 5 seconds. This intersection consists of 4 incoming roads  $R_{in} = \{R_2, R_5, R_8, R_{11}\}$  and 4 outcome roads  $R_{out} = \{R_1, R_6, R_7, R_{12}\}$ .

Figure 3.2: Configure traffic lights on intersection  $J_1$ .

The set of available lanes  $\mathcal{A}_k$  of  $k$ th phase on intersection  $J_1$  showed as Figure 3.2. is given as

follows:

$$\begin{aligned}
\mathcal{A}_1 &= \{(R_2, 1), (R_2, 2), (R_2, 3), (R_5, 1)\} & \mathcal{A}_5 &= \{(R_8, 1), (R_8, 2), (R_8, 3), (R_2, 1)\} \\
\mathcal{A}_2 &= \{(R_5, 1)\} & \mathcal{A}_6 &= \{(R_8, 1)\} \\
\mathcal{A}_3 &= \{(R_5, 1), (R_5, 2), (R_5, 3), (R_4, 1)\} & \mathcal{A}_7 &= \{(R_{11}, 1), (R_{11}, 2), (R_{11}, 3), (R_8, 1)\} \\
\mathcal{A}_4 &= \{\phi\} & \mathcal{A}_8 &= \{\phi\}
\end{aligned}$$

The set of available source  $\mathcal{S}_i$  of road  $R_i$  on intersection  $J_1$  showed as Figure 3.2. is given as follows:

$$\begin{aligned}
\mathcal{S}_1 &= \{(R_5, 1), (R_8, 3), (R_{11}, 2)\} & \mathcal{S}_7 &= \{(R_2, 1), (R_5, 2), (R_{11}, 3)\} \\
\mathcal{S}_2 &= \{\phi\} & \mathcal{S}_8 &= \{\phi\} \\
\mathcal{S}_5 &= \{\phi\} & \mathcal{S}_{11} &= \{\phi\} \\
\mathcal{S}_6 &= \{(R_2, 3), (R_8, 2), (R_{11}, 1)\} & \mathcal{S}_{12} &= \{(R_2, 2), (R_5, 3), (R_8, 1)\}
\end{aligned}$$

The splitting ratio  $p_i$  of road  $R_i$  on intersection  $J_1$  are evaluated from routing configuration is given as follows:

$$\begin{aligned}
p_1 &= [1]^T & p_7 &= [1]^T \\
p_2 &= [0.0206, 0.0619, 0.9175]^T & p_8 &= [0.3250, 0.3312, 0.3438]^T \\
p_5 &= [0.0833, 0.8472, 0.0694]^T & p_{11} &= [0.8732, 0.0563, 0.0704]^T \\
p_6 &= [1]^T & p_{12} &= [1]^T
\end{aligned}$$

### Configuration of intersection $J_2$

The traffic light signal of intersection  $J_2$  is configured of 8 phases which showed on Figure 3.3. Phase index 2,4,6 and 7 are defined as the yellow phase which the time duration are fixed at 5 seconds. This intersection consists of 4 incoming roads  $R_{in} = \{R_4, R_7, R_{10}, R_{13}\}$  and 4 outcome roads  $R_{out} = \{R_3, R_8, R_9, R_{14}\}$ .

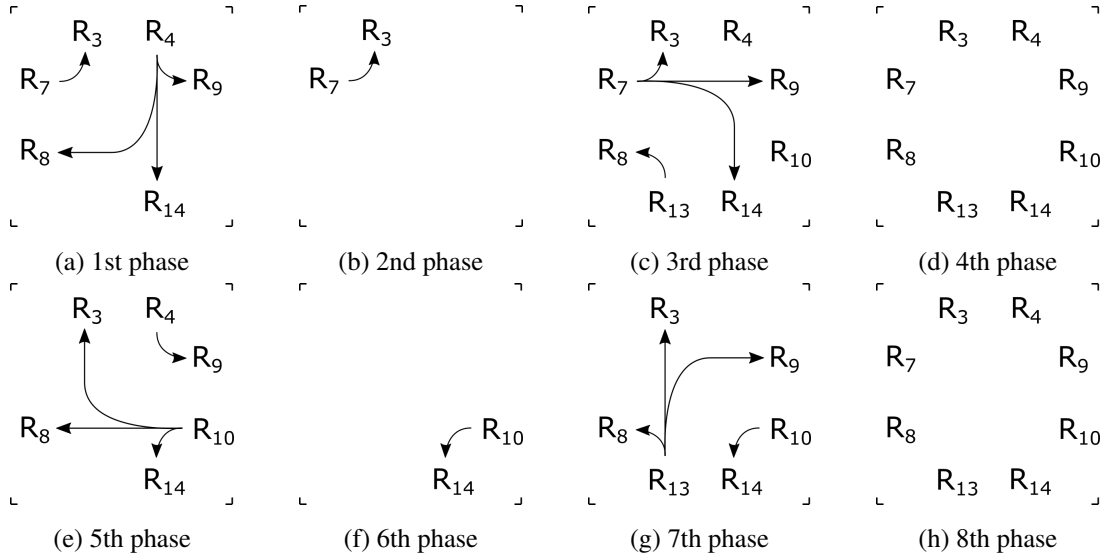


Figure 3.3: Configure traffic lights on intersection  $J_2$ .

The set of available lanes  $\mathcal{A}_k$  of  $k$ th phase on intersection  $J_2$  showed as Figure 3.3. is given as follows:

$$\begin{aligned}
 \mathcal{A}_1 &= \{(R_4, 1), (R_4, 2), (R_4, 3), (R_7, 1)\} & \mathcal{A}_5 &= \{(R_{10}, 1), (R_{10}, 2), (R_{10}, 3), (R_4, 1)\} \\
 \mathcal{A}_2 &= \{(R_7, 1)\} & \mathcal{A}_6 &= \{(R_{10}, 1)\} \\
 \mathcal{A}_3 &= \{(R_7, 1), (R_7, 2), (R_7, 3), (R_{13}, 1)\} & \mathcal{A}_7 &= \{(R_{13}, 1), (R_{13}, 2), (R_{13}, 3), (R_{10}, 1)\} \\
 \mathcal{A}_4 &= \{\phi\} & \mathcal{A}_8 &= \{\phi\}
 \end{aligned}$$

The set of available source  $\mathcal{S}_i$  of road  $R_i$  on intersection  $J_2$  showed as Figure 3.3. is given as follows:

$$\begin{aligned}
 \mathcal{S}_3 &= \{(R_7, 1), (R_{10}, 3), (R_{13}, 2)\} & \mathcal{S}_9 &= \{(R_4, 1), (R_7, 2), (R_{13}, 3)\} \\
 \mathcal{S}_4 &= \{\phi\} & \mathcal{S}_{10} &= \{\phi\} \\
 \mathcal{S}_7 &= \{\phi\} & \mathcal{S}_{13} &= \{\phi\} \\
 \mathcal{S}_8 &= \{(R_4, 3), (R_{10}, 2), (R_{13}, 1)\} & \mathcal{S}_{14} &= \{(R_4, 2), (R_7, 3), (R_{10}, 1)\}
 \end{aligned}$$

The splitting ratio  $p_i$  of road  $R_i$  on intersection  $J_2$  are evaluated from routing configuration is given as follows:

$$\begin{aligned}
 p_3 &= [1]^T & p_9 &= [1]^T \\
 p_4 &= [0.6753, 0.1299, 0.1948]^T & p_{10} &= [0.1351, 0.6622, 0.2027]^T \\
 p_7 &= [0.1792, 0.5000, 0.3208]^T & p_{13} &= [0.2247, 0.1124, 0.6629]^T \\
 p_8 &= [1]^T & p_{14} &= [1]^T
 \end{aligned}$$

### 3.2 Simulation results

The simulation used the SUMO traffic simulator that is the microscopic and continuous traffic simulation model. Simulation length is 3 hour period, which compared the results from HDC cases to fixed time control. For HDC simulation cases, its were sweep the gamma value ( $\gamma$ ) in cost objective (2.23) as  $\gamma = 0, 100, 200, \dots, 20000$  with three trial per one gamma value. According to the scenario, traffic demand from area  $A_1$  to area  $A_2$  is higher than from area  $A_2$  to area  $A_1$ . If the traffic signal on intersection  $J_1$  is inappropriate scheduled then, the traffic on road  $R_7$  will be congested and led the road  $R_2, R_5,$  and  $R_{11}$  in area  $A_1$  will congested also. While the traffic signal on intersection  $J_1$  has appropriately scheduled then, the traffic-congested on area  $A_1$  is possible to treat.

#### 3.2.1 Fixed time control

First, we consider the results in the case of fixed time control. In this case, the scheme of traffic signal timing for each phase is calculated from equation (1.19) with using the traffic volume as each road from Table 3.3.

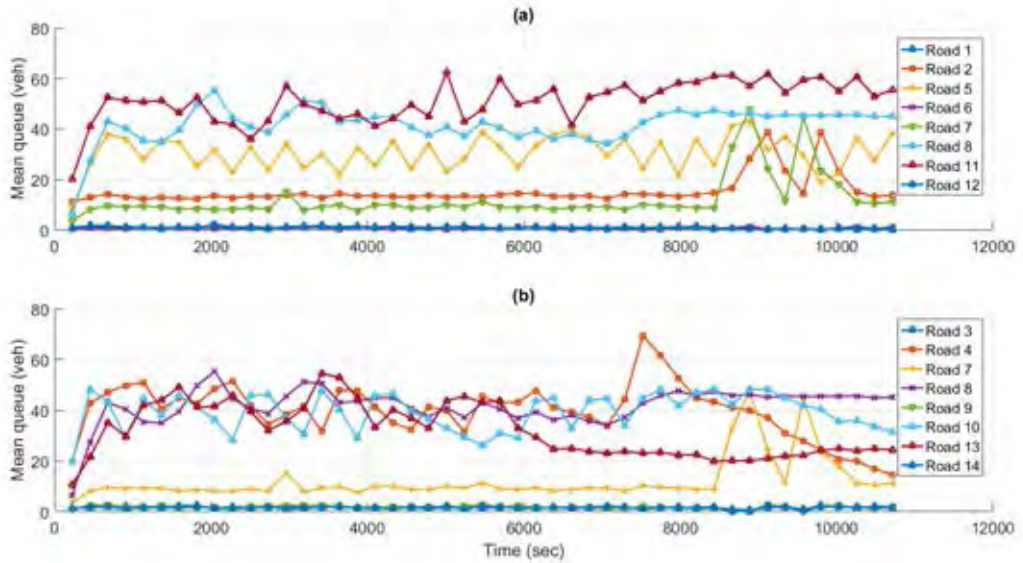


Figure 3.4: Plot of states on fixed control: (a) intersection  $J_1$ , (b) intersection  $J_2$ .

Figure 3.4 shows the average vehicle queue-length  $\bar{y}_{J_i}(t_s)$  for  $t_s = 30, 60, \dots, 10800$  seconds, where the average vehicle queue-length  $\bar{y}_{J_i}(t_s)$  is calculated from output measurement  $y_{J_i}(t_s)$  in (2.11) as follows:

$$\bar{y}_{J_i}(t_s) = \frac{1}{30} \sum_{k=t_s-30}^{t_s} y_{J_i}(k) \quad \text{for } t_s = 30, 60, \dots, 10800. \quad (3.1)$$

The traffic signal scheduling on intersection  $J_a$  is  $u = [94, 5, 62, 5, 13, 5, 31, 5]^T$  and the traffic signal scheduling on intersection  $J_2$  is  $u = [15, 5, 155, 5, 15, 5, 15, 5]^T$ . In the 3th phase of traffic signal scheduling of 2nd intersection showed the highest time duration than other phases because

of the traffic demand on road  $R_7$  from the information in Table 3.3 is higher than other roads in intersection  $J_2$ . Therefore, the average vehicle on road  $R_7$  is lower than the other incoming road in intersection  $J_2$ . It effects to the traffic congestion on the intersection  $J_1$  which the good vehicles released the to area  $A_2$ .

### 3.2.2 Hierarchical distributed control

These simulation results are used the hierarchical distributed control to adjust the traffic signal scheduling with choosing the gamma value  $\gamma = 20000$  in the cost objective (2.19) for an example results. The reason for choosing this case to explain because this case gives better results than the other cases.

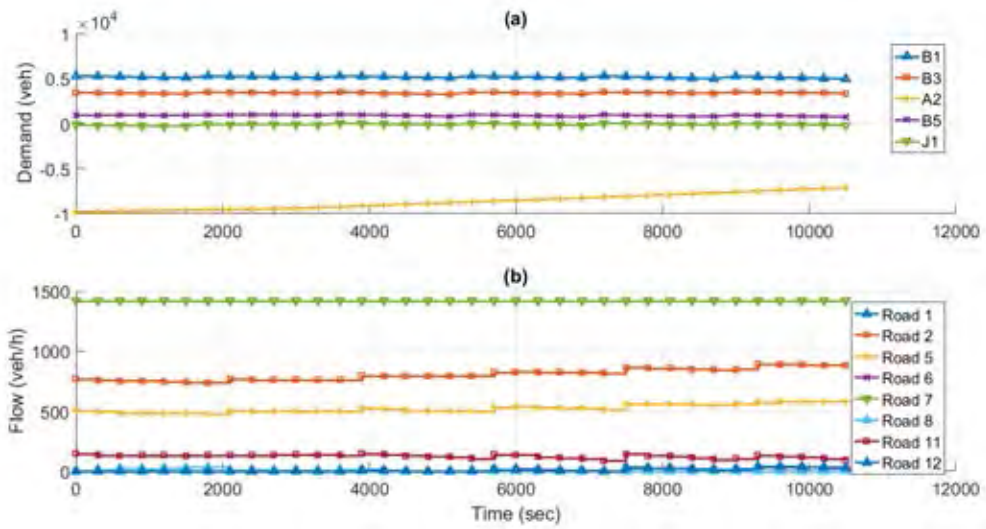


Figure 3.5: Plot of area  $A_1$  on HDC with  $\gamma = 20000$ ; (a) state, (b) control signal.

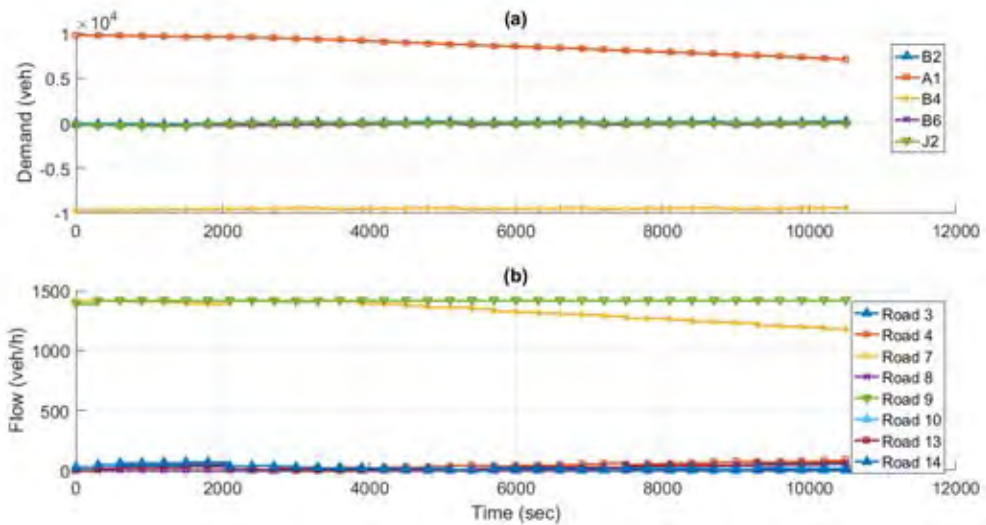


Figure 3.6: Plot of area  $A_2$  on HDC with  $\gamma = 20000$ ; (a) state, (b) control signal.

Figure 3.5(a) and 3.6(a) show the state  $x_{A_i}(t_{A_j})$  of area  $A_1$  and  $A_2$  respectively, and Figure 3.5(b) and 3.6(b) show the optimal traffic flow obtained from (2.30) which has converted the unit to vehicles per hour as given by

$$\text{Optimal flow} = 3600 \times \left[ q_{\max} \frac{u_{A_i}(t_{A_j})}{\|u_{A_i}(t_{A_j})\|_1} \right] \quad \text{for } t_{A_j} = 1, 2, \dots, 36.$$

where  $i$  is the area index, and  $t_{A_j}$  is the sample time index of area layer. Area's state  $x_{A_i}(t_{A_j})$  shown the traffic demand on each node. While the demand is the positive value, the traffic type on these nodes will be the source. In the other hand, if the demand is the negative value, the traffic type on these nodes will be the sink.

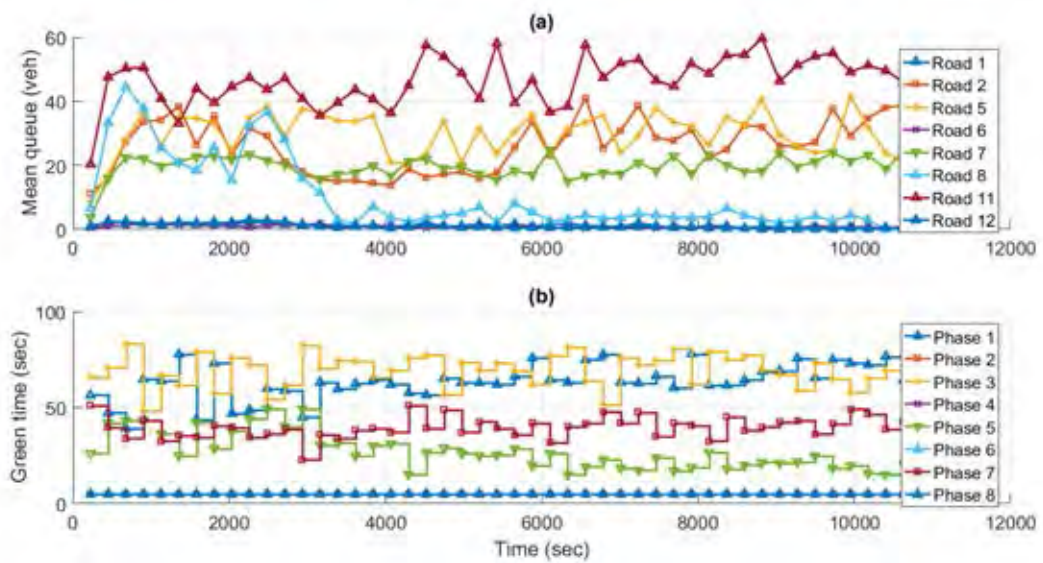


Figure 3.7: Plot of intersection  $J_1$  on HDC with  $\gamma = 20000$ ; (a) state, (b) control signal.

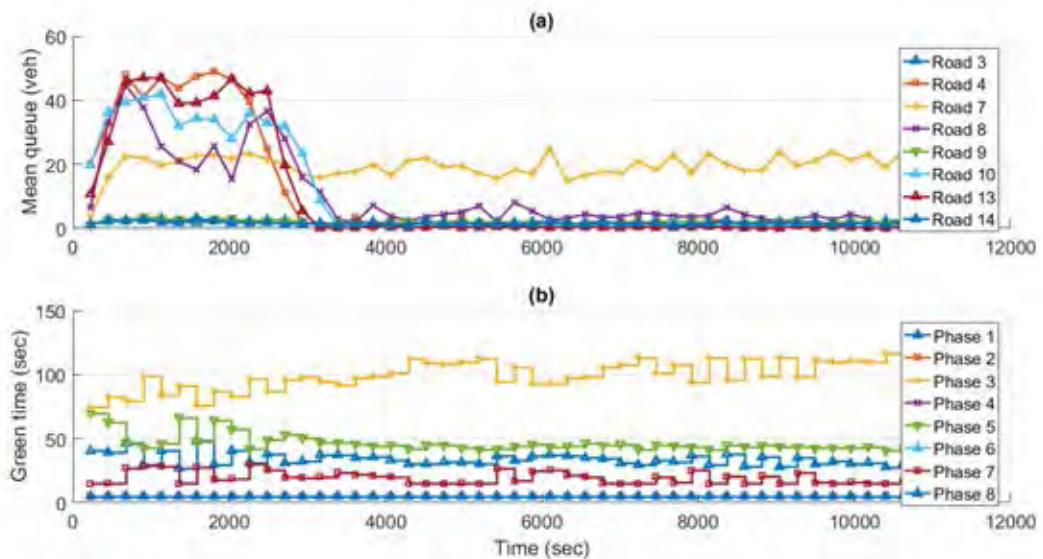


Figure 3.8: Plot of intersection  $J_2$  on HDC with  $\gamma = 20000$ ; (a) state, (b) control signal.

Figure 3.7(a) and 3.8(a) show the average vehicle queue-length  $y_{J_i}(t_{J_i})$  for  $t_{J_i} = 30, 60, \dots, 10800$  seconds, where the average vehicle queue-length  $y_{J_i}(t_{J_i})$  is calculated from (3.1). Figure 3.7(b) and 3.8(b) show the optimal traffic signal obtained from (2.19). In the first moment of simulation, the vehicle queue-length of each road in intersection  $J_2$  which are  $R_4, R_7, R_{10}$ , and  $R_{13}$  are similar volume but the duration of green time in road  $R_7$  is higher than other roads because of the controller is used the demand information that showed the demand on road  $R_7$  is highest.

### 3.2.3 Comparison and summary

This part is compared the results from three cases, first is the results from the FTC, second is the results from HDC with  $\gamma = 0$  and finally, the results from HDC with  $\gamma = 20000$ .

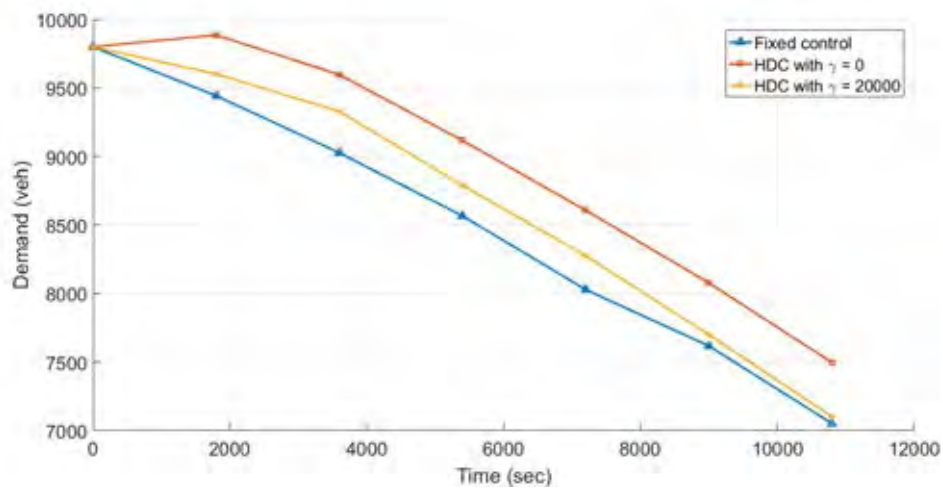


Figure 3.9: Plot of demand on area  $A_1$  with varying  $\gamma$ .

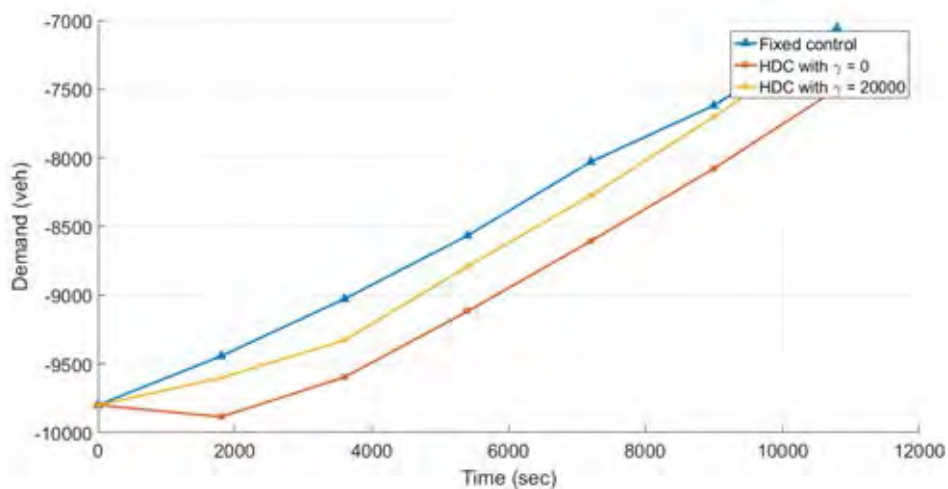


Figure 3.10: Plot of demand on area  $A_2$  with varying  $\gamma$ .

Figure 3.9 and 3.10 is showed the predicted traffic demand  $x_N(t_N)$  on both area for  $t_N = 1, 2, \dots, 6$  with sampling period 1800 seconds. The simulation results show the decay rate to zero of

the FTC which is higher than other control techniques. However, when the simulation ran to a time that the traffic demand was changed, the decay rate of HDC has switched to a higher rate than the FTC. Caused by the traffic signal of the FTC is not adaptive to the traffic demand. Therefore, the traffic flow controller is not provided the optimal traffic signal for every time controls on the changing of traffic demand.

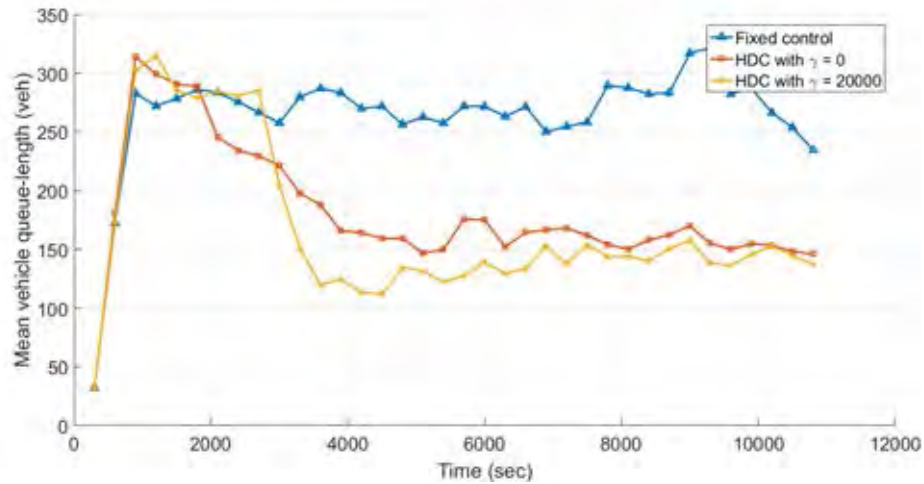


Figure 3.11: Total mean vehicle queue-length comparison on the network.

The total mean vehicle queue-length (TMVQ) of all roads which illustrated in Figure 3.11 on HDC with  $\gamma = 20000$  is calculated by

$$\text{TMVQ}(t_{JCi}) = \sum_{i=1}^N \left\{ \frac{1}{300} \sum_{k=t_{JCi}-30}^{300} y_{Ji}(k) \right\} \quad \text{for } t_{JCi} = 300, 600, \dots, 10800. \quad (3.2)$$

where  $N$  is the number of road in the network, and  $y_{Ji}(k)$  is the output measurement of  $i$ th road at time  $k$ . It's obvious that TMVQ of HDC is lower than fixed time control in each simulation time.

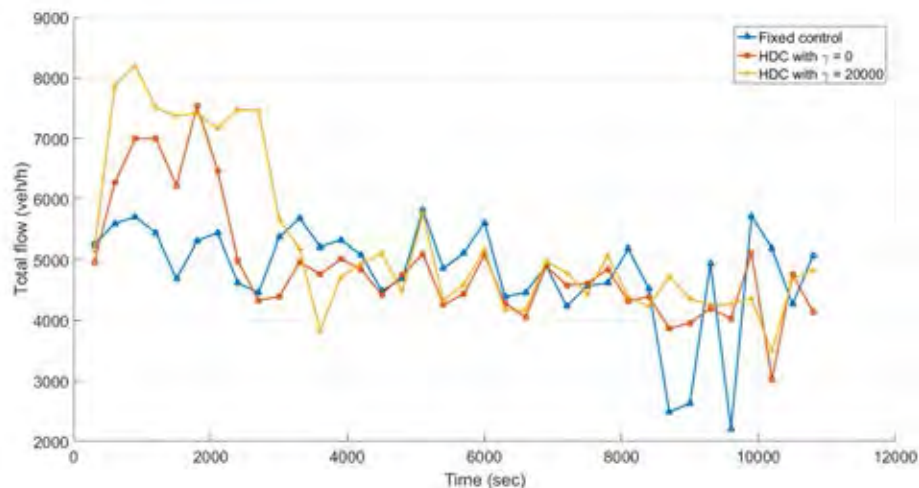


Figure 3.12: Total traffic flow comparison on the network.

However, the comparison of total traffic flow (TTF) of all roads that illustrated in Figure 3.12. on HDC with  $\gamma = 20000$  is calculated by

$$\text{TTF}(t_{JCi}) = \sum_{i=1}^N \left\{ \frac{1}{300} \sum_{k=t_{JCi}-300}^{300} q_i(k) \right\} \quad \text{for } t_{JCi} = 300, 600, \dots, 10800. \quad (3.3)$$

where  $N$  is the number of roads in the network, and  $q_i(k)$  is the flow measurement of  $i$ th road at time  $k$ . It's unclear to predicates that which controller is getting the best performance on TTF.

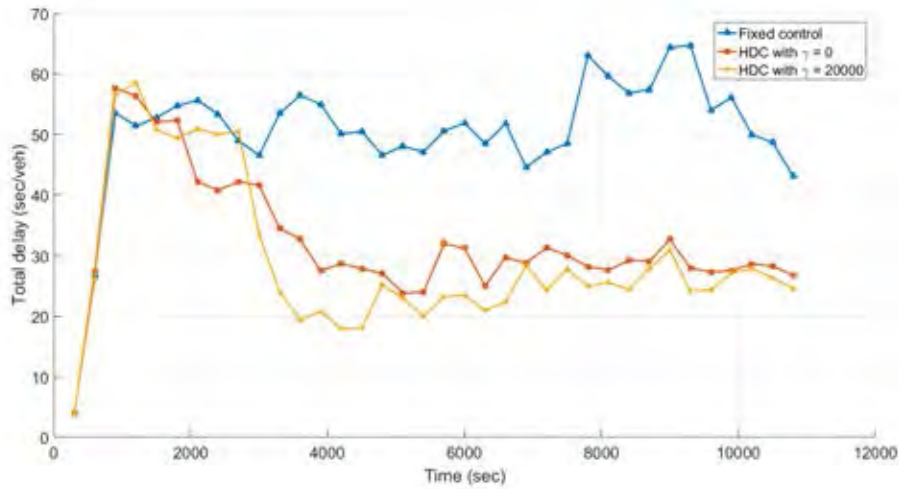


Figure 3.13: Total delay comparison on the network.

The Total delay of all roads which illustrated in Figure 3.13 on HDC with  $\gamma = 20000$  is calculated from (1.14) by using the traffic queue-length approximate from (3.2). The results are still showing the same tend with the total mean vehicle queue-length as Figure 3.11.

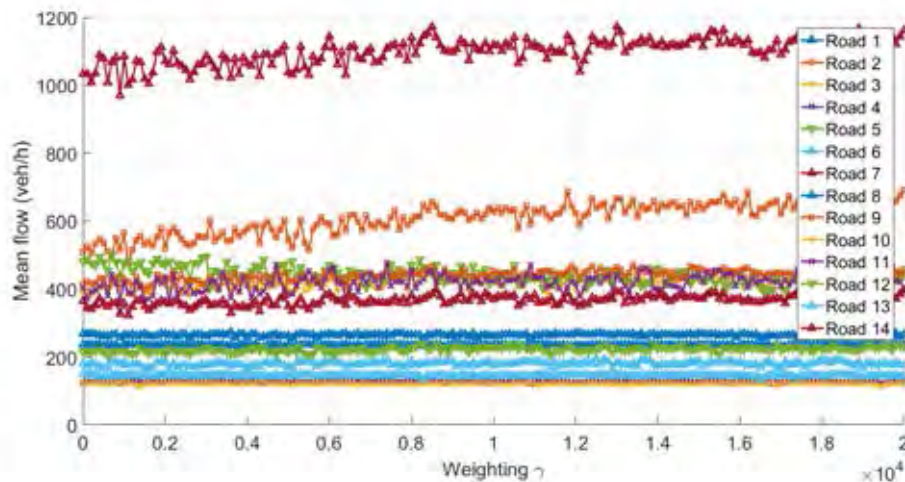


Figure 3.14: Mean traffic flow rate on each road with varying  $\gamma$ .

Figure 3.14 shows the mean traffic flow rate on each road that the road  $R_7$  at highest over other roads in the network. When the mean flow rate on road  $R_7$  is increased, the mean flow rate on certain

roads is also increased. It's meant that the network tries to allocate the traffic flow on each road to an optimal point.

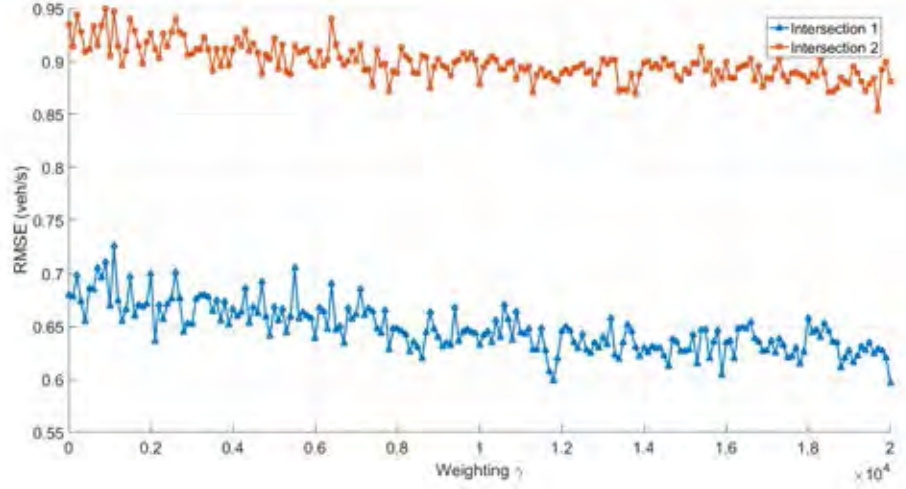


Figure 3.15: RMSE on flow tracking on each intersection.

Figure 3.15 shows the root mean square error (RMSE) between the traffic flow measurement  $q_i(t_{A_j})$  and control signal  $q_i^*(t_{A_j})$  from area layer (2.30) for  $t_{A_j} = 1, 2, \dots, 36$ , which calculated by

$$\text{RMSE} = \sum_{j=1}^{N_{\text{rd}}^{(i)}} \sqrt{\frac{1}{N} \sum_{t_{A_j}=1}^N \left( q_{ij}(t_{A_j}) - q_{ij}^*(t_{A_j}) \right)^2} \quad \text{for } i = 1, 2.$$

where  $N$  is the number of area control index which is 36,  $i$  is the intersection index, and  $N_{\text{rd}}^{(i)}$  is the number of road in  $i$ th intersection which is 8. Figure 3.15 shows the decreasing trend of RMSE in vehicles per second on both intersections when gamma  $\gamma$  is increased. It showed that the second term on cost objective (2.19) is achievable.

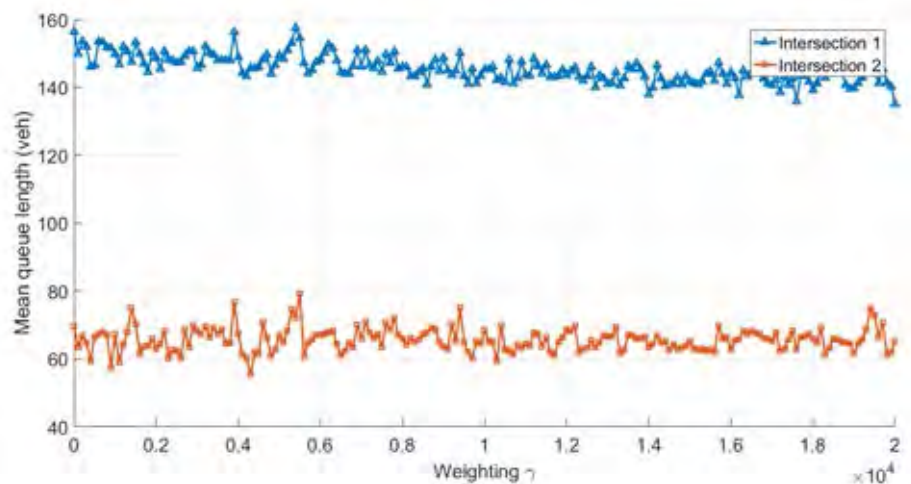


Figure 3.16: Mean vehicle-queue length on each intersection with varying  $\gamma$ .

Also to mean vehicle queue-length (MVQL) that showed as Figure 3.16 which related to the first term in cost objective (2.19). The MVQL of  $i$ th intersection is calculated by

$$\text{MVQL} = \sum_{j=1}^{N_{\text{rd}}^{(i)}} \left\{ \frac{1}{N} \sum_{t_{\text{JC}i}=1}^N \mathbf{y}(t_{\text{JC}i}) \right\} \quad \text{for } i = 1, 2.$$

When gamma  $\gamma$  is increased, the mean vehicle queue length is decreased. It showed that the control references received from the area layer are significant to traffic congestion mitigating.

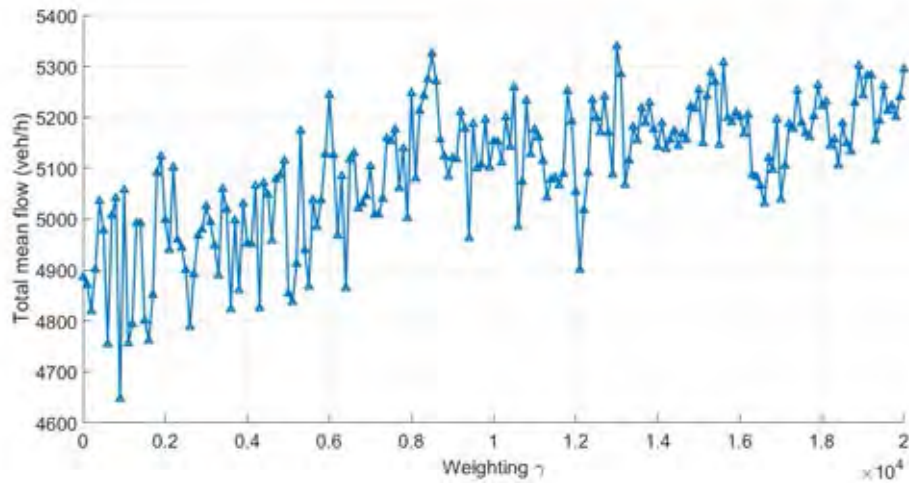


Figure 3.17: Total mean traffic flow on the network.

Figure 3.17. is showed the effect of gamma value  $\gamma$  on TTF in the network on HDC control cases calculated from (3.3). It showed the increasing of TTF over the network when the gamma value  $\gamma$  is increased. It obvious that the gamma value  $\gamma$  in second term of cost objective (2.19) is significant.

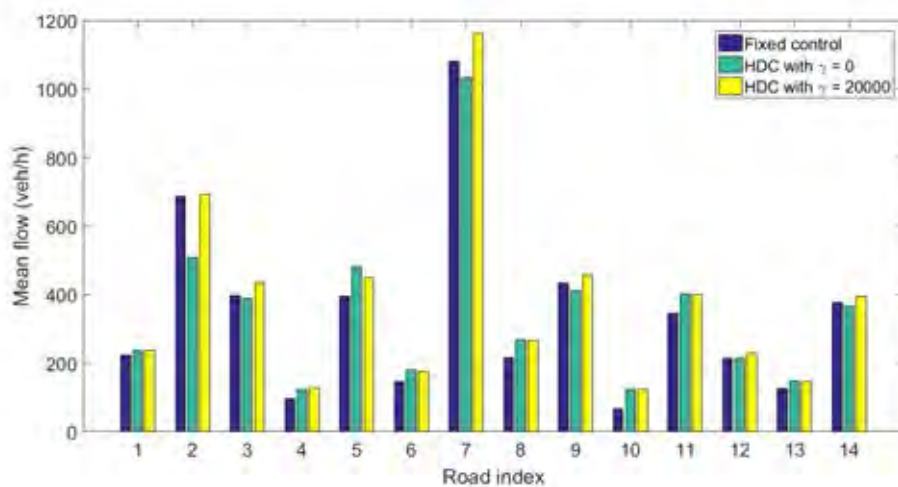


Figure 3.18: Mean traffic flow comparison on each road.

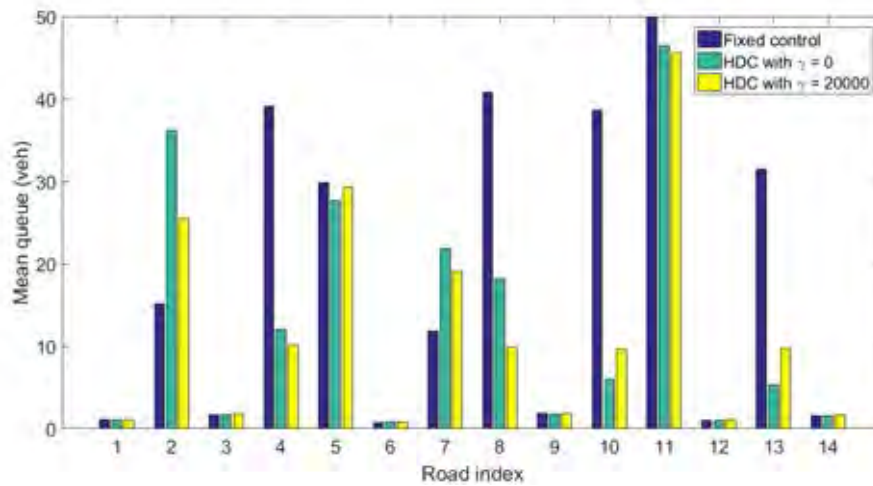


Figure 3.19: Mean vehicle queue-length comparison on each road.

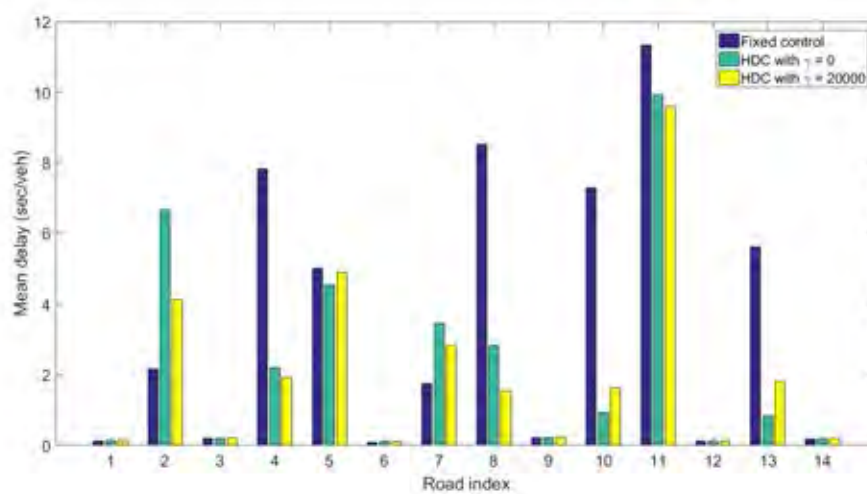


Figure 3.20: Mean delay comparison on each road.

Figure 3.18, 3.19, and 3.20. are showed the mean traffic flow, mean vehicle queue-length, and mean delay of each road comparing with FTC and HDC respectively. While the network employs the HDC, the traffic flow and traffic congestion on a certain road are better but some roads are worse. Because the traffic controllers are concern about the traffic network conditions which made well handle on the overview.

Table 3.4: Summary of simulation results.

| <b>Controller</b>         | <b>Total Mean<br/>Flow (veh/h)</b> | <b>Total Mean<br/>Queue (veh)</b> | <b>Total Mean<br/>Delay (sec/veh)</b> |
|---------------------------|------------------------------------|-----------------------------------|---------------------------------------|
| Fixed Time                | 4,808                              | 264.53                            | 50.42                                 |
| HDC with $\gamma = 0$     | 4,886 (1.61%)                      | 181.52 (-31.38%)                  | 32.37 (-35.80%)                       |
| HDC with $\gamma = 20000$ | 5,171 (7.55%)                      | 157.78 (-40.35%)                  | 29.41 (-41.67%)                       |

The comparison of the mean traffic flow rate on each road is summarized in Table 3.4 which are consist of fixed time control, HDC with  $\gamma = 0$ , and HDC with  $\gamma = 20000$ . The results from HDC with  $\gamma = 20000$  showed the total traffic flow rate inside the network is higher than other control cases and the total mean vehicle queue-length that showed in Figure 3.19 is lower than other control cases. Caused by the length of each road are not equal. Therefore, the improvement of total delay is better than the improvement of total mean vehicle queue-length. That shows the significant improvement when comparing with the fixed time traffic control in this scenario.

## CHAPTER IV

### APPLICATION TO SATHORN MODEL

#### 4.1 Traffic scenario description

This section describes the used scenario of Chula-SSS [31] which is developed on the SUMO platform in an over-saturated Sathorn road network scenario by the team of Associate Professor Chaodit Aswakul, Department of Electrical Engineering, Faculty of Engineering, Chulalongkorn University. This scenario is engulfed of 10 intersections around Sathorn's zone, Bangkok city which is shown on Figures 4.1. The traffic light plans were recorded from the practice which is controlled by Bangkok's traffic police.

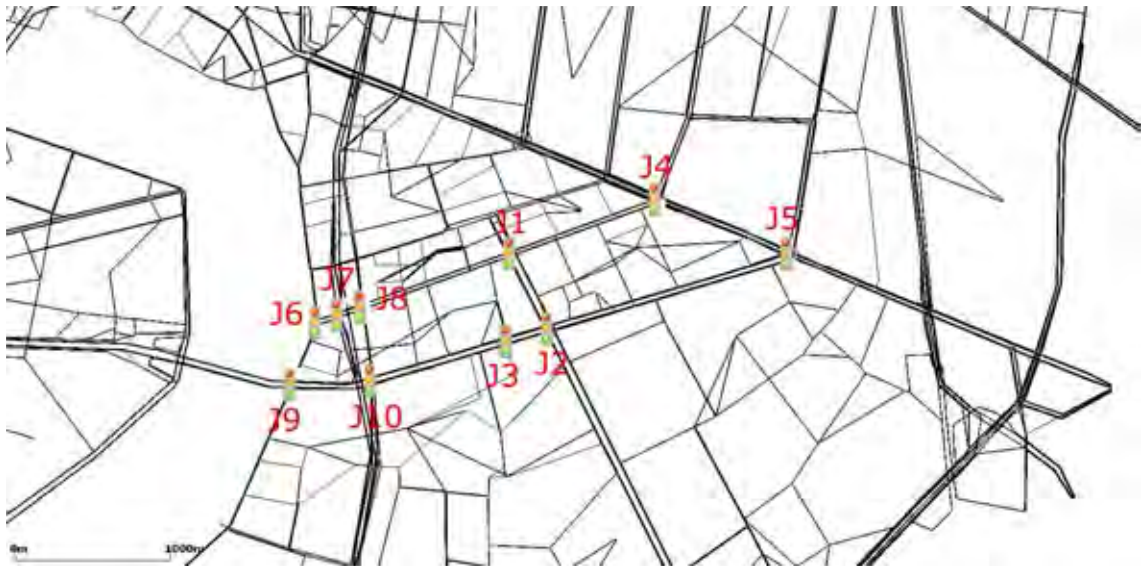


Figure 4.1: Traffic scenario of Sathorn's network.

The scenario is set up on the morning time of rush hour traffic condition from 8 am to 11 am, and the whole input vehicle on the network is around 35,211 vehicles. This work has divided the network into three areas and defined 10 boundaries as illustrates in Figure 4.2 which are divided by considering the distance between intersections. This work has placed the inductor loop detectors on the stop line of incoming direction road to an intersection, 150 meters from the stop line for measuring the queue length, and the entrance point of the outcome direction road on an intersection. The performance measurement is measured by observing the departure flow rate (veh/h) on each intersection. The average performance of the Fixed control case which recorded from traffic police is 25,940 veh/h.

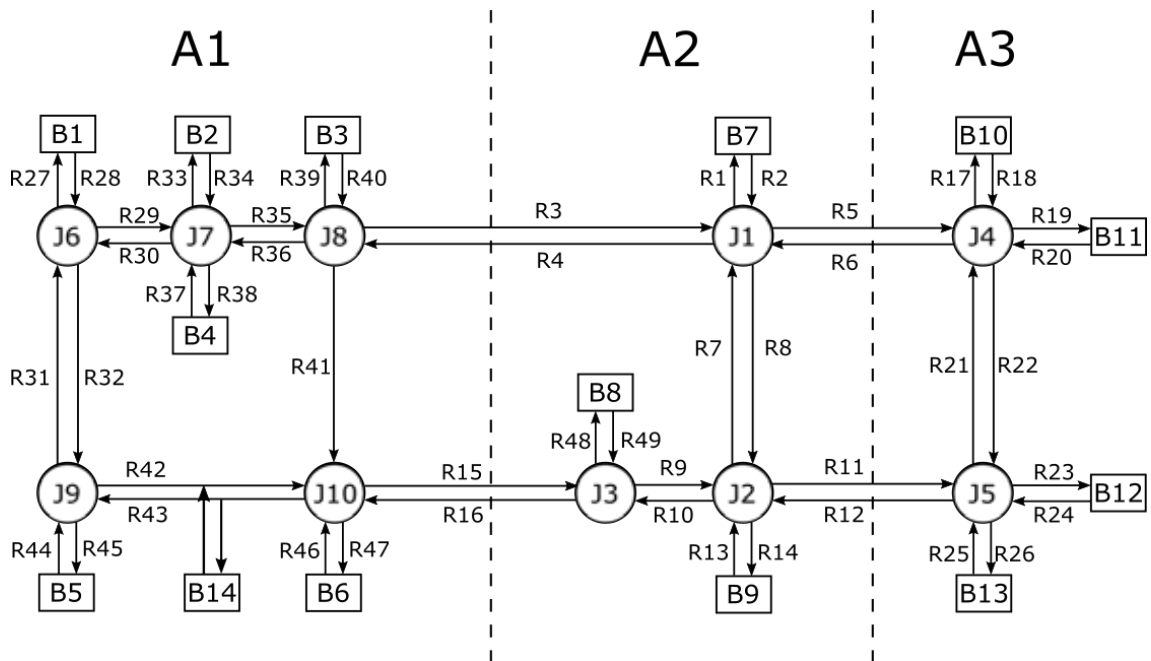


Figure 4.2: Area allocation on a scenario of Sathorn's network.

The objective of this work is to increase the ability of traffic flow on the network. Then, the designed controller in this work will be compared to performance with a Fixed control case. We summarized the traffic demand information (veh) of the boundaries in the network which obtained from the measurement into Table 4.1.

Table 4.1: Summary of traffic demand (veh/h) on the boundaries (outer area).

| Node | Source | Sink | Node | Source | Sink | Node | Source | Sink  |
|------|--------|------|------|--------|------|------|--------|-------|
| B1   | 0      | 0    | B6   | 847    | 517  | B11  | 660    | 374   |
| B2   | 374    | 0    | B7   | 297    | 484  | B12  | 1,100  | 1,254 |
| B3   | 737    | 0    | B8   | 0      | 0    | B13  | 1,727  | 880   |
| B4   | 330    | 0    | B9   | 484    | 704  | B14  | 1,551  | 1,353 |
| B5   | 660    | 1900 | 704  | 627    | 935  |      |        |       |

The next following part will describe the intersection information which is consist of traffic light patterns, splitting flows and intersection capacity.

### Configuration of intersection $J_1$ (Nararom)

The traffic light signal of intersection  $J_1$  is configured at 3 phases which is showed on Figure 4.3. This intersection is consists of 4 incoming roads  $R_{in} = \{R_2, R_3, R_6, R_7\}$  and 4 outcome roads  $R_{out} = \{R_1, R_2, R_4, R_8\}$ . This intersection has the capacity  $C_{int,i}^1 = 3,000$  veh/h which is measured from Fixed control case.

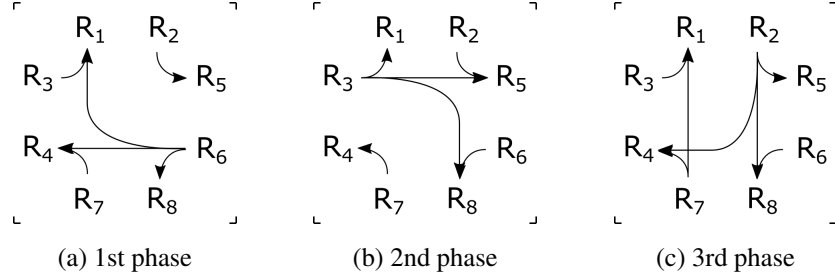


Figure 4.3: The traffic light pattern of intersection  $J_1$ .

The set of available lanes  $\mathcal{A}_k$  on intersection  $J_1$  which are showed as Figure 4.3 are defined as follows:

$$\mathcal{A}_1 = \{(R_2, 1), (R_2, 2), (R_2, 3), (R_5, 1)\}$$

$$\mathcal{A}_2 = \{(R_5, 1)\}$$

$$\mathcal{A}_3 = \{(R_5, 1), (R_5, 2), (R_5, 3), (R_4, 1)\}$$

The set of available sources  $\mathcal{S}_i$  of road  $R_i$  on intersection  $J_1$  which are showed as Figure 4.3 are defined as follows:

$$\mathcal{S}_1 = \{(R_3, 1), (R_7, 2), (R_6, 3)\}$$

$$\mathcal{S}_2 = \{\phi\}$$

$$\mathcal{S}_3 = \{\phi\}$$

$$\mathcal{S}_4 = \{(R_7, 1), (R_6, 2), (R_2, 3)\}$$

$$\mathcal{S}_5 = \{(R_2, 1), (R_3, 2)\}$$

$$\mathcal{S}_6 = \{\phi\}$$

$$\mathcal{S}_7 = \{\phi\}$$

$$\mathcal{S}_8 = \{(R_6, 1), (R_2, 2), (R_3, 3)\}$$

The splitting ratio  $p_i$  of road  $R_i$  on intersection  $J_1$  are obtained from Eq (2.8) with the measurement data which are given as follows:

$$p_1 = [1]^T$$

$$p_2 = [0.716, 0.284, 0.0]^T$$

$$p_3 = [0.247, 0.449, 0.304]^T$$

$$p_4 = [1]^T$$

$$p_5 = [1]^T$$

$$p_6 = [0.434, 0.305, 0.261]^T$$

$$p_7 = [0.675, 0.325, 0.0]^T$$

$$p_8 = [1]^T$$

The traffic light constraints of intersection  $J_1$  are defined as follows:

$$\rho_{fix,1} = []$$

$$\tau_{fix,1} = [0, 0, 0]$$

$$\tau_{min,1} = [15, 15, 15]$$

$$\tau_{max,1} = [90, 90, 90]$$

$$\tau_1 = 150$$

### Configuration of intersection $J_2$ (Narinthon)

The traffic light signal of intersection  $J_2$  is configured at 4 phases which is showed on Figure 4.4. This intersection is consists of 4 incoming roads  $R_{in} = \{R_8, R_9, R_{12}, R_{13}\}$  and 4 outcome roads  $R_{out} = \{R_7, R_{10}, R_{11}, R_{14}\}$ . This intersection has the capacity  $C_{int,i}^2 = 4,800$  veh/h which is measured from Fixed control case.

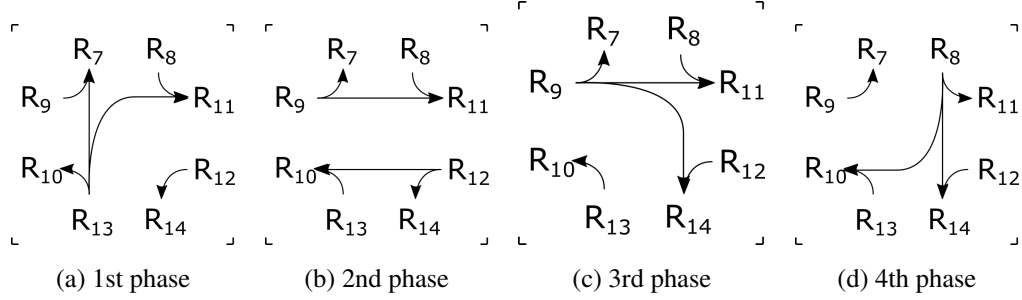


Figure 4.4: The traffic light pattern of intersection  $J_2$ .

The set of available lanes  $\mathcal{A}_k$  on intersection  $J_2$  which are showed as Figure 4.4 are defined as follows:

$$\begin{aligned}\mathcal{A}_1 &= \{(R_8, 1), (R_9, 1), (R_{12}, 1), (R_{13}, 1), (R_{13}, 2), (R_{13}, 3)\} \\ \mathcal{A}_2 &= \{(R_8, 1), (R_9, 1), (R_{12}, 1), (R_{13}, 1), (R_9, 2), (R_{12}, 2)\} \\ \mathcal{A}_3 &= \{(R_8, 1), (R_9, 1), (R_{12}, 1), (R_{13}, 1), (R_9, 2), (R_9, 3)\} \\ \mathcal{A}_4 &= \{(R_8, 1), (R_9, 1), (R_{12}, 1), (R_{13}, 1), (R_8, 2), (R_8, 3)\}\end{aligned}$$

The set of available sources  $\mathcal{S}_i$  of road  $R_i$  on intersection  $J_2$  which are showed as Figure 4.4 are defined as follows:

$$\begin{aligned}\mathcal{S}_7 &= \{(R_9, 1), (R_{13}, 2)\} & \mathcal{S}_8 &= \{\phi\} & \mathcal{S}_9 &= \{\phi\} \\ \mathcal{S}_{10} &= \{(R_{13}, 1), (R_{12}, 2), (R_8, 3)\} & \mathcal{S}_{11} &= \{(R_8, 1), (R_9, 2), (R_{13}, 3)\} & \mathcal{S}_{12} &= \{\phi\} \\ \mathcal{S}_{13} &= \{\phi\} & \mathcal{S}_{14} &= \{(R_{12}, 1), (R_8, 2), (R_9, 3)\}\end{aligned}$$

The splitting ratio  $p_i$  of road  $R_i$  on intersection  $J_2$  are obtained from Eq (2.8) with the measurement data which are given as follows:

$$\begin{aligned}p_7 &= [1]^T & p_8 &= [0.535, 0.288, 0.177]^T & p_9 &= [0.676, 0.269, 0.055]^T \\ p_{10} &= [1]^T & p_{11} &= [1]^T & p_{12} &= [0.696, 0.304, 0.0]^T \\ p_{13} &= [0.731, 0.093, 0.176]^T & p_{14} &= [1]^T\end{aligned}$$

The traffic light constraints of intersection  $J_2$  are defined as follows:

$$\begin{aligned}\rho_{\text{fix},2} &= [] & \tau_{\text{fix},2} &= [0, 0, 0, 0] \\ \tau_{\text{min},2} &= [15, 15, 15, 15] & \tau_{\text{max},2} &= [90, 90, 90, 90] \\ \tau_2 &= 135\end{aligned}$$

### Configuration of intersection $J_3$ (Sathorn - Pan)

The traffic light signal of intersection  $J_3$  is configured at 3 phases which is showed on Figure 4.4. This intersection is consists of 3 incoming roads  $R_{in} = \{R_{10}, R_{15}, R_{49}\}$  and 3 outcome roads  $R_{out} = \{R_9, R_{16}, R_{49}\}$ . This intersection has the capacity  $C_{int,i}^3 = 4,200$  veh/h which is measured from Fixed control case.

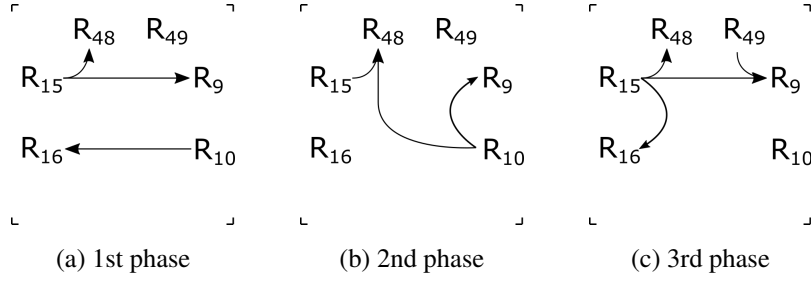


Figure 4.5: The traffic light pattern of intersection  $J_3$ .

The set of available lanes  $\mathcal{A}_k$  on intersection  $J_3$  which are showed as Figure 4.5 are defined as follows:

$$\mathcal{A}_1 = \{(R_{15}, 1), (R_{15}, 2), (R_{10}, 1)\}$$

$$\mathcal{A}_2 = \{(R_{15}, 1), (R_{10}, 2), (R_{10}, 3)\}$$

$$\mathcal{A}_3 = \{(R_{15}, 1), (R_{15}, 2), (R_{15}, 3), (R_{49}, 1)\}$$

The set of available sources  $\mathcal{S}_i$  of road  $R_i$  on intersection  $J_3$  which are showed as Figure 4.5 are defined as follows:

$$\mathcal{S}_9 = \{(R_{10}, 2), (R_{15}, 2)\}$$

$$\mathcal{S}_{10} = \{\phi\}$$

$$\mathcal{S}_{15} = \{\phi\}$$

$$\mathcal{S}_{16} = \{(R_{10}, 1), (R_{15}, 2)\}$$

$$\mathcal{S}_{48} = \{(R_{10}, 2), (R_{15}, 1)\}$$

$$\mathcal{S}_{49} = \{\phi\}$$

The splitting ratio  $p_i$  of road  $R_i$  on intersection  $J_3$  are obtained from Eq (2.8) with the measurement data which are given as follows:

$$p_9 = [1]^T$$

$$p_{10} = [0.616, 0.186, 0.198]^T$$

$$p_{15} = [0.132, 0.868, 0.0]^T$$

$$p_{16} = [1]^T$$

$$p_{48} = [1]^T$$

$$p_{49} = [1]^T$$

The traffic light constraints of intersection  $J_3$  are defined as follows:

$$\rho_{\text{fix},3} = [2, 4]$$

$$\tau_{\text{fix},3} = [0, 3, 0, 3, 0]$$

$$\tau_{\text{min},3} = [15, 3, 15, 3, 15]$$

$$\tau_{\text{max},3} = [90, 3, 90, 3, 90]$$

$$\tau_3 = 150$$

### Configuration of intersection $J_4$ (Sala Daeng)

The traffic light signal of intersection  $J_4$  is configured at 5 phases which are shown in Figure 4.6. This intersection consists of 4 incoming roads  $R_{in} = \{R_5, R_{18}, R_{20}, R_{21}\}$  and 4 outcome roads  $R_{out} = \{R_6, R_{17}, R_{19}, R_{22}\}$ . This intersection has the capacity  $C_{int,i}^4 = 2,500$  veh/h which is measured from Fixed control case.

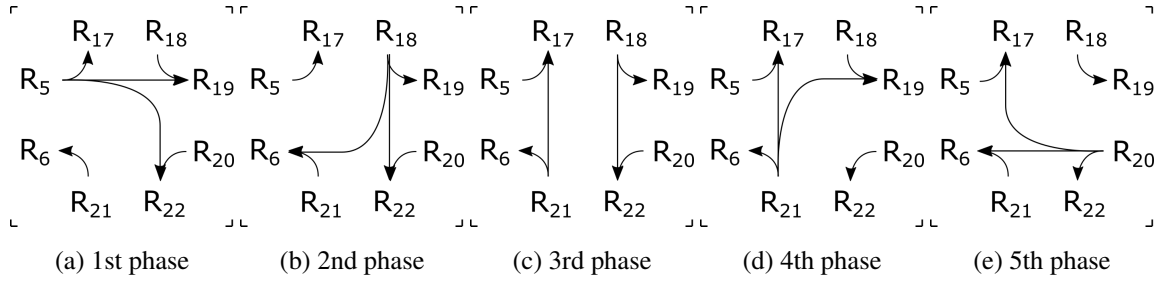


Figure 4.6: The traffic light pattern of intersection  $J_4$ .

The set of available lanes  $\mathcal{A}_k$  on intersection  $J_4$  which are showed as Figure 4.6 are defined as follows:

$$\begin{aligned}\mathcal{A}_1 &= \{(R_5, 1), (R_{18}, 1), (R_{20}, 1), (R_{21}, 1), (R_5, 2), (R_5, 3)\} \\ \mathcal{A}_2 &= \{(R_5, 1), (R_{18}, 1), (R_{20}, 1), (R_{21}, 1), (R_{18}, 2), (R_{18}, 3)\} \\ \mathcal{A}_3 &= \{(R_5, 1), (R_{18}, 1), (R_{20}, 1), (R_{21}, 1), (R_{18}, 2), (R_{21}, 2)\} \\ \mathcal{A}_4 &= \{(R_5, 1), (R_{18}, 1), (R_{20}, 1), (R_{21}, 1), (R_{21}, 2), (R_{21}, 3)\} \\ \mathcal{A}_5 &= \{(R_5, 1), (R_{18}, 1), (R_{20}, 1), (R_{21}, 1), (R_{20}, 2), (R_{17}, 3)\}\end{aligned}$$

The set of available sources  $\mathcal{S}_i$  of road  $R_i$  on intersection  $J_4$  which are showed as Figure 4.6 are defined as follows:

$$\begin{aligned}\mathcal{S}_5 &= \{\phi\} & \mathcal{S}_6 &= \{(R_{21}, 1), (R_{20}, 2), (R_{18}, 3)\} & \mathcal{S}_{17} &= \{(R_5, 1), (R_{21}, 2), (R_{20}, 3)\} \\ \mathcal{S}_{18} &= \{\phi\} & \mathcal{S}_{19} &= \{(R_{18}, 1), (R_5, 2), (R_{21}, 3)\} & \mathcal{S}_{20} &= \{\phi\} \\ \mathcal{S}_{21} &= \{\phi\} & \mathcal{S}_{22} &= \{(R_{20}, 1), (R_{18}, 2), (R_5, 3)\}\end{aligned}$$

The splitting ratio  $p_i$  of road  $R_i$  on intersection  $J_4$  are obtained from Eq (2.8) with the measurement data which are given as follows:

$$\begin{aligned}p_5 &= [0.691, 0.309, 0.0]^T & p_6 &= [1]^T & p_{17} &= [1]^T \\ p_{18} &= [0.234, 0.427, 0.339]^T & p_{19} &= [1]^T & p_{20} &= [0.378, 0.285, 0.336]^T \\ p_{21} &= [0.440, 0.559, 0.001]^T & p_{22} &= [1]^T\end{aligned}$$

The traffic light constraints of intersection  $J_4$  are defined as follows:

$$\rho_{\text{fix},4} = [], \quad \tau_{\text{fix},4} = [0, 0, 0, 0, 0], \quad \tau_{\text{min},4} = [15, 15, 15, 15, 15], \quad \tau_{\text{max},4} = [50, 50, 50, 50, 50], \quad \tau_4 = 150.$$

### Configuration of intersection $J_5$ (Witthayu)

The traffic light signal of intersection  $J_5$  is configured at 4 phases which are shown in Figure 4.7. This intersection consists of 4 incoming roads  $R_{in} = \{R_{11}, R_{22}, R_{24}, R_{25}\}$  and 4 outcome roads  $R_{out} = \{R_{12}, R_{21}, R_{23}, R_{26}\}$ . This intersection has the capacity  $C_{int,i}^5 = 3,000$  veh/h which is measured from Fixed control case.

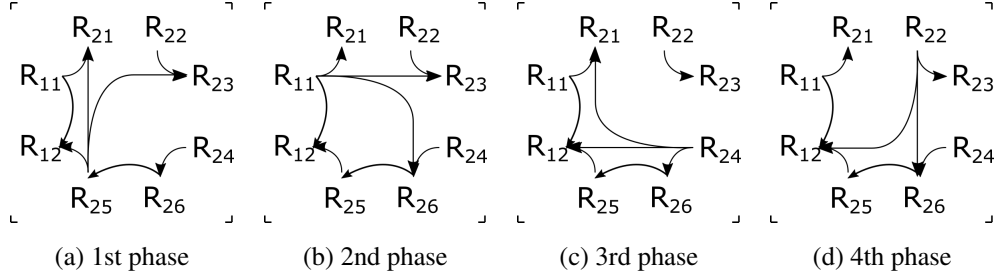


Figure 4.7: The traffic light pattern of intersection  $J_5$ .

The set of available lanes  $\mathcal{A}_k$  on intersection  $J_4$  which are showed as Figure 4.6 are defined as follows:

$$\mathcal{A}_1 = \{(R_{11}, 1), (R_{11}, 4), (R_{22}, 1), (R_{24}, 1), (R_{25}, 1), (R_{25}, 4), (R_{25}, 3)\}$$

$$\mathcal{A}_2 = \{(R_{11}, 1), (R_{11}, 4), (R_{22}, 1), (R_{24}, 1), (R_{25}, 1), (R_{25}, 4), (R_{11}, 2), (R_{11}, 3)\}$$

$$\mathcal{A}_3 = \{(R_{11}, 1), (R_{11}, 4), (R_{22}, 1), (R_{24}, 1), (R_{25}, 1), (R_{25}, 4), (R_{24}, 2), (R_{24}, 3)\}$$

$$\mathcal{A}_4 = \{(R_{11}, 1), (R_{11}, 4), (R_{22}, 1), (R_{24}, 1), (R_{25}, 1), (R_{25}, 4), (R_{22}, 2), (R_{22}, 3)\}$$

The set of available sources  $\mathcal{S}_i$  of road  $R_i$  on intersection  $J_4$  which are showed as Figure 4.6 are defined as follows:

$$\mathcal{S}_{11} = \{\phi\}$$

$$\mathcal{S}_{12} = \{(R_{25}, 1), (R_{24}, 2), (R_{22}, 3), (R_{11}, 4)\}$$

$$\mathcal{S}_{21} = \{(R_{11}, 1), (R_{25}, 2), (R_{24}, 3)\}$$

$$\mathcal{S}_{22} = \{\phi\}$$

$$\mathcal{S}_{23} = \{(R_{22}, 1), (R_{11}, 2), (R_{25}, 3)\}$$

$$\mathcal{S}_{24} = \{\phi\}$$

$$\mathcal{S}_{25} = \{\phi\}$$

$$\mathcal{S}_{26} = \{(R_{24}, 1), (R_{22}, 2), (R_{11}, 3), (R_{25}, 4)\}$$

The splitting ratio  $p_i$  of road  $R_i$  on intersection  $J_4$  are obtained from Eq (2.8) with the measurement data which are given as follows:

$$p_{11} = [0.099, 0.340, 0.184, 0.377]^T$$

$$p_{12} = [1]^T$$

$$p_{21} = [1]^T$$

$$p_{22} = [0.842, 0.0, 0.158]^T$$

$$p_{23} = [1]^T$$

$$p_{24} = [0.623, 0.312, 0.064]^T$$

$$p_{25} = [0.721, 0.0, 0.211, 0.068]^T$$

$$p_{26} = [1]^T$$

The traffic light constraints of intersection  $J_5$  are defined as follows:

$$\rho_{fix,5} = [], \quad \tau_{fix,5} = [0, 0, 0, 0, 0], \quad \tau_{min,5} = [15, 15, 15, 15], \quad \tau_{max,5} = [60, 60, 60, 60], \quad \tau_5 = 150.$$

### Configuration of intersection $J_6$ (Bang Rak)

The traffic light signal of intersection  $J_6$  is configured at 3 phases which are shown in Figure 4.8. This intersection consists of 3 incoming roads  $R_{in} = \{R_{28}, R_{30}, R_{31}\}$  and 3 outcome roads  $R_{out} = \{R_{27}, R_{29}, R_{32}\}$ . This intersection has the capacity  $C_{int,i}^6 = 800$  veh/h which is measured from Fixed control case.

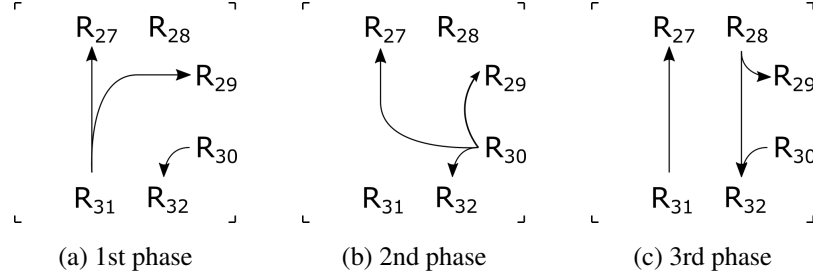


Figure 4.8: The traffic light pattern of intersection  $J_6$ .

The set of available lanes  $\mathcal{A}_k$  on intersection  $J_6$  which are showed as Figure 4.8 are defined as follows:

$$\mathcal{A}_1 = \{(R_{30}, 1), (R_{31}, 1), (R_{31}, 2)\}$$

$$\mathcal{A}_2 = \{(R_{30}, 1), (R_{30}, 2), (R_{30}, 3)\}$$

$$\mathcal{A}_3 = \{(R_{30}, 1), (R_{31}, 1), (R_{28}, 2)\}$$

The set of available sources  $\mathcal{S}_i$  of road  $R_i$  on intersection  $J_6$  which are showed as Figure 4.8 are defined as follows:

$$\mathcal{S}_{27} = \{(R_{31}, 1), (R_{30}, 2)\}$$

$$\mathcal{S}_{28} = \{\phi\}$$

$$\mathcal{S}_{29} = \{(R_{28}, 1), (R_{31}, 2), (R_{30}, 3)\}$$

$$\mathcal{S}_{30} = \{\phi\}$$

$$\mathcal{S}_{31} = \{\phi\}$$

$$\mathcal{S}_{32} = \{(R_{30}, 1), (R_{28}, 2)\}$$

The splitting ratio  $p_i$  of road  $R_i$  on intersection  $J_4$  are obtained from Eq (2.8) with the measurement data which are given as follows:

$$p_{27} = [1]^T$$

$$p_{28} = [0.5, 0.5]^T$$

$$p_{29} = [1]^T$$

$$p_{30} = [0.821, 0.075, 0.104]^T$$

$$p_{31} = [0.057, 0.942]^T$$

$$p_{32} = [1]^T$$

The traffic light constraints of intersection  $J_6$  are defined as follows:

$$\rho_{fix,6} = []$$

$$\tau_{fix,6} = [0, 0, 0]$$

$$\tau_{min,6} = [15, 15, 15]$$

$$\tau_{max,6} = [60, 60, 60]$$

$$\tau_6 = 165$$

### Configuration of intersection $J_7$ (Duan Si Lom)

The traffic light signal of intersection  $J_7$  is configured at 3 phases which are shown in Figure 4.9. This intersection consists of 4 incoming roads  $R_{in} = \{R_{29}, R_{34}, R_{36}, R_{37}\}$  and 4 outcome roads  $R_{out} = \{R_{30}, R_{33}, R_{35}, R_{38}\}$ . This intersection has the capacity  $C_{int,i}^7 = 1,700$  veh/h which is measured from Fixed control case.

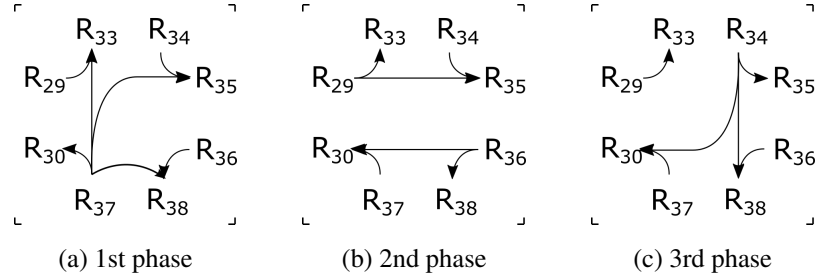


Figure 4.9: The traffic light pattern of intersection  $J_7$ .

The set of available lanes  $\mathcal{A}_k$  on intersection  $J_7$  which are showed as Figure 4.9 are defined as follows:

$$\mathcal{A}_1 = \{(R_{29}, 1), (R_{34}, 1), (R_{36}, 1), (R_{37}, 1), (R_{37}, 2), (R_{37}, 3), (R_{37}, 4)\}$$

$$\mathcal{A}_2 = \{(R_{29}, 1), (R_{34}, 1), (R_{36}, 1), (R_{37}, 1), (R_{29}, 2), (R_{36}, 2)\}$$

$$\mathcal{A}_3 = \{(R_{29}, 1), (R_{34}, 1), (R_{36}, 1), (R_{37}, 1), (R_{34}, 2), (R_{34}, 3)\}$$

The set of available sources  $\mathcal{S}_i$  of road  $R_i$  on intersection  $J_7$  which are showed as Figure 4.9 are defined as follows:

$$\mathcal{S}_{29} = \{\phi\}$$

$$\mathcal{S}_{30} = \{(R_{37}, 1), (R_{36}, 2), (R_{34}, 3)\}$$

$$\mathcal{S}_{33} = \{(R_{29}, 1), (R_{37}, 2)\}$$

$$\mathcal{S}_{34} = \{\phi\}$$

$$\mathcal{S}_{35} = \{(R_{34}, 1), (R_{29}, 2), (R_{37}, 3)\}$$

$$\mathcal{S}_{36} = \{\phi\}$$

$$\mathcal{S}_{37} = \{\phi\}$$

$$\mathcal{S}_{38} = \{(R_{36}, 1), (R_{34}, 2), (R_{37}, 4)\}$$

The splitting ratio  $p_i$  of road  $R_i$  on intersection  $J_7$  are obtained from Eq (2.8) with the measurement data which are given as follows:

$$p_{29} = [0.518, 0.482]^T$$

$$p_{30} = [1]^T$$

$$p_{33} = [1]^T$$

$$p_{34} = [0.758, 0.0, 0.242]^T$$

$$p_{35} = [1]^T$$

$$p_{36} = [0.437, 0.563]^T$$

$$p_{37} = [0.238, 0.0162, 0.745, 0.001]^T$$

$$p_{38} = [1]^T$$

The traffic light constraints of intersection  $J_7$  are defined as follows:

$$\rho_{fix,7} = []$$

$$\tau_{fix,7} = [0, 0, 0]$$

$$\tau_{min,7} = [15, 15, 15]$$

$$\tau_{max,7} = [60, 40, 60]$$

$$\tau_7 = 150$$

### Configuration of intersection $J_8$ (Surasak)

The traffic light signal of intersection  $J_8$  is configured at 4 phases which are shown in Figure 4.10. This intersection consists of 3 incoming roads  $R_{in} = \{R_4, R_{35}, R_{40}\}$  and 4 outcome roads  $R_{out} = \{R_3, R_{36}, R_{39}, R_{41}\}$ . This intersection has the capacity  $C_{int,i}^8 = 2,900$  veh/h which is measured from Fixed control case.

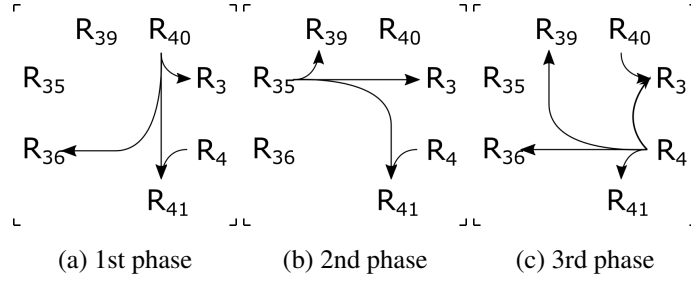


Figure 4.10: The traffic light pattern of intersection  $J_8$ .

The set of available lanes  $\mathcal{A}_k$  on intersection  $J_8$  which are shown as Figure 4.10 are defined as follows:

$$\mathcal{A}_1 = \{(R_4, 1), (R_{40}, 1), (R_{40}, 2), (R_{40}, 3)\}$$

$$\mathcal{A}_2 = \{(R_4, 1), (R_{40}, 1), (R_{35}, 1), (R_{35}, 2), (R_{35}, 3)\}$$

$$\mathcal{A}_3 = \{(R_4, 1), (R_{40}, 1), (R_4, 2), (R_4, 3), (R_4, 4)\}$$

The set of available sources  $\mathcal{S}_i$  of road  $R_i$  on intersection  $J_8$  which are shown as Figure 4.10 are defined as follows:

$$\mathcal{S}_3 = \{(R_{40}, 1), (R_{35}, 2), (R_4, 4)\}$$

$$\mathcal{S}_4 = \{\phi\}$$

$$\mathcal{S}_{35} = \{\phi\}$$

$$\mathcal{S}_{36} = \{(R_4, 2), (R_{40}, 3)\}$$

$$\mathcal{S}_{39} = \{(R_{18}, 1), (R_5, 2), (R_{21}, 3)\}$$

$$\mathcal{S}_{40} = \{(R_{35}, 1), (R_4, 3)\}$$

$$\mathcal{S}_{41} = \{(R_4, 1), (R_{40}, 2), (R_{35}, 3)\}$$

The splitting ratio  $p_i$  of road  $R_i$  on intersection  $J_8$  are obtained from Eq (2.8) with the measurement data which are given as follows:

$$p_3 = [1]^T \quad p_4 = [0.586, 0.292, 0.122, 0.0]^T \quad p_{35} = [0.1017, 0.562, 0.337]^T$$

$$p_{36} = [1]^T \quad p_{39} = [1]^T \quad p_{40} = [0.306, 0.299, 0.395]^T$$

$$p_{41} = [1]^T$$

The traffic light constraints of intersection  $J_8$  are defined as follows:

$$\rho_{\text{fix},8} = [], \quad \tau_{\text{fix},8} = [0, 0, 0], \quad \tau_{\text{min},8} = [15, 15, 15], \quad \tau_{\text{max},8} = [80, 50, 80], \quad \tau_8 = 150.$$

### Configuration of intersection $J_9$ (Chaloem Phan)

The traffic light signal of intersection  $J_9$  is configured at 6 phases which are shown in Figure 4.11. This intersection consists of 3 incoming roads  $R_{in} = \{R_{32}, R_{43}, R_{44}\}$  and 3 outcome roads  $R_{out} = \{R_{31}, R_{42}, R_{45}\}$ . This intersection has the capacity  $C_{int,i}^9 = 1,600$  veh/h which is measured from Fixed control case.

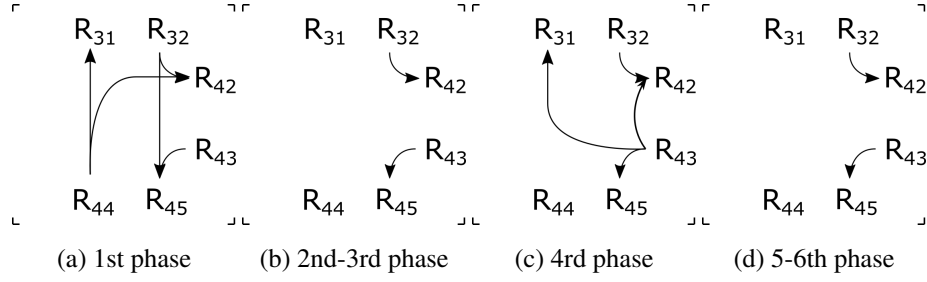


Figure 4.11: The traffic light pattern of intersection  $J_9$ .

The set of available lanes  $\mathcal{A}_k$  on intersection  $J_9$  which are showed as Figure 4.11 are defined as follows:

$$\begin{aligned} \mathcal{A}_1 &= \{(R_{32}, 1), (R_{43}, 1), (R_{32}, 2), (R_{44}, 1), (R_{44}, 2)\} & \mathcal{A}_2 &= \{(R_{32}, 1), (R_{43}, 1)\} \\ \mathcal{A}_4 &= \{(R_{32}, 1), (R_{43}, 1), (R_{43}, 2), (R_{43}, 3)\} & \mathcal{A}_5 &= \{(R_{32}, 1), (R_{43}, 1)\} \\ \mathcal{A}_6 &= \{(R_{32}, 1), (R_{43}, 1)\} \end{aligned}$$

The set of available sources  $\mathcal{S}_i$  of road  $R_i$  on intersection  $J_9$  which are showed as Figure 4.11 are defined as follows:

$$\begin{aligned} \mathcal{S}_{31} &= \{(R_{44}, 1), (R_{43}, 2)\} & \mathcal{S}_{32} &= \{\phi\} \\ \mathcal{S}_{42} &= \{(R_{32}, 1), (R_{44}, 2), (R_{43}, 3)\} & \mathcal{S}_{43} &= \{\phi\} \\ \mathcal{S}_{44} &= \{\phi\} & \mathcal{S}_{45} &= \{(R_{43}, 1), (R_{32}, 2)\} \end{aligned}$$

The splitting ratio  $p_i$  of road  $R_i$  on intersection  $J_9$  are obtained from Eq (2.8) with the measurement data which are given as follows:

$$\begin{aligned} p_{31} &= [1]^T & p_{32} &= [0.585, 0.415]^T \\ p_{42} &= [1]^T & p_{43} &= [0.971, 0.029, 0.0]^T \\ p_{44} &= [0.894, 0.106]^T & p_{45} &= [1]^T \end{aligned}$$

The traffic light constraints of intersection  $J_9$  are defined as follows:

$$\begin{aligned} \rho_{\text{fix},9} &= [2, 3, 5, 6] & \tau_{\text{fix},9} &= [0, 2, 3, 0, 3, 2] \\ \tau_{\text{min},9} &= [15, 2, 3, 15, 3, 2] & \tau_{\text{max},9} &= [70, 2, 3, 70, 3, 2] \\ \tau_9 &= 150 \end{aligned}$$

### Configuration of intersection $J_{10}$ (Sathorn - Surasak)

The traffic light signal of intersection  $J_{10}$  is configured at 4 phases which is showed on Figure 4.12. This intersection is consists of 4 incoming roads  $R_{in} = \{R_{16}, R_{41}, R_{42}, R_{46}\}$  and 4 outcome roads  $R_{out} = \{R_{15}, R_{43}, R_{47}\}$ . This intersection has the capacity  $C_{int,i}^{10} = 6,500$  veh/h which is measured from Fixed control case.

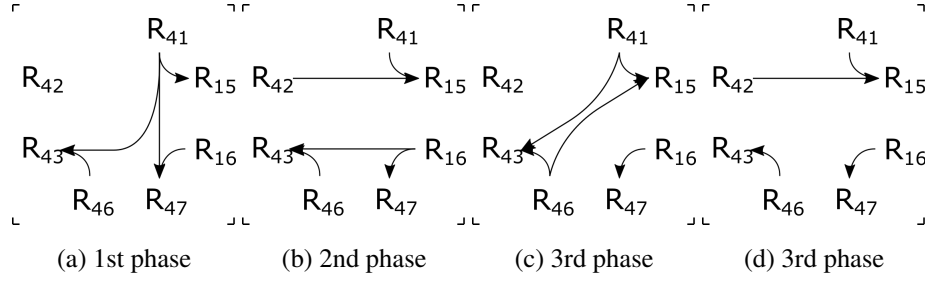


Figure 4.12: The traffic light pattern of intersection  $J_{10}$ .

The set of available lanes  $\mathcal{A}_k$  on intersection  $J_{10}$  which are showed as Figure 4.12 are defined as follows:

$$\begin{aligned} \mathcal{A}_1 &= \{(R_{16}, 1), (R_{41}, 1), (R_{46}, 1), (R_{41}, 2), (R_{41}, 3)\} & \mathcal{A}_2 &= \{(R_{16}, 1), (R_{41}, 1), (R_{46}, 1), (R_{42}, 1), (R_{16}, 2)\} \\ \mathcal{A}_3 &= \{(R_{16}, 1), (R_{41}, 1), (R_{46}, 1), (R_{41}, 3), (R_{46}, 2)\} & \mathcal{A}_4 &= \{(R_{16}, 1), (R_{41}, 1), (R_{46}, 1), (R_{42}, 1)\} \end{aligned}$$

The set of available sources  $\mathcal{S}_i$  of road  $R_i$  on intersection  $J_{10}$  which are showed as Figure 4.12 are defined as follows:

$$\begin{aligned} \mathcal{S}_{15} &= \{(R_{41}, 1), (R_{42}, 2), (R_{46}, 2)\} & \mathcal{S}_{16} &= \{\phi\} \\ \mathcal{S}_{41} &= \{\phi\} & \mathcal{S}_{42} &= \{\phi\} \\ \mathcal{S}_{43} &= \{(R_{46}, 1), (R_{16}, 2), (R_{41}, 3)\} & \mathcal{S}_{46} &= \{\phi\} \\ \mathcal{S}_{47} &= \{(R_{16}, 1), (R_{41}, 2)\} \end{aligned}$$

The splitting ratio  $p_i$  of road  $R_i$  on intersection  $J_{10}$  are obtained from Eq (2.8) with the measurement data which are given as follows:

$$\begin{aligned} p_{15} &= [1]^T & p_{16} &= [0.644, 0.356]^T \\ p_{41} &= [0.459, 0.156, 0.385]^T & p_{42} &= [1]^T \\ p_{43} &= [1]^T & p_{46} &= [0.735, 0.265]^T \\ p_{47} &= [1]^T \end{aligned}$$

The traffic light constraints of intersection  $J_{10}$  are defined as follows:

$$\begin{aligned} \rho_{fix,10} &= [] & \tau_{fix,10} &= [0, 0, 0, 0] \\ \tau_{min,10} &= [15, 15, 15, 15] & \tau_{max,10} &= [60, 60, 60, 60] \\ \tau_{10} &= 150 \end{aligned}$$

## 4.2 Experimental procedure

This work has established the controller with three layers which are the network, area, and intersections. Those controllers are independent worked from other controllers but they have a communication socket for sending the signal to other layer controllers.

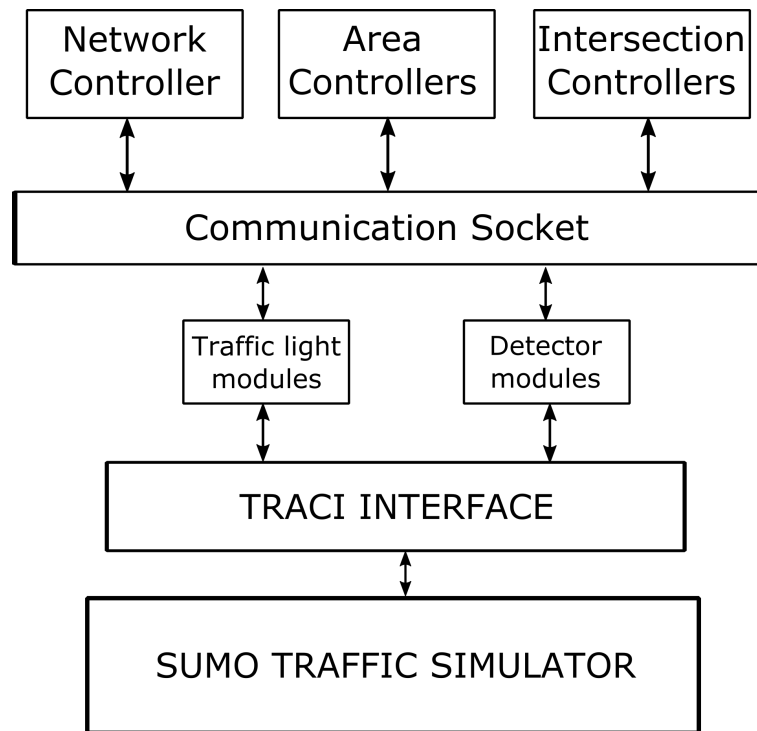


Figure 4.13: The diagram of controllers, modules, and simulator.

The diagram from Figure 4.13 shows the module components in this work which divided into 4 levels which are the controller level, communication level, module level, and simulator level. This work has created only the controller level and communication level to control the traffic lights and read the detectors which connect the SUMO Traffic microscopic simulator via the Traci interface.

The experimental procedure of this work is illustrated in Figure 4.14 to obtain the best control performance that is measured from the average traffic flow (veh/h) through the intersection. Firstly, prepare the simulation for the traffic scenario with an initial cycle length by considering the number of incoming roads. If the number of incoming roads is less than 4, the suggested the initial cycle length is 120 seconds. If the number of incoming roads is more than or equal to 4, the suggested the initial cycle length is 150 seconds.

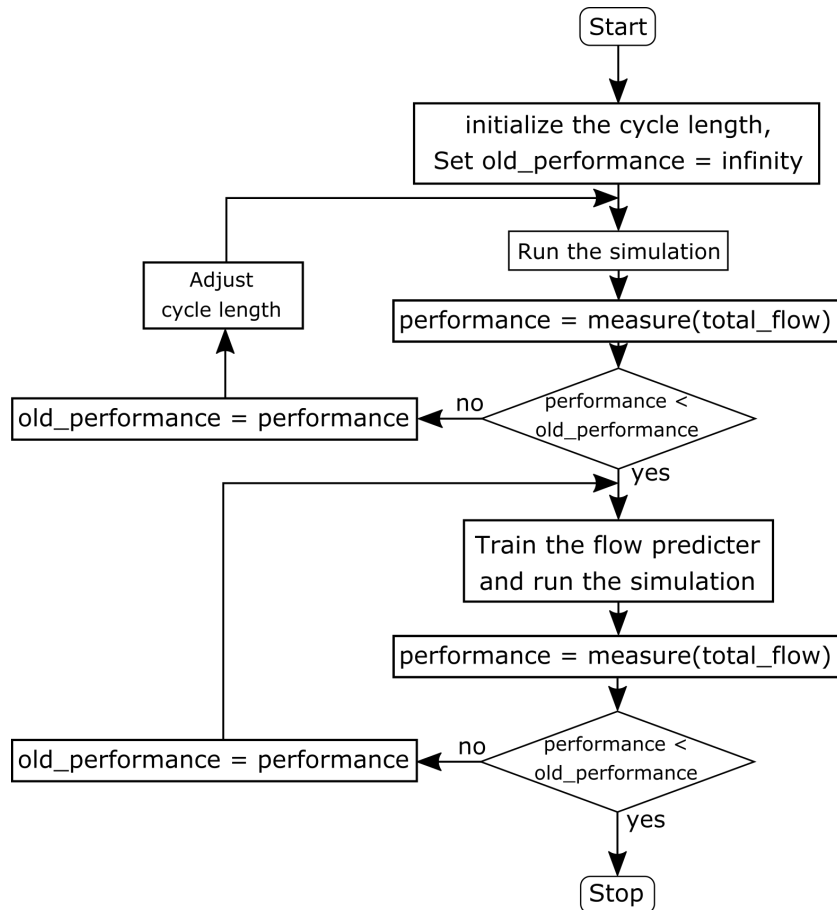


Figure 4.14: The diagram of experimental procedure.

Secondly, run the traffic simulation by using the initial cycle length without the flow predictor model and measure the control performance. If the control performance is not satisfied, the simulation will be run again by increasing or decreasing the cycle length of the considering intersection with 15 seconds.

Thirdly, create the traffic flow predictor model by using the historical data from the prior step and run the traffic simulation by using the trained model. If the performance is not satisfied, go back to the third step to train the traffic flow predictor model by using the new dataset and run the traffic simulation by using the trained model.

Finally, if the performance is satisfied, the traffic flow predictor model and cycle length will be used in the practice.

### 4.3 Simulation results

This section illustrates the control results of an example case which are consist of the state and control signal on each layer. The simulation The control results are consist of network, area, and intersection layer are illustrated as follows. Then, the performance of the hierarchical distributed control will be compared with the fixed control result.

#### Control results of the network layer

The control results of the network layer which showed in Figure 4.15 displays the total of the vehicle in each area and a control signal which represents the desired traffic flow (veh/h) on each link.

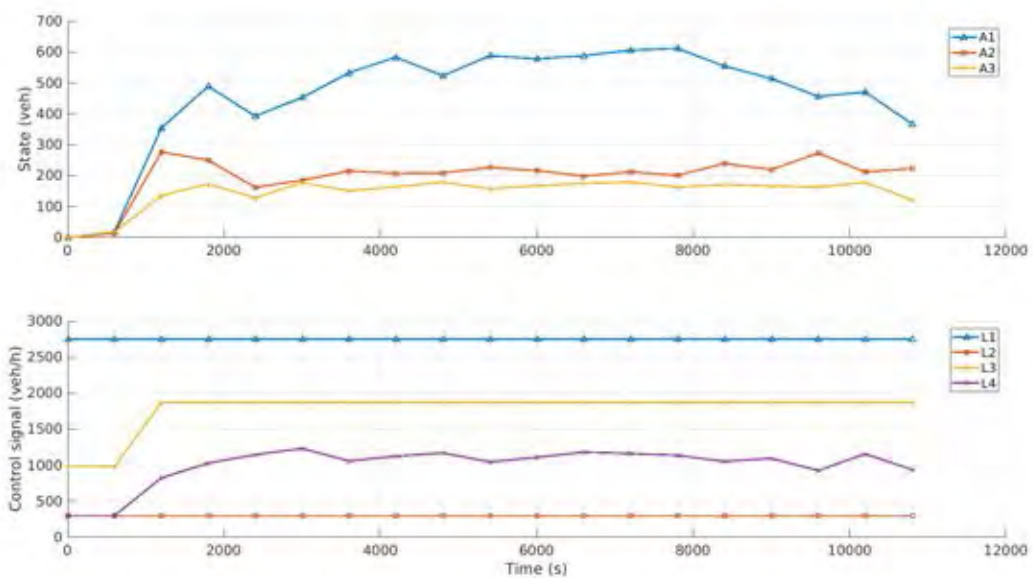


Figure 4.15: Plot of control results of the network layer; (top) state, (bottom) control signal.

From the traffic demand information, the most traffic of the 1st area in the morning time will be transferred into the 2nd area and the 3rd area. The control signal shows the traffic flow on the 1st link is higher than the other links because of the traffic demand in the 1st area is highest. However, the behavior of traffic in the practice is not the one-way transferred but the traffic flow on the coupling area is exchanged with differing rates. Thus, the traffic flow from the 3rd area to the 2nd area, and the 2nd area to the 1st area will greater than zero.

**Control results of the area layer**

The control results of area layer which are showed in Figure 4.16, 4.17, and 4.18 are displayed the state on each node which represents the number of vehicle in each intersection and estimated waiting vehicle from outer area, and the control signal which represents the desired traffic flow.

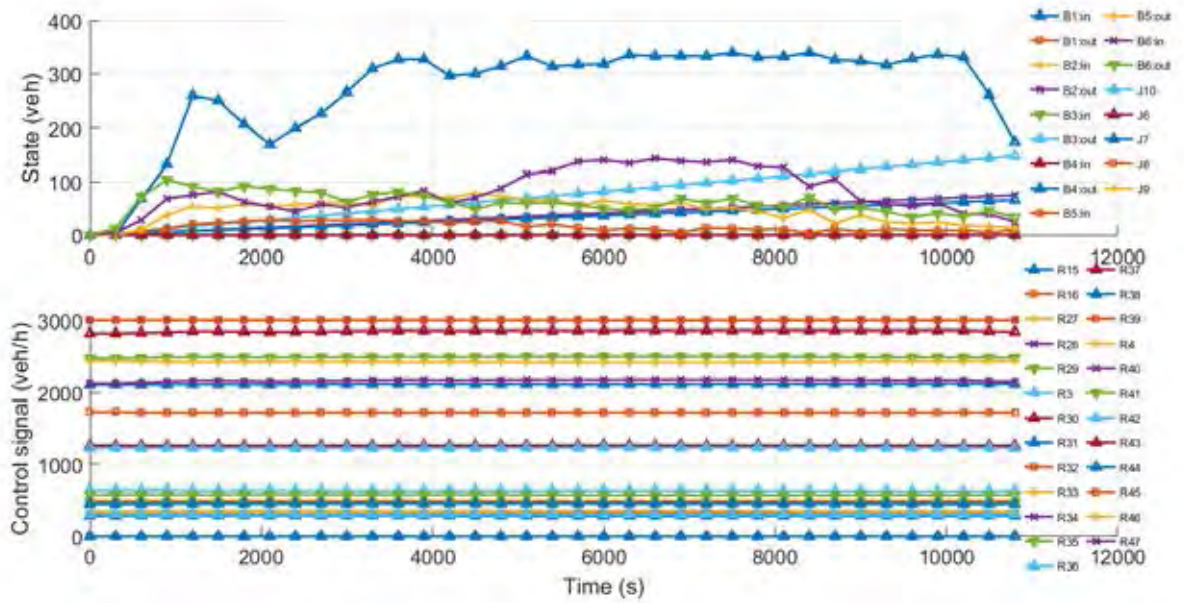


Figure 4.16: Plot of control results of the 1st area; (top) state, (bottom) control signal.

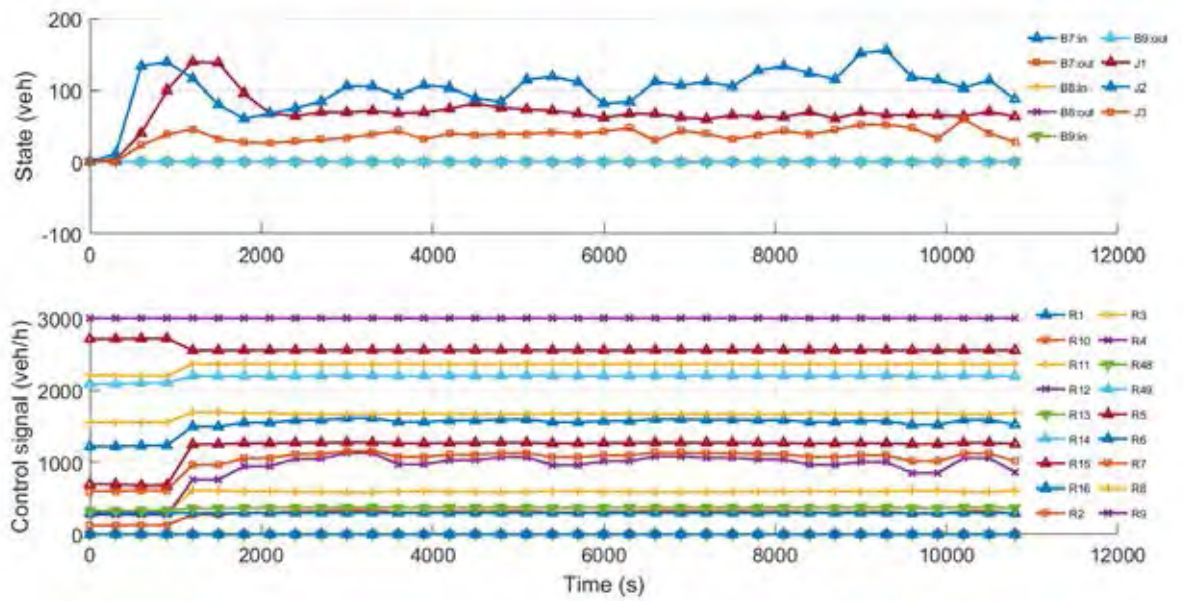


Figure 4.17: Plot of control results of the 2nd area; (top) state, (bottom) control signal.

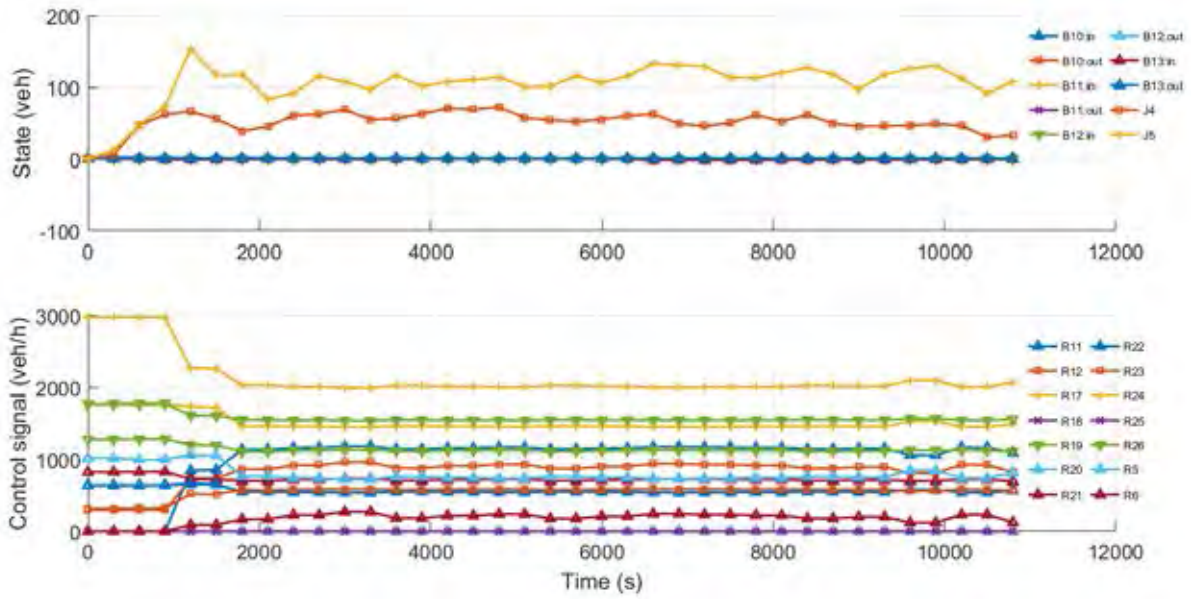


Figure 4.18: Plot of control results of the 3rd area; (top) state, (bottom) control signal.

The control signal from three areas can be summarized by drawing into the heat map that compares the desired traffic flow on each road, which illustrates in Figure 4.19.

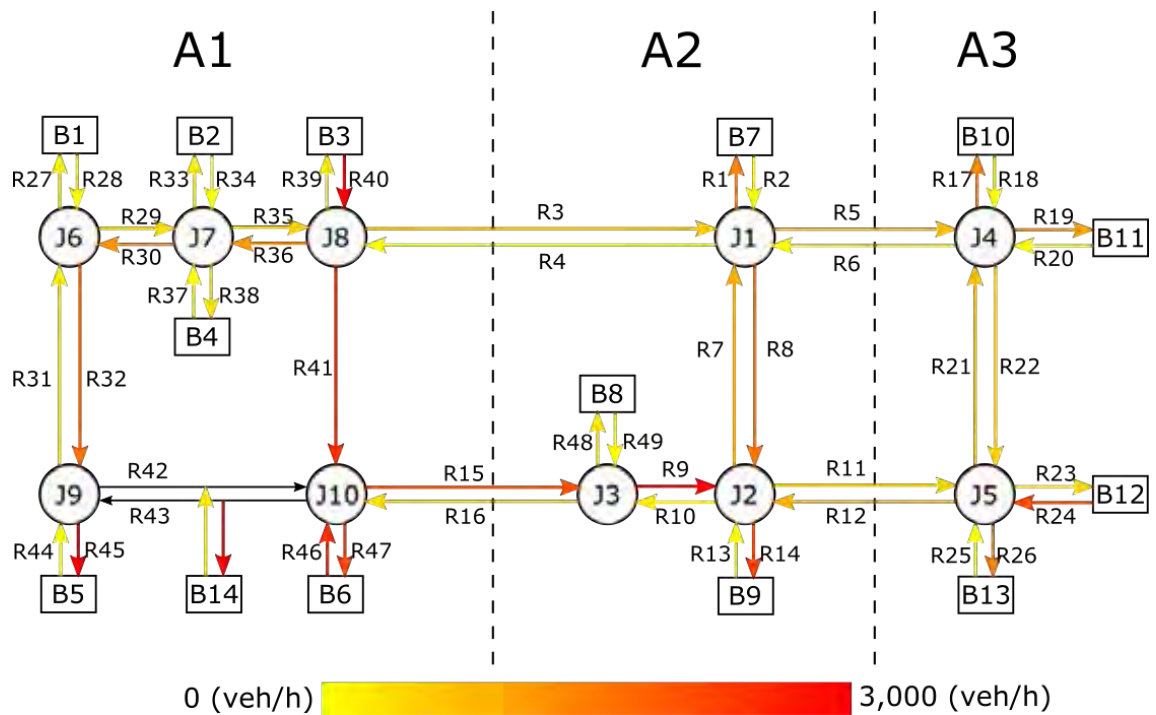


Figure 4.19: Plot of heat map on the network of Sathorn's network.

### Control results of the intersection layer

The control results of area layer which are showed in Figure 4.20, 4.21, 4.22, 4.23, and 4.24 are displayed the state which represents the number of vehicle in each road, and the control signal which represents the optimal traffic signal.

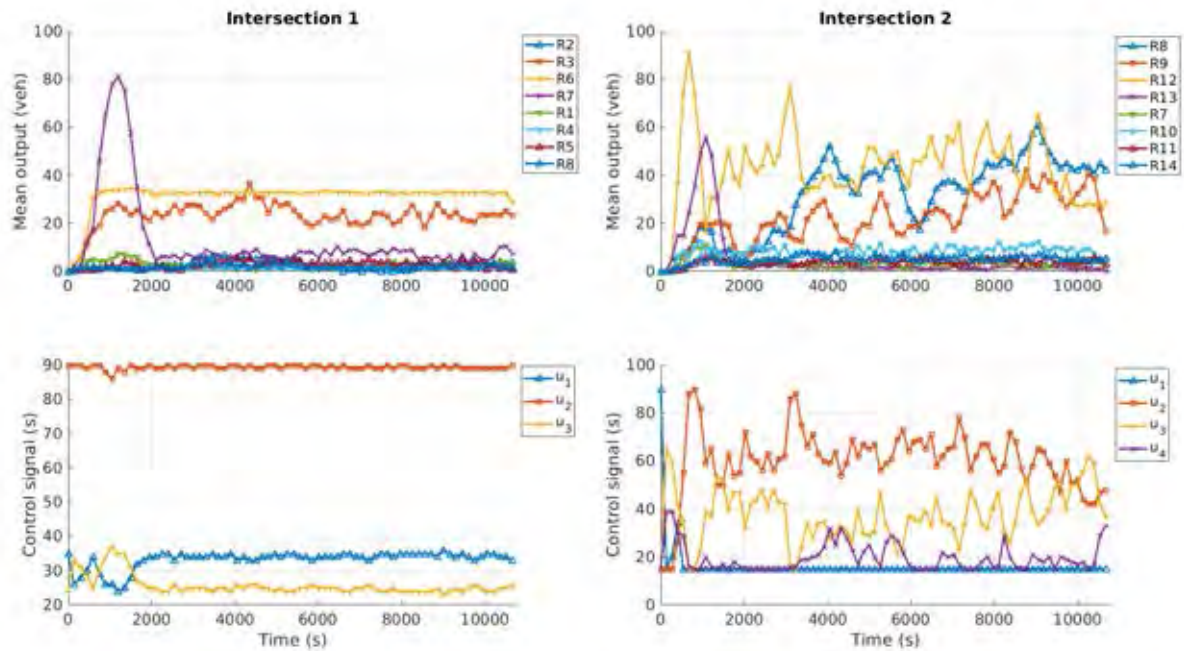


Figure 4.20: Plot of control results of the 1st and 2nd intersection; (top) state, (bottom) control signal.

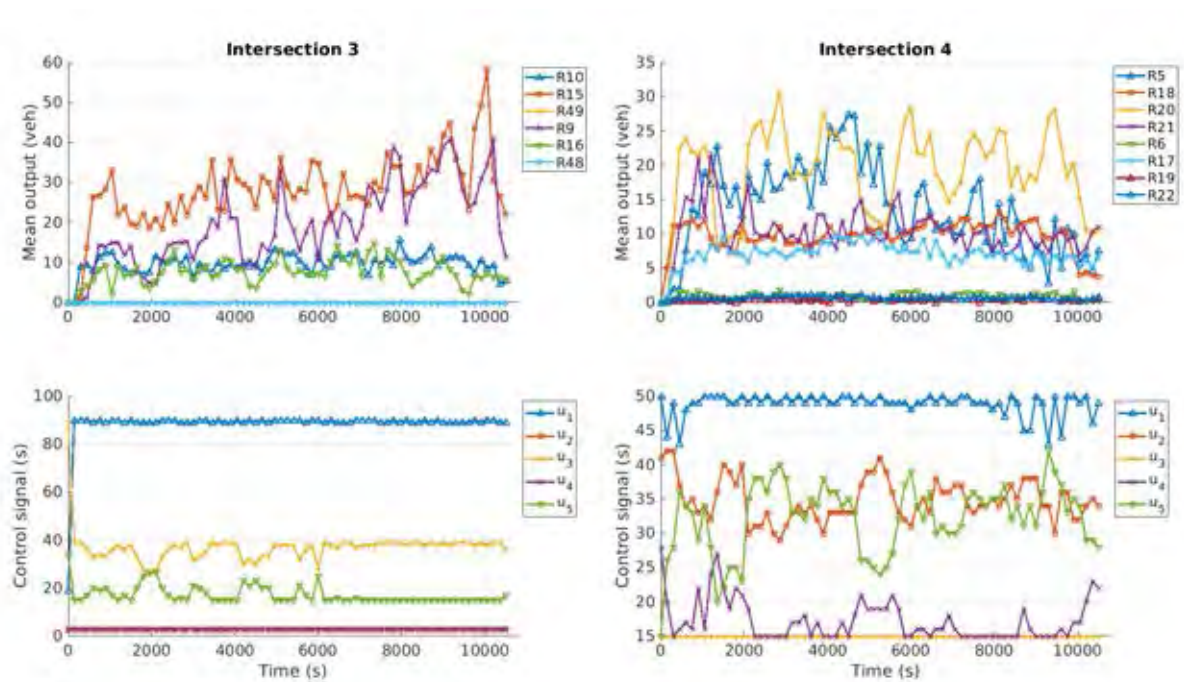


Figure 4.21: Plot of control results of the 3rd and 4th intersection; (top) state, (bottom) control signal.

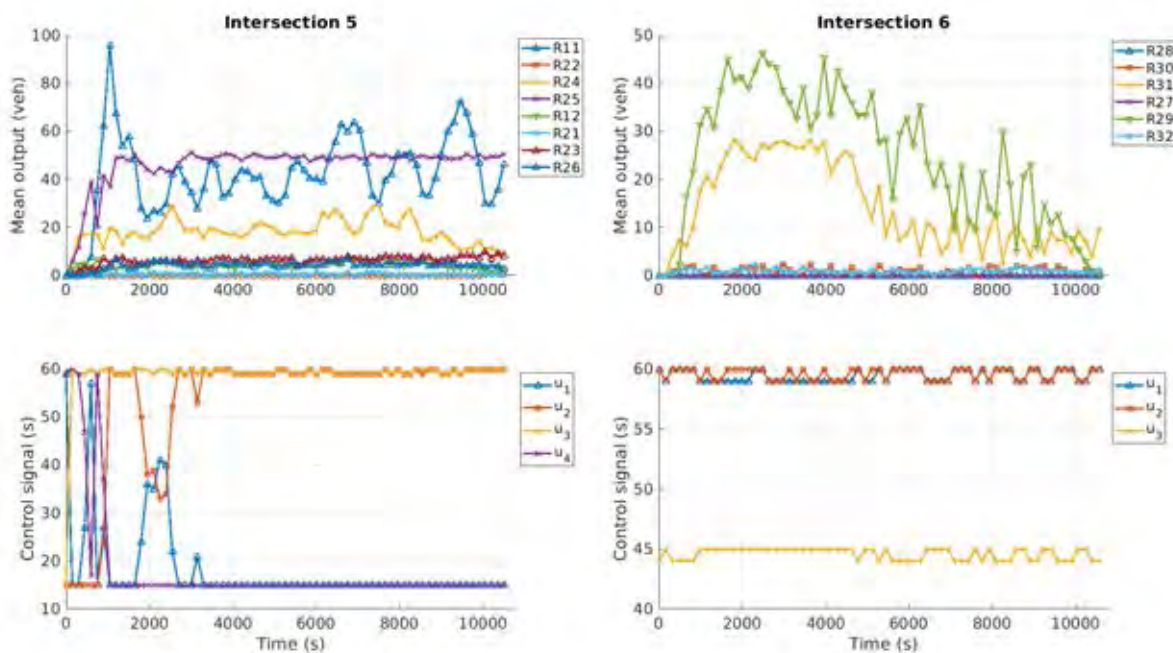


Figure 4.22: Plot of control results of the 5th and 6th intersection; (top) state, (bottom) control signal.

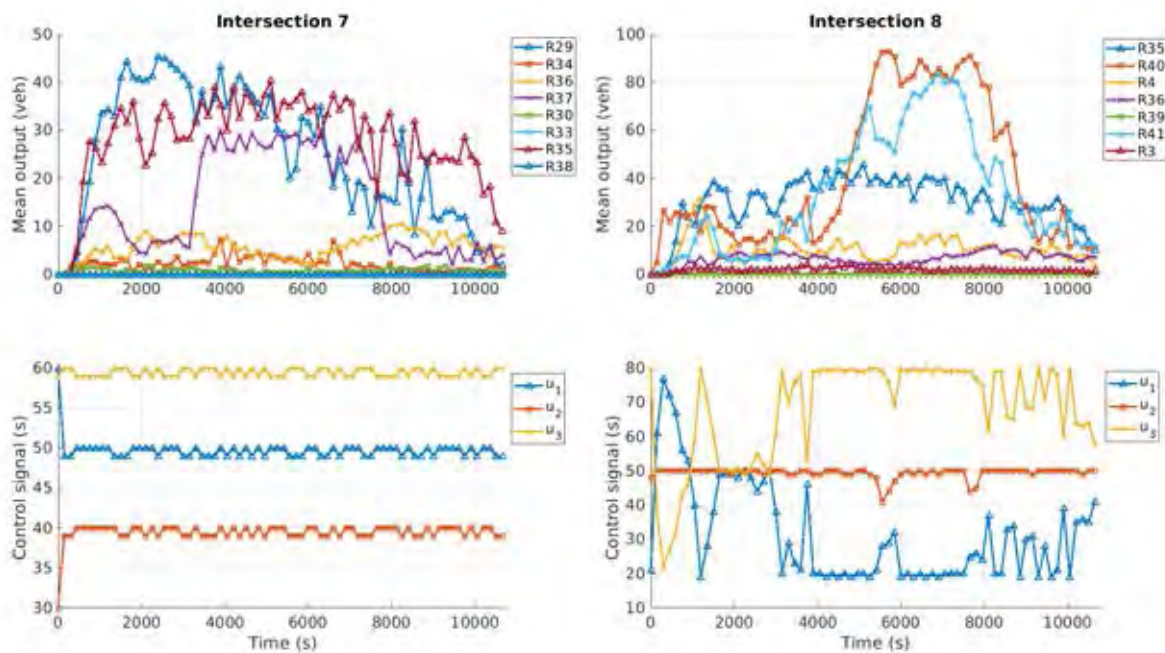


Figure 4.23: Plot of control results of the 7th and 8th intersection; (top) state, (bottom) control signal.

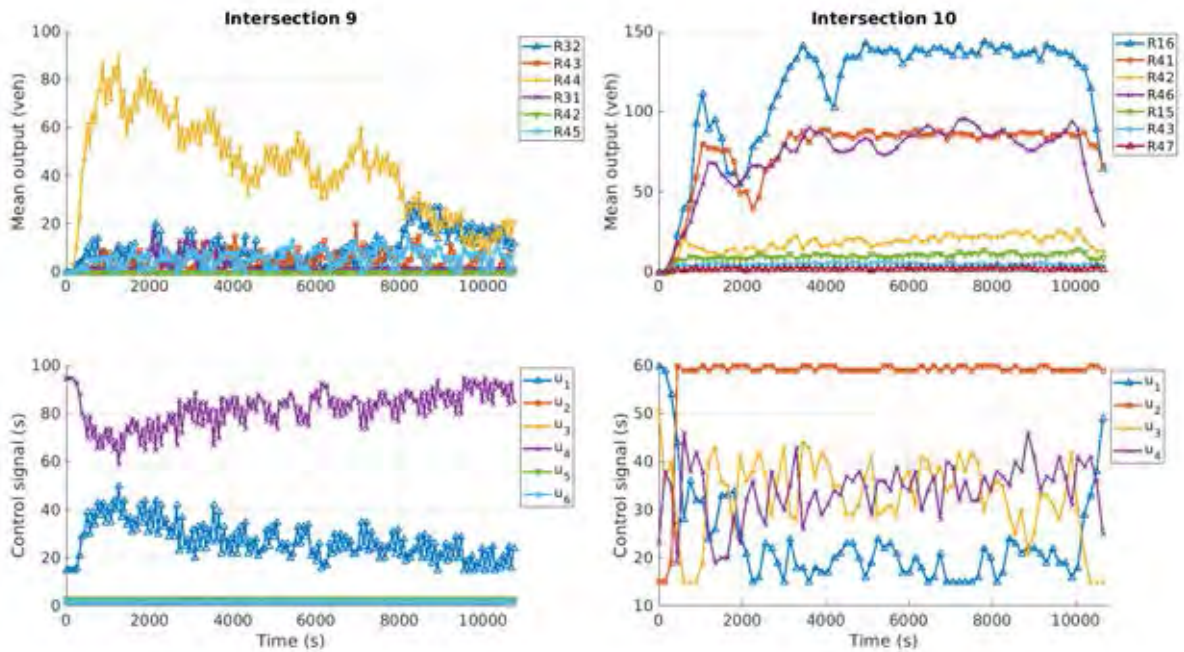


Figure 4.24: Plot of control results of the 9th and 10th intersection; (top) state, (bottom) control signal.

**Control performance of the network layer on 100% traffic**

This part shows the control performance on the traffic network which consists of the total traffic flow (veh/h) and the average of estimated travel time (sec) which shows in Figure 4.25. The total traffic flow of 3 controllers of the network is measured from the departure traffic flow on each intersection.

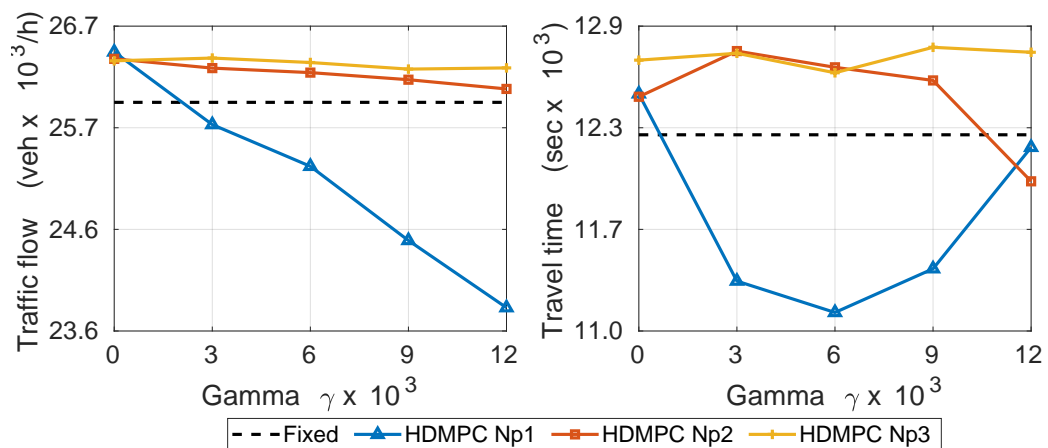


Figure 4.25: Plot of control performance of network layer on 100% traffic; (left) traffic flow, (right) average of estimated travel time.

This traffic network has 10 intersections, the total performance of the network is obtained from

$$\text{TOTAL FLOW} = \sum_{i \in I_N} \sum_{r_{in} \in R_{in}^i} q_{r_{in}} \times 3,600$$

where  $I_N$  is the set of intersection's index in the network,  $R_{in}^i$  is the set of incoming road's index on  $i$ th intersection, and  $q_r$  is the traffic flow (veh/s) on  $r$ th road.

**Control performance of the area layer on 100% traffic**

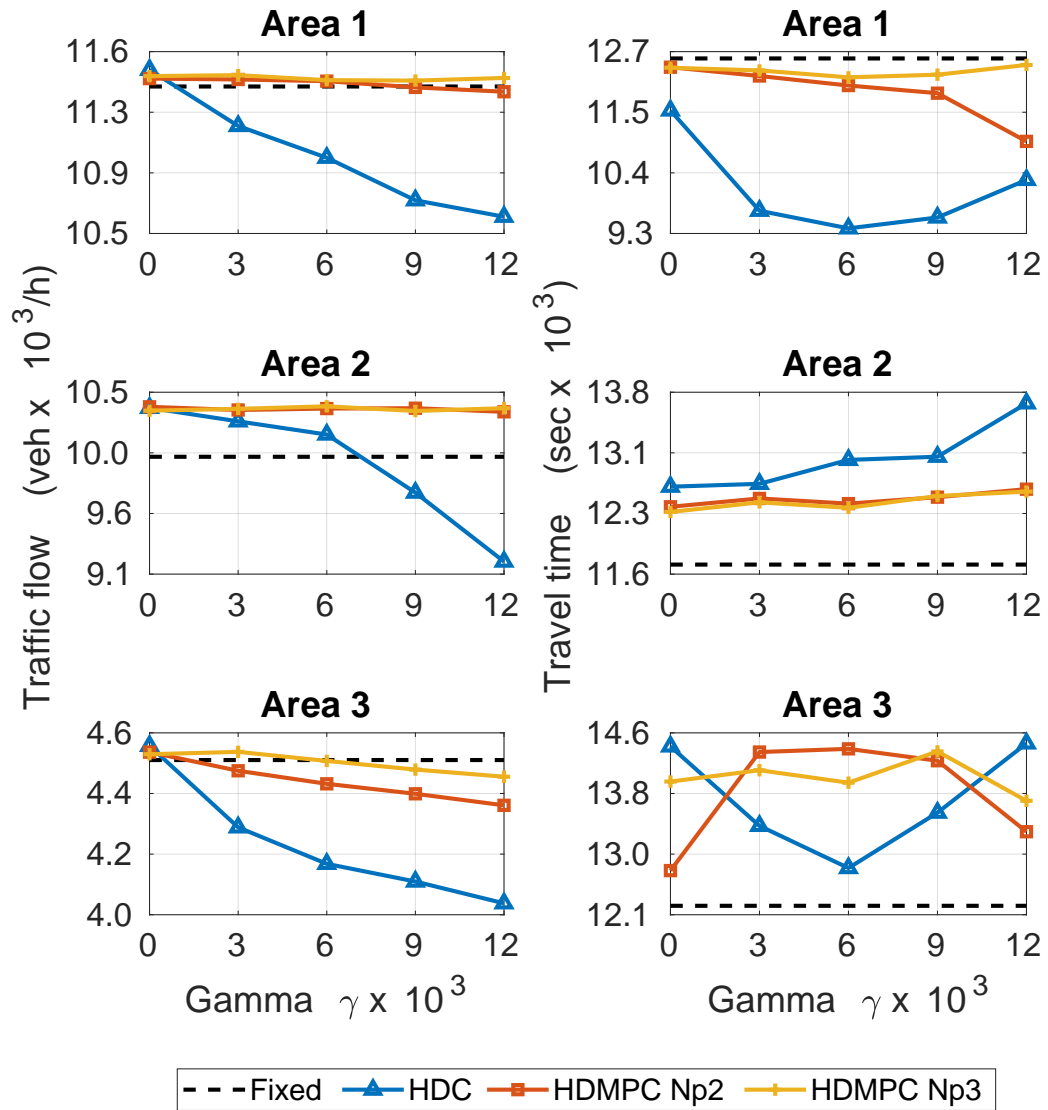


Figure 4.26: Plot of control performance of 3 areas on 100% traffic; (left) traffic flow, (right) average of estimated travel time.

### Control performance of the area intersection on 100% traffic

This part illustrates the performance of each network which are measured from the total departure flow (veh/h) of incoming roads in the intersection.

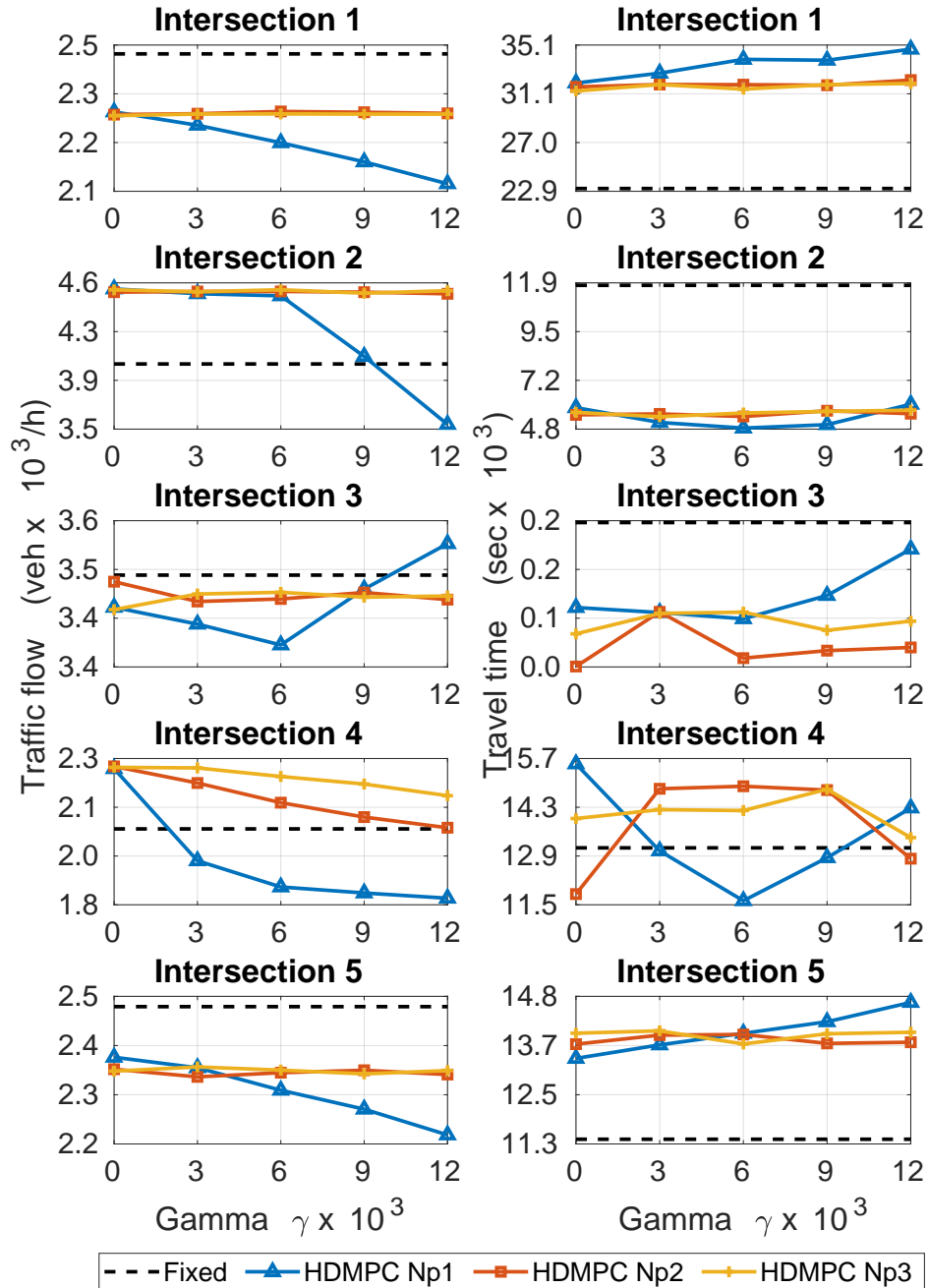


Figure 4.27: Plot of control performance of intersection  $J_1 - J_5$  on 100% traffic; (left) traffic flow, (right) average of estimated travel time.

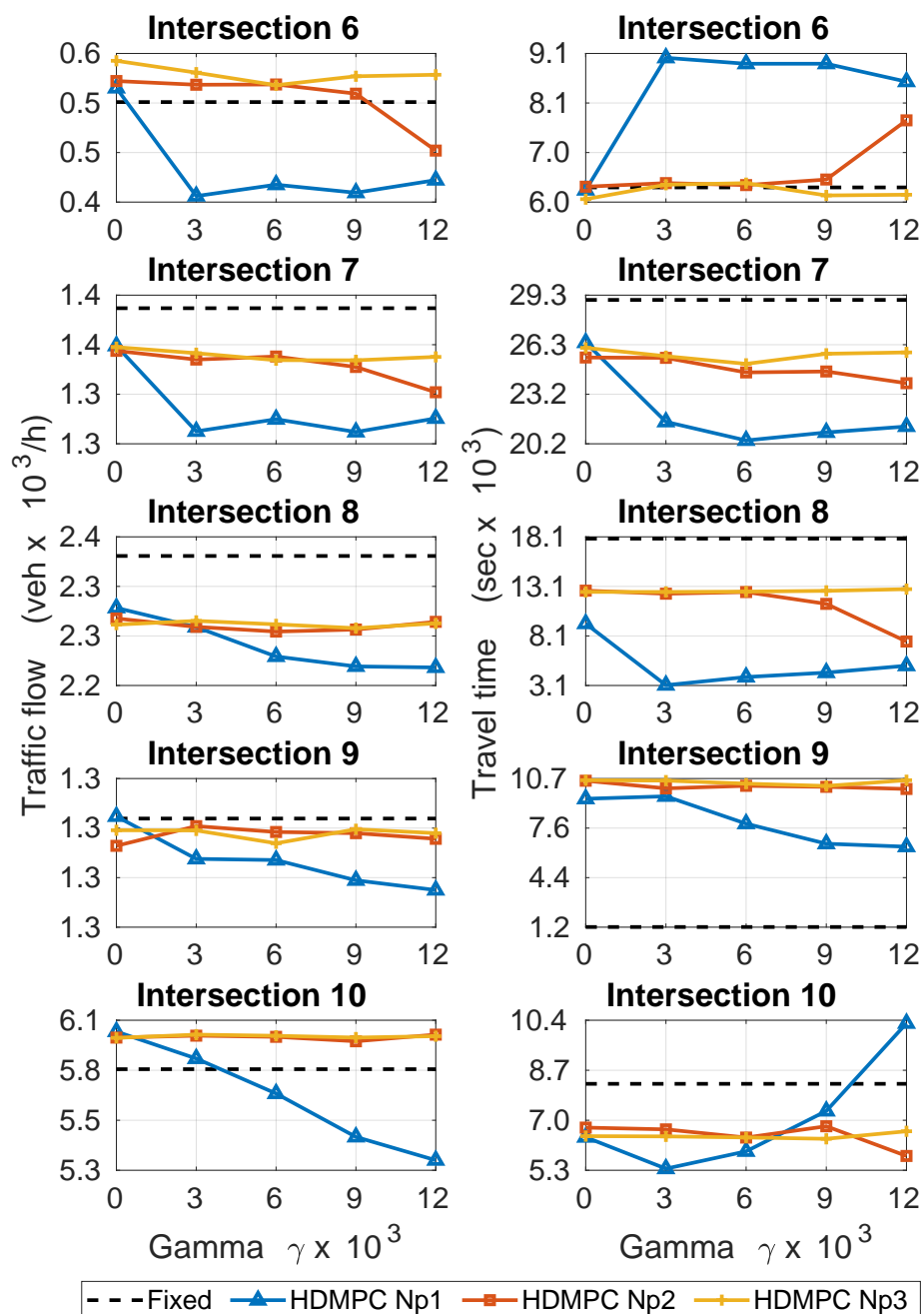


Figure 4.28: Plot of control performance of intersection  $J_6 - J_{10}$  on 100% traffic; (left) traffic flow, (right) average of estimated travel time.

### Control performance of the network layer on 85% traffic

This part shows the control performance on the traffic network when the traffic demand had reduced to 85%. We observe the behavior of the performance while varying the gamma when the traffic demand is lighter.

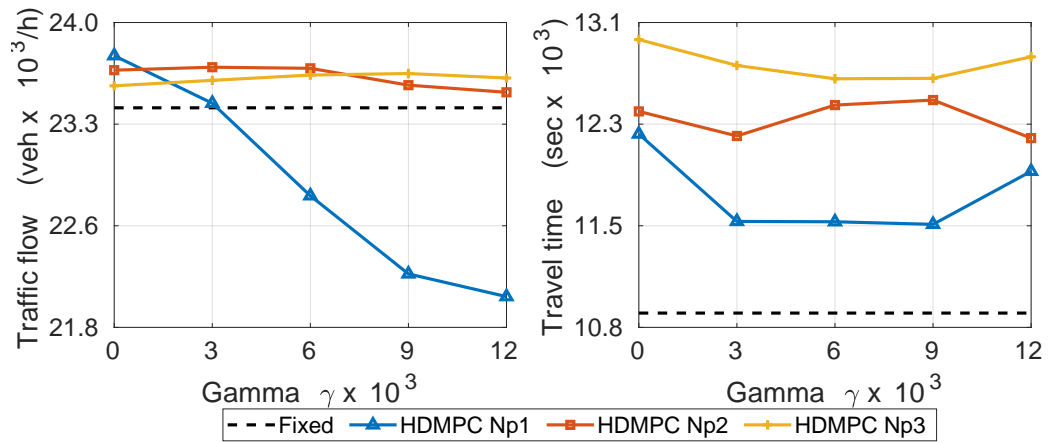


Figure 4.29: Plot of control performance of network layer on 85% traffic; (left) traffic flow, (right) average of estimated travel time.

The performance of the network layer on 85% traffic of HDMPC Np=1, Np=2, and, Np=3 are showed in Figure 4.29 which are compared to Fixed control. The HDC shows the best performance with 1.59% on gamma  $\gamma = 0$ .

## Control performance of the area layer on 85% traffic

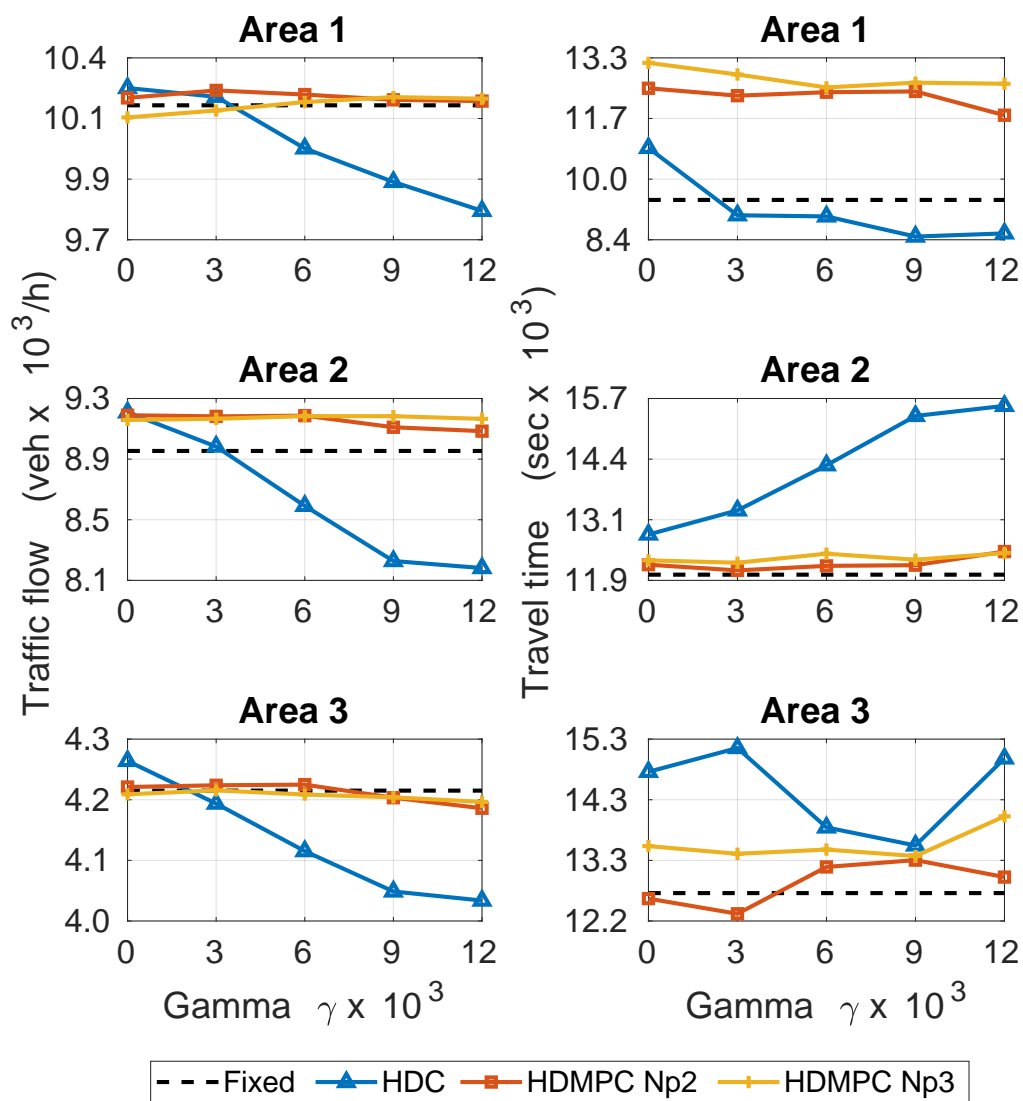


Figure 4.30: Plot of control performance of 3 areas on 85% traffic; (left) traffic flow, (right) average of estimated travel time.

### Control performance of the area intersection on 85% traffic

This part illustrates the performance of each network which are measured from the total departure flow (veh/h) of incoming roads in the intersection.

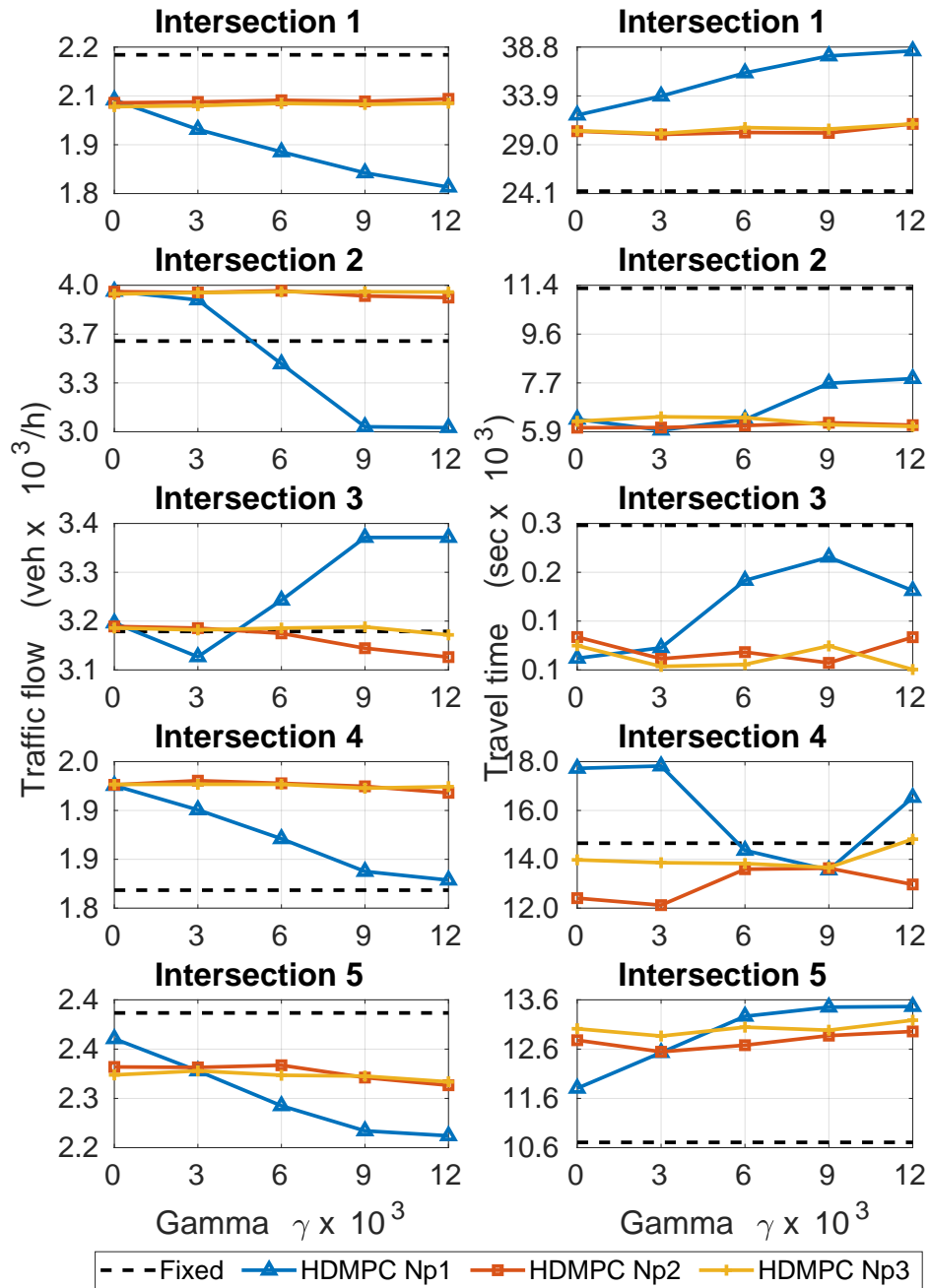


Figure 4.31: Plot of control performance of intersection  $J_1 - J_5$  on 85% traffic; (left) traffic flow, (right) average of estimated travel time.

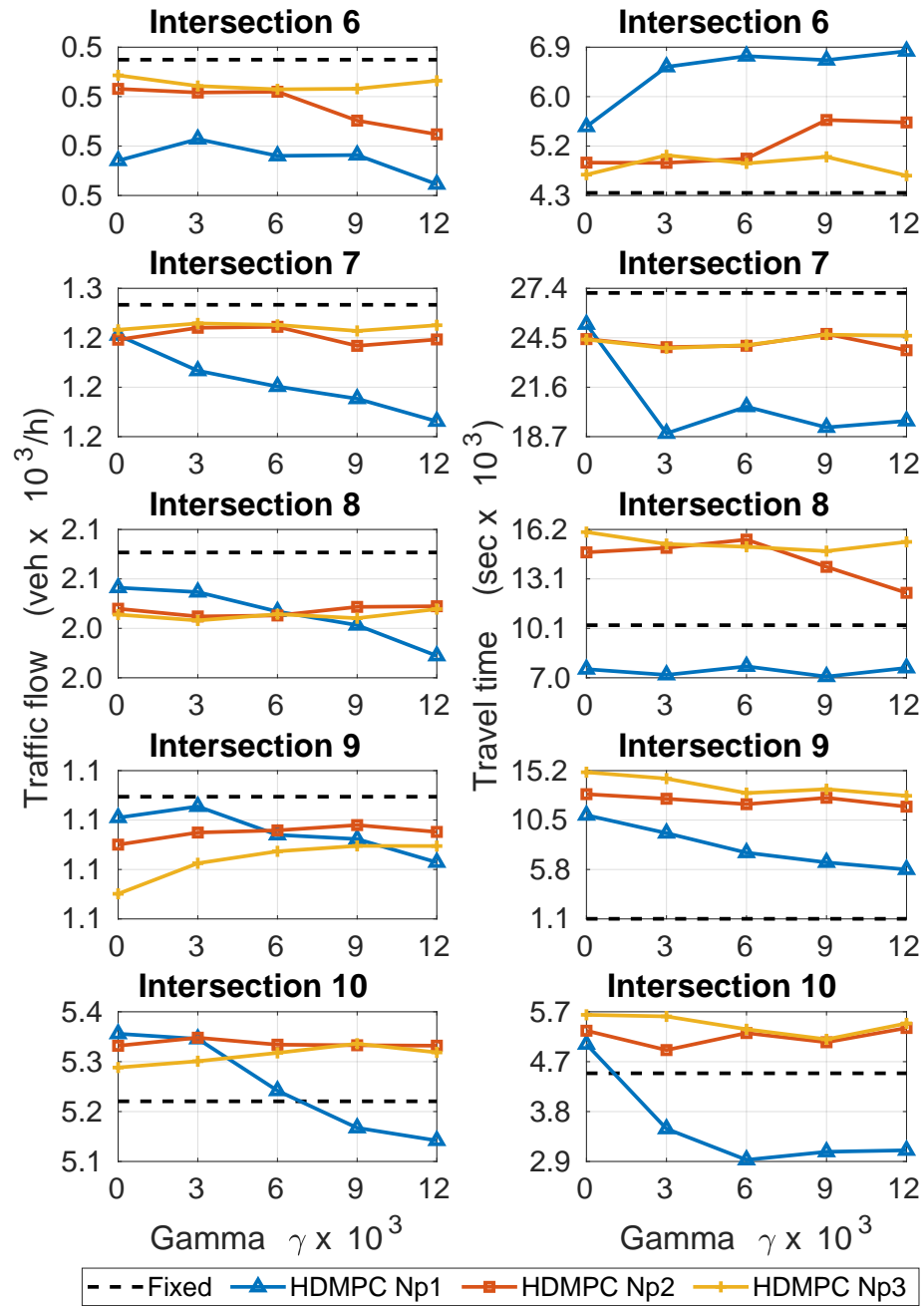


Figure 4.32: Plot of control performance of intersection  $J_6 - J_{10}$  on 85% traffic; (left) traffic flow, (right) average of estimated travel time.

### Control performance of the network layer on 75% traffic

This part shows the control performance on the traffic network when the traffic demand had reduced to 75%. We observe the behavior of the performance while varying the gamma when the traffic demand is lighter.

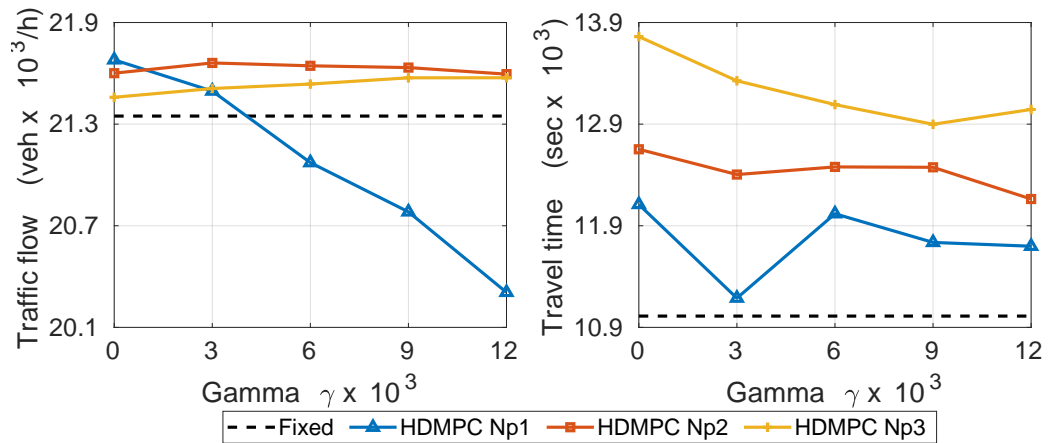


Figure 4.33: Plot of control performance of network layer on 75% traffic; (left) traffic flow, (right) average of estimated travel time.

The performance of the network layer on 75% traffic of HDMPC Np=1, Np=2, and, Np=3 are showed in Figure 4.33 which are compared to Fixed control. The HDC shows the best performance with 1.53% on gamma  $\gamma = 0$ .

## Control performance of the area layer on 75% traffic

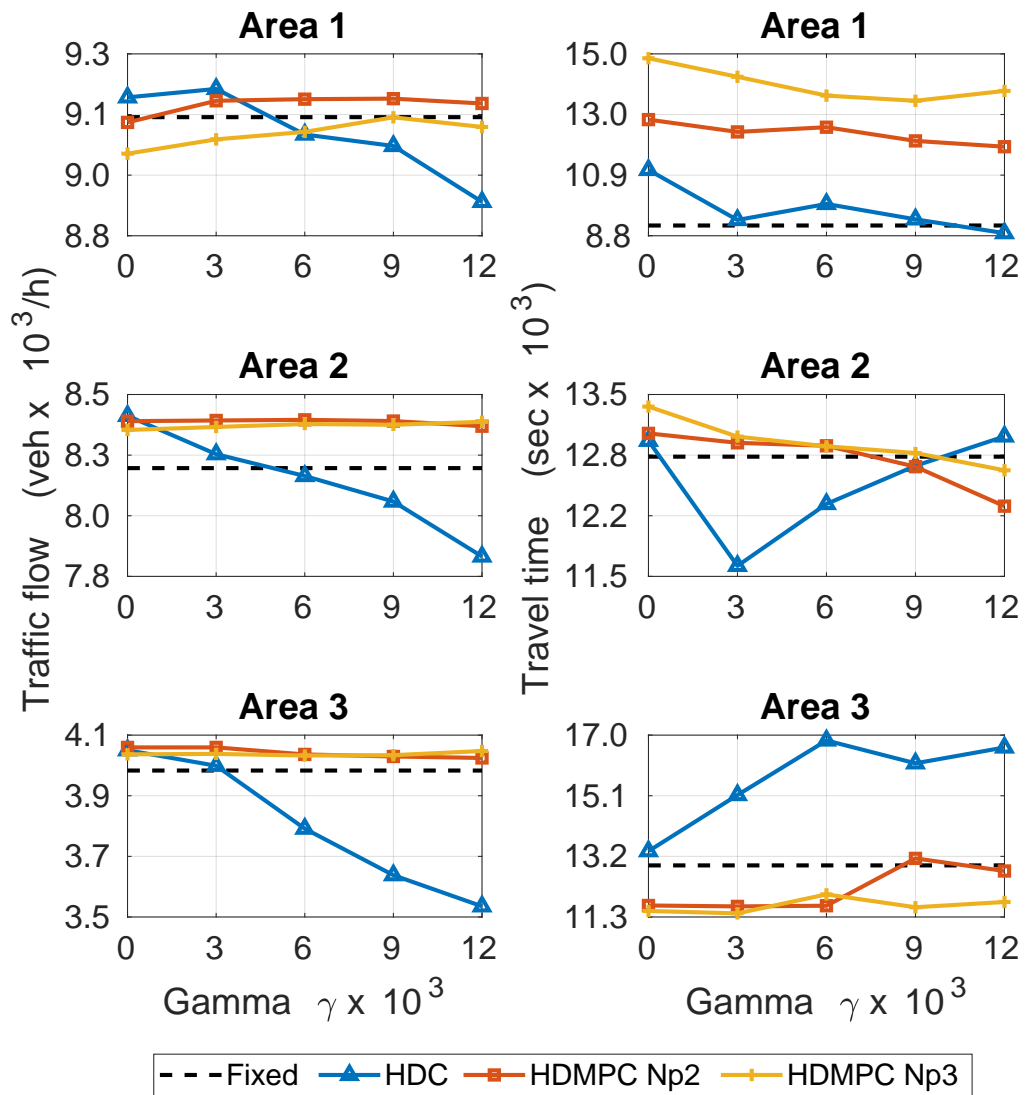


Figure 4.34: Plot of control performance of 3 areas on 75% traffic; (left) traffic flow, (right) average of estimated travel time.

### Control performance of the area intersection on 75% traffic

This part illustrates the performance of each network which are measured from the total departure flow (veh/h) of incoming roads in the intersection.

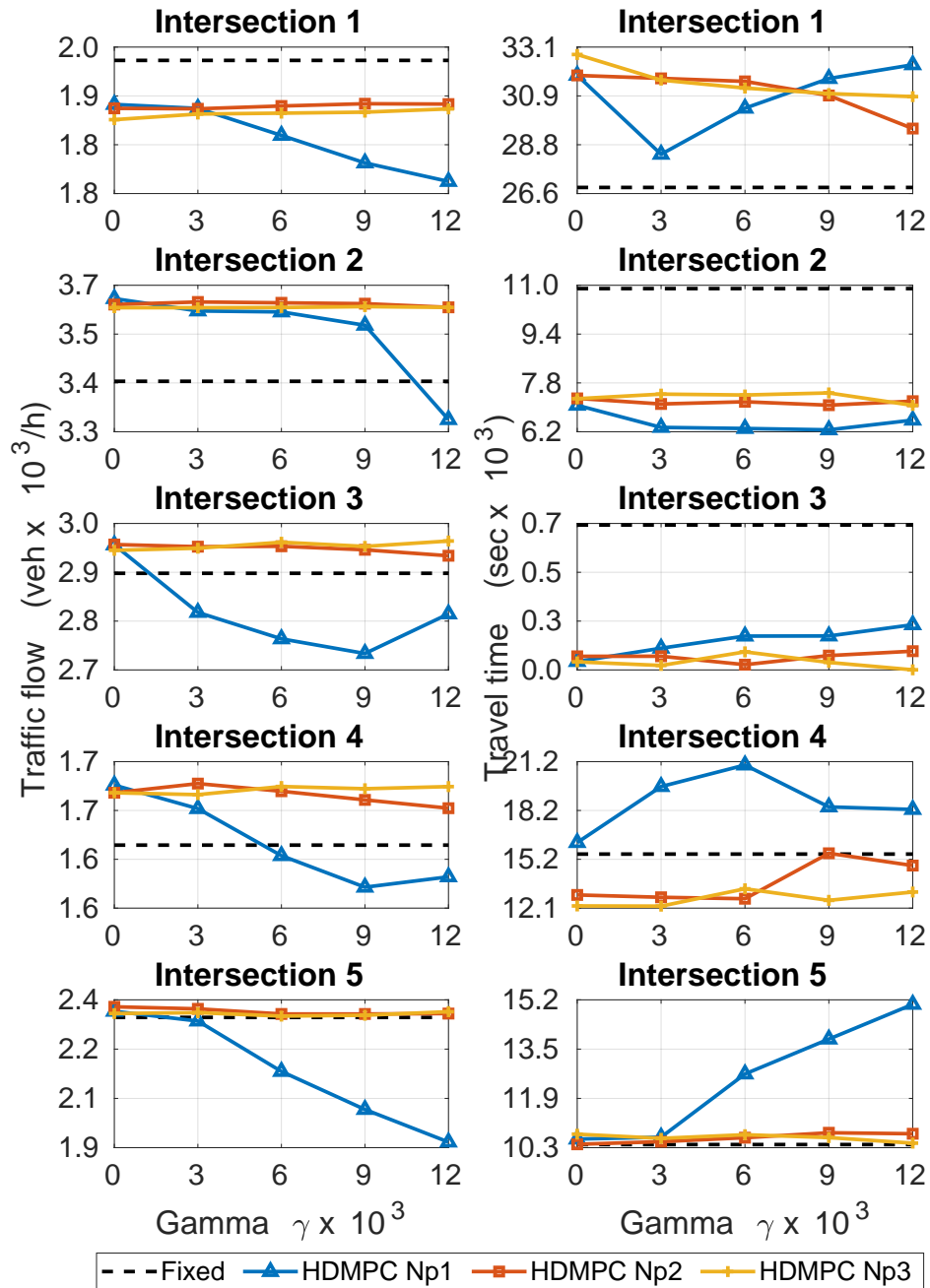


Figure 4.35: Plot of control performance of intersection  $J_1 - J_5$  on 75% traffic; (left) traffic flow, (right) average of estimated travel time.

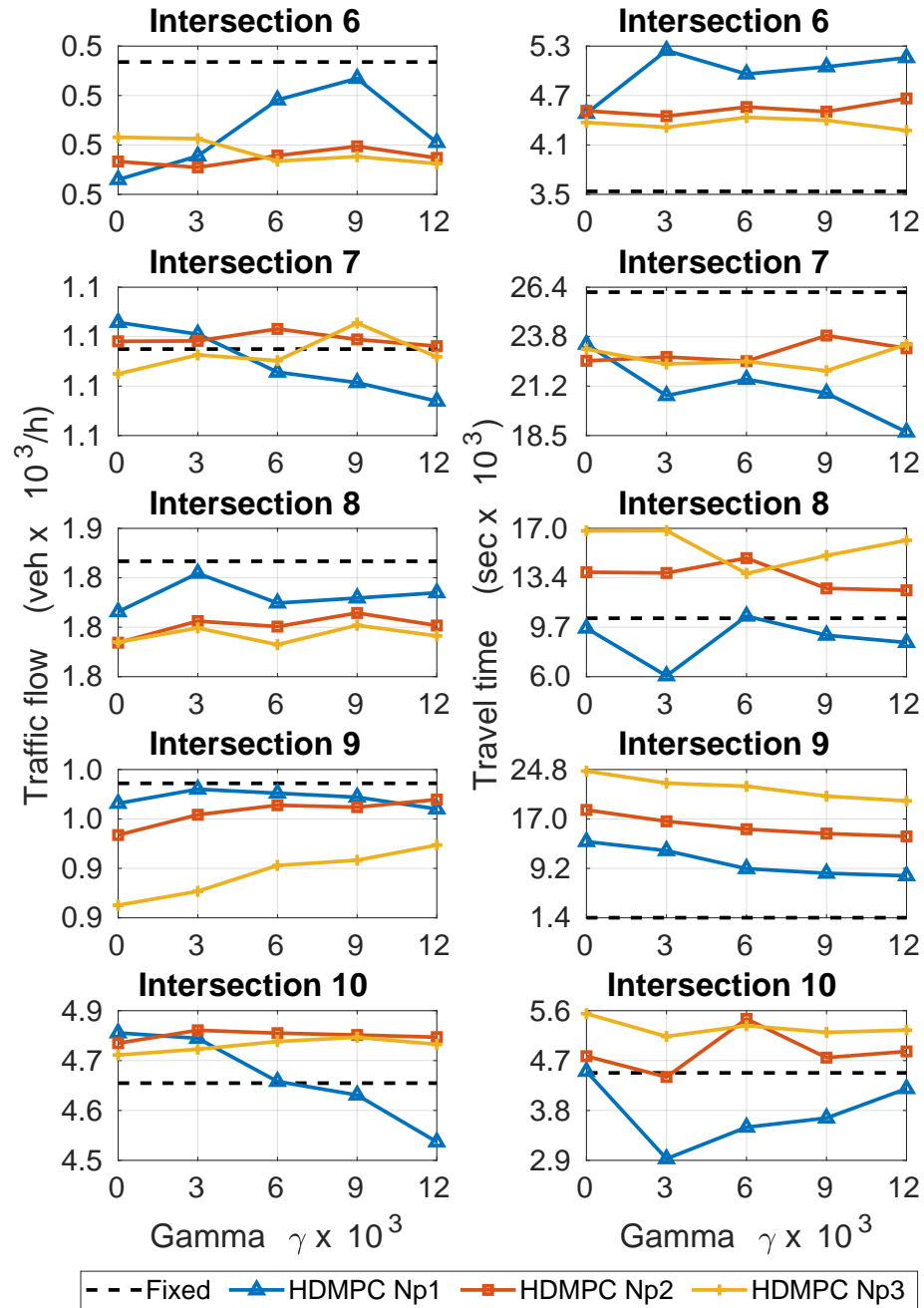


Figure 4.36: Plot of control performance of intersection  $J_6 - J_{10}$  on 75% traffic; (left) traffic flow, (right) average of estimated travel time.

#### 4.4 Summary

This work simulated the traffic and compared the performance of three controllers which are HDMPC  $N_p=1$ ,  $N_p=2$ , and  $N_p=3$  to the Fixed control that is controlled and recorded from the Bangkok traffic police. The simulations on three cases, where the 1st case is 75% of traffic demand, the 2nd case is 85% of traffic demand, and the 3rd case is 100% of traffic demand which is simulated on 3 hours and averaged the performance with five trails.

The traffic performance indices which used in this work are the traffic flow and travel time. The results from the three cases show the inconsistency of both performance indices on the network layer which is illustrated in Figure 4.25, 4.29, and 4.33. The travel time and traffic flow measurement should be displayed as the results in the opposites tend. In other words, while the traffic flow is increased, it mitigates the traffic to less congestion, the travel time should be decreased in the opposites way. However, the results show on the 4th, 5th, and 9th intersection are showed the opposites tend of performance measurement which is correct to the hypothesis. The reason that the results of the other intersection are caused by the arrived vehicles on those intersections are decreased, it has increased the mean speed which makes the estimated travel time is less than it.

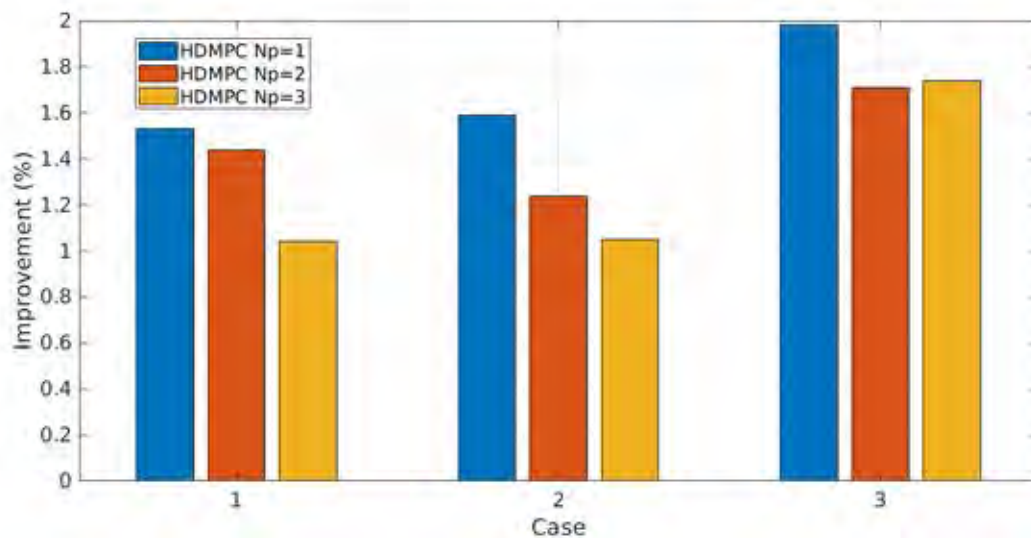


Figure 4.37: Summary of the best control performances on three traffic conditions.

The summary of control performances on three traffics which shows in Figure 4.37 is compared to the control performances of the fixed case giving the total traffic flow 25,947 (veh/h). The best performance on 100% traffic is 1.98% of HDMPC  $N_p=1$  at gamma  $\gamma = 0$ , the best performance on 85% traffic is 1.59% of HDMPC  $N_p=1$  at gamma  $\gamma = 0$ , and the best performance on 75% traffic is 1.53% of HDMPC  $N_p=1$  at gamma  $\gamma = 0$ . It appears to be better than a fixed case giving the total traffic flow 26,457 (veh/h).

## **CHAPTER V**

### **CONCLUSION**

The goal of this work is to establish the traffic signal control method to mitigate traffic congestion in the network based on hierarchical distributed control by applying the model predictive control. Each traffic signal controllers on the interconnection's layer are shared the traffic information such that traffic flow measurement through the higher layer. The higher layers are composed of a network layer and area layer which are used to reduce the complexity of the traffic network and used to find the optimal traffic flow on each road. It also solves the practical problem that some intersections cannot control and measure by grouping the controllable intersections into the same area. The optimal traffic flow information from the area layer is fed into each traffic signal controller in the interconnection layer. It is used for scheduling the traffic signal by concerning the traffic demand on the network, not only the traffic density in an individual intersection.

The study case of this work is Sathorn's zone (Chula-SSS) from the team of Associate Professor Chaodit Aswakul, Department of Electrical Engineering, Faculty of Engineering, Chulalongkorn University, which is composed of 10 intersections. This scenario is set up on the morning traffic condition which is calibrated to the real traffic measurement. Then, the performance of the designed controller in this work is compared to the traffic signal recorded from the Bangkok traffic police.

The simulation results are showed the optimal traffic flow information from the area layer is useful to mitigate the traffic congestion on the overview of the traffic network when the traffic condition is undersaturated. However, when the traffic condition became oversaturated, the model can not provide the efficiency of the optimal signal from the area layer. It may be improved by using the state-dependence model or nonlinear model to the model of the intersection's layer to track the reference signal from the area's layer as better.

## REFERENCES

- [1] I. Ioslovich, P.O. Gutman, D. Mahalel, J. Haddad, "Design of optimal traffic flow control at intersection with regard for queue length constraints," *Automation and Remote Control*, 72, 9, (2011): 1833.
- [2] I. Varga, "A Congestion Detection Based Traffic Control for Signalized Intersection," *Periodica Polytechnica Civil Engineering*, 62, 2, (2018): 398–403.
- [3] A. A. Zaidi, B. Kulcsar, H. Wymeersch, "Traffic-adaptive signal control and vehicle routing using a decentralized back-pressure method," in *Proc. of 2015 European Control Conference*, (2015): 3029–3034.
- [4] L. Fan, "Coordinated Control of Traffic Signals for Multiple Intersections," *Applied Mathematics*, 5, 13, (2014): 2042.
- [5] Y. Li, Z. Hou, J. Hao, "Decentralized Model-Free Adaptive Control for Signalized Intersections Network," *IFAC Proceedings*, 46, 13, (2013): 88–93.
- [6] P. Coll, P. Factorovich, I. Loiseau, R. Gómez, "A linear programming approach for adaptive synchronization of traffic signals," *International Transactions in Operational Research*, 20, 5, (2013): 667–679.
- [7] T. Tettamanti, I. Varga, B. Kulcsár, J. Bokor, "Model predictive control in urban traffic network management," *2008 16th Mediterranean Conference on Control and Automation*, (2008): 1538–1543.
- [8] M. Papageorgiou, C. Diakaki, V. Dinopoulou, A. Kotsialos, Y. Wang, "Review of road traffic control strategies," *Proceedings of the IEEE*, 91, 12, (2003): 2043–2067.
- [9] K. Aboudolas, M. Papageorgiou, A. Kouvelas, E. Kosmatopoulos, "A rolling-horizon quadratic-programming approach to the signal control problem in large-scale congested urban road networks," *Transportation Research Part C: Emerging Technologies*, 18, 5, (2010): 680–694.
- [10] S. Peeta, H.S. Mahmassani, "Multiple user classes real-time traffic assignment for online operations: a rolling horizon solution framework," *Transportation Research Part C: Emerging Technologies*, 3, 2, (1995): 83–98.
- [11] K. Aboudolas, M. Papageorgiou, E. Kosmatopoulos, "Store-and-forward based methods for the signal control problem in large-scale congested urban road networks," *Transportation Research Part C: Emerging Technologies*, 17, 2, (2009): 163–174.

- [12] X.H. Yu, W.W. Recker, "Stochastic adaptive control model for traffic signal systems," *Transportation Research Part C: Emerging Technologies*, 14, 4, (2006): 263–282.
- [13] O. De, B. Lucas, E. Camponogara, "Multi-agent model predictive control of signaling split in urban traffic networks," *Transportation Research Part C: Emerging Technologies*, 18, 1, (2010): 120–139.
- [14] S. Lämmer, D. Helbing, "Self-control of traffic lights and vehicle flows in urban road networks," *Journal of Statistical Mechanics: Theory and Experiment*, 2008, 4, (2008): P04019.
- [15] D. Srinivasan, M.C. Choy, R.L. Cheu, "Neural networks for real-time traffic signal control," *IEEE Transactions on Intelligent Transportation Systems*, 7, 3, (2006): 261–272.
- [16] M.C. Choy, D. Srinivasan, R.L. Cheu, "Cooperative, hybrid agent architecture for real-time traffic signal control," *IEEE Transactions on Systems, Man, and Cybernetics-Part A: systems and humans*, 33, 5, (2003): 597–607.
- [17] B. Abdulhai, R. Pringle, G.J. Karakoulas, "Reinforcement learning for true adaptive traffic signal control," *Journal of Transportation Engineering*, 129, 3, (2003): 278–285.
- [18] D. Houli, L. Zhiheng, Z. Yi, "Multiobjective reinforcement learning for traffic signal control using vehicular ad hoc network," *EURASIP journal on advances in signal processing*, 2010, 7, (2010).
- [19] Y. Bie, Z. Liu, Y. Wang, "A real-time traffic control method for the intersection with pre-signals under the phase swap sorting strategy," *PloS one*, 12, 5, (2017): e0177637.
- [20] P.I. Richards, "Shock waves on the highway," *Operations research*, 4, 1, (1956): 42–51.
- [21] M. Mircea, F. Nicolae, "Increasing of the urban traffic surveillance by automatic information device," *Central European Journal of Engineering*, 4, 2, (2014): 133–141.
- [22] Transportation Research Board National Research Council, "Highway capacity manual," *TRB Business Office*, (2000).
- [23] J. Barzilai, J.M. Borwein, "Two-point step size gradient methods," *IMA journal of numerical analysis*, 8, 1, (1988): 141–148.
- [24] P. Van Overschee, B.L. De Moor, "Subspace identification for linear systems: Theory—Implementation—Applications," *Springer Science & Business Media*, (2012).
- [25] M. Arnold, G. Andersson, "Model predictive control of energy storage including uncertain forecasts," *In Power systems computation conference (PSCC), Stockholm, Sweden*, 23, (1989): 24–29.

- [26] T. Geyer, "Model predictive control of high power converters and industrial drives," *John Wiley & Sons*, (2016).
- [27] C.E. Garcia, D.M. Prett, M. Morari, "Model predictive control: theory and practice—a survey," *Automatica*, 25(3), (1989): 335–348.
- [28] M.J. Lighthill, G.B. Whitham, "On kinematic waves II. A theory of traffic flow on long crowded roads," *Proc. R. Soc. Lond. A*, 229, 1178, (1955): 317–345.
- [29] K. Wada, T. Ohata, K. Kobayashi, M. Kuwahara, "Traffic measurements on signalized arterials from vehicle trajectories," *Interdisciplinary Information Sciences*, 21, 1, (2015): 77–85.
- [30] M. Behrisch, L. Bieker, J. Erdmann, D. Krajzewicz, "SUMO—simulation of urban mobility: an overview," *Proceedings of SIMUL 2011, The Third International Conference on Advances in System Simulation*, 42, (2011).
- [31] C. Aswakul, S. Watarakitpaisarn, P. Komolkiti, C. Krisanachantara, K. Techakittiroj, "Chula-SSS: Developmental Framework for Signal Actuated Logics on SUMO Platform in Over-saturated Sathorn Road Network Scenario," *EPiC Series in Engineering*, 2, (2018): 67–81.

## **APPENDIX**

## APPENDIX A

### Notation

| Variable            | Meaning   | Unit    |
|---------------------|---|---------|
| ▼ Network layer ▼   |   |         |
| $T_N$               | Sampling period of network layer                  | sec     |
| $t_N$               | Sample index of network layer                     | -       |
| $x_N$               | Traffic demand of network                         | veh     |
| $u_N$               | Traffic movement of network layer                 | veh/sec |
| $v_N$               | Number of waiting vehicles from outside demand    | veh     |
| $\dot{v}_N$         | Arrival rate of vehicles from outside demand      | veh/sec |
| $z$                 | Traffic demand inside the area                    | veh/sec |
| $B_{NF}$            | Input matrix of network layer from link flow      | -       |
| $B_{NB}$            | Input matrix of network layer from outside demand | -       |
| $q_{\min}$          | Minimum traffic flow on each link                 | veh/sec |
| $C_{\text{link},k}$ | Maximum traffic flow on $k$ th link               | veh/sec |
| $\mu_{lk}$          | Gain of departure vehicles on $k$ th link         | -       |
| ▼ Area layer ▼      |   |         |
| $T_A$               | Sampling period of area layer                     | sec     |
| $t_{Aj}$            | Sample index of $j$ th area                       | -       |
| $x_{Aj}$            | Traffic demand of $j$ th area                     | veh     |
| $u_{Aj}$            | Traffic movement of $j$ th area                   | veh/sec |
| $\dot{v}_{aj}$      | Traffic demand from outside of $j$ th area        | veh/sec |
| $B_{AFj}$           | Input matrix of $j$ th area from road flow        | -       |
| $B_{ABj}$           | Input matrix of $j$ th area from outside demand   | -       |
| $W_{Aj}$            | Demand from adjacent $j$ th area                  | veh     |
| $\Sigma_{Aj}$       | Aggregation matrix of $j$ th area                 | -       |
| $D_{Aj}$            | Distribution matrix of $j$ th area                | -       |
| $q_{\max,r}$        | Maximum traffic flow on $r$ th road               | veh/sec |
| $C_{\text{int},i}$  | Maximum throughput on $i$ th intersection         | veh/sec |

|                                 |   |         |
|---------------------------------|---|---------|
| $\mu_r$                         | Gain of departure vehicles on $r$ th road                             | -       |
| ▼ Intersection layer ▼          |   |         |
| $T_s$                           | Sampling period of intersection layer                                 | sec     |
| $t_{JCi}$                       | Sample index of $i$ th intersection                                   | -       |
| $\tau_i$                        | Cycle length of traffic signal of $i$ th intersection                 | sec     |
| $\tau_{\min,ij}$                | Minimum duration of green time of $i$ th intersection on $j$ th phase | sec     |
| $\tau_{\max,ij}$                | Maximum duration of green time of $i$ th intersection on $j$ th phase | sec     |
| $\tau_{\text{fix},ij}$          | Duration of fixed time of $i$ th intersection on $j$ th phase         | sec     |
| $\rho_{\text{fix},i}$           | Set of index of fixed phase of $i$ th intersection                    | -       |
| $q_{\max,i}$                    | Maximum flow rate on $i$ th intersection                              | veh/sec |
| $x_{Ji}$                        | State vector of $i$ th intersection                                   | veh     |
| $\bar{x}_{Ji}$                  | Mean vehicles of $i$ th intersection over a time cycle                | veh     |
| $y_{Ji}$                        | Output vector of $i$ th intersection                                  | veh     |
| $u_{Ji}$                        | Input vector of $i$ th intersection                                   | sec     |
| $q_i$                           | Flow measurement vector of $i$ th intersection                        | veh/sec |
| $\hat{q}_i$                     | Predicted flow vector of $i$ th intersection                          | veh/sec |
| $w_{Ji}$                        | Traffic input of $i$ th intersection over a cycle                     | veh     |
| $C_i$                           | Output matrix of $i$ th intersection                                  | -       |
| $B_i$                           | Input matrix of $i$ th intersection                                   | -       |
| $\Sigma_{Ji}$                   | Aggregation matrix of $i$ th intersection                             | -       |
| $D_{Ji}$                        | Distribution matrix of $i$ th intersection                            | -       |
| ▼ Intersection layer with MPC ▼ |   |         |
| $N_p$                           | Prediction length of MPC  | -       |
| $\gamma$                        | Weighting gamma on 2nd cost objective                                 | -       |
| $X_{J,CL,i}$                    | State vector of MPC on $i$ th intersection                            | veh     |
| $U_{J,CL,i}$                    | Input vector of MPC on $i$ th intersection                            | sec     |

## Biography

Jeerapat Jitnuant was born in Bangkok, Thailand, in 1993. He received his Bachelor's degree in electrical engineering from Silpakorn University, in 2015. He conducted his graduate study with the Control Systems Research Laboratory, Department of Electrical Engineering, Faculty of Engineering, Chulalongkorn University. His research interests include traffic control systems design by the method of hierarchical distributed control framework and the model predictive control.

## List of Publications

1. J. Jitnuant, D. Banjerdpongchai, "Design of State Feedback Traffic Control Using Hierarchical Distributed Control Framework," in *Proc. of 2019 First International Symposium on Instrumentation, Control, Artificial Intelligence, and Robotics (ICA-SYMP)*, Bangkok, Thailand, (2019): 191–194.
2. J. Jitnuant, D. Banjerdpongchai, "Application of Model Predictive Control to Traffic Network Systems Based on Hierarchical Distributed Control Framework," in *Proc. 16th ECTI Conference*, Pattaya, Thailand, (2019). (accepted)